The primary cilium encourages osteogenic behavior in periosteal osteochondroprogenitors and osteocytes during juvenile skeletal development and adult bone adaptation

Emily R. Moore

Submitted in partial fulfillment of the
requirements for the degree of
Doctor of Philosophy
in the Graduate School of Arts and Sciences

COLUMBIA UNIVERSITY

2018

ABSTRACT

The primary cilium encourages osteogenic behavior in periosteal osteochondroprogenitors and osteocytes during juvenile skeletal development and adult bone adaptation

Emily R. Moore

Primary cilia are sensory organelles that facilitate early skeletal development, as well as maintenance and adaptation of bone later in life. These solitary, immotile organelles are known to be involved in cell differentiation, proliferation, and mechanotransduction, a process by which cells sense and covert external physical stimuli into intracellular biochemical signals. Bone is a metabolically active tissue that continuously recruits osteogenic precursors and relies on osteocytes, the sensory cells of bone, to coordinate skeletal maintenance. Overall bone quality is dependent on the integrity of the initial structure formed, as well as this organ's ability to adapt to physical loads. Proper differentiation and controlled proliferation of osteogenic progenitors are critical to the initial formation of the skeleton, while osteocyte mechanotransduction is essential for adaptation of developed bone. These phenomena rely on primary cilia, but little is known about the origin of osteogenic precursors and the ciliary mechanisms that promote osteogenesis.

In this thesis, we first characterize an osteochondroprogenitor (OCP) population that rapidly and extensively populates skeletal tissues during juvenile skeletal development (Chapter 2). We also demonstrate that the primary cilium is critical for these cells to differentiate and contribute to skeletogenesis. We then show this OCP population is required for adult bone adaptation and is mechanoresponsive (Chapter 3). Again, we demonstrate that primary cilia are necessary for these OCPs to sense physical stimuli and differentiate into active bone-forming cells. Finally, we identify a novel link between ciliary calcium and cAMP dynamics in the

osteocyte primary cilium (Chapter 4). Specifically, we show that a calcium channel (TRPV4) and adenylyl cyclases, which produce cAMP, bind calcium to mediate calcium entry and cAMP production, respectively, and these phenomena are critical to fluid flow-induced osteogenesis. Collectively, our results demonstrate that an easily extracted progenitor population is pre-programmed towards an osteogenic fate and extensively contributes to bone generation through primary cilium-mediated mechanisms at multiple stages of life. Furthermore, we identified ciliary proteins that are potentially unique to the osteocyte and can be manipulated to encourage osteogenesis by tuning calcium/ cAMP dynamics. For these reasons, we propose that this OCP population and their primary cilia, as well as osteocyte ciliary proteins that coordinate calcium/ cAMP dynamics, are attractive therapeutic targets to encourage bone regeneration.

Table of Contents

List of Figures

Acknowledgements

I have too many friends and family to thank so I will be focusing my acknowledgements to those that were immediately involved with the science presented in my thesis. I would first like to thank my PI, Chris Jacobs, for accepting me as a member of the Cell and Molecular Biomechanics Lab and providing the best training an aspiring young investigator could hope for. Without his insight and guidance, this work would never have been imagined and developed into a series of exciting experiments outside our lab's expertise.

I thank my defense committee for their participation in my dissertation, especially Ed Guo for his insight on the primary periosteal cell fluid shear experiments, Steve Thomopoulos for his input on the cell ablation model, and Helen Lu for her feedback on the R01 submission inspired by this work. I have come to know many of my panelists on a more personal level and would like to acknowledge what generally wonderful people they are. Their passion for their career and excellent treatment of their students is something I aspire to replicate as a PI. I would also like to recognize our former postdoc, Dr. Julia Chen, who initiated the exploration of Prx1-expressing cells and their cilia in bone formation. She has been in constant contact with me since her departure from our lab and was very patient with all of my questions. The majority of my thesis work came to fruition as a result of her vision so I thank her for the inspiration.

I would like to thank Dr. Thorsten Kirsch and his group at NYU, Dr. Annie Schwartz at Washington University in St. Louis, and Thomas Novak at Abcam for their invaluable consultation on histological analysis, imaging, and staining. I also thank the members of the Fairchild mouse facility for their attentive care and consultation regarding the animals used in the presented studies, the technical assistants in the Columbia University Medical Center (CUMC)

Molecular Pathology Core Facility for their help with histological preparation, and Luke and Wei in the Herbert Irving Comprehensive Cancer Center at CUMC for sorting the primary cells used in our fluid flow studies. I am also extremely grateful to our Biomedical Engineering department staff, particularly Paulette Louissaint, Michelle Cintron, and Zach Corter for processing and managing our numerous supply orders, as well as Wendy Goldberg for her assistance with submitting our grant application. Our lab's research, funding, and general operation is dependent on the often thankless job these staff members perform on a daily basis.

Three amazing students generated the bulk of the data presented in this thesis: Yu Chen Yang, Ya Xing "Amy" Zhu, and Han Seul "Kelly" Ryu. These women are extremely hardworking, dedicated, and passionate when it comes to research. I was equally impressed by their self-awareness and ability to fit seamlessly into our lab's social environment. Yu Chen, I will always keep the minion scientist figurine you brought me from China at my desk. Amy, thank you for walking to 7/11 with me on free slurpee day and I hope we can repeat this tradition when we are in Boston together this summer! Kelly, I fully intend to recruit you as a postdoc for my lab so no need to prepare a resume…I already know it. I am forever in their debt and have enjoyed being a part of their growth into brilliant researchers that have very bright careers ahead.

A significant portion of writing this thesis, as well as the publications resulting from the work presented in this document, could not have been done without the support of several (mainly pop) musicians. Specifically, my submission to Development was fueled by Demi Lovato's "Confident" and "Glory" by Britney Spears. Revisions to my co-authorship with Julia Chen and my JOR review paper on primary cilia in the growth plate were assisted by Taylor Swift's "1989", Lady Gaga's "Joanne", and an assortment of Betty Who songs. My publication on periosteal progenitors in adult bone formation was constructed with help from Marlon

Williams and throwbacks from Ashlee Simpson and Lorde's "Pure Heroine". Taylor Swift's new album "Reputation"—as well as Spencer Pratt's track-by-track review of this album—Gabbrielle Aplin's song "Night Bus", and various songs by Pinc Louds (discovered via another PhD student, Chris Mosher's, Snapchat of an interesting subway platform performance) gave me the strength to write my first postdoctoral fellowship and my manuscript for characterizing calcium/ cAMP dynamics in the osteocyte in less than 3 weeks. Lastly, the body of this thesis was inspired by a series of albums that dropped in 2017 and were straight fire: (in order of importance) Kesha's "Rainbow", Lorde's "Melodrama", Demi Lovato's "Tell Me You Love Me", and Miley Cyrus's "Younger Now." NO thank you to 2017 Katy Perry.

I feel compelled to acknowledge the Cleveland Browns, my beloved sports team. I particularly want to thank the 2017 Browns for a "perfect season". Your persistence despite being so utterly terrible is admirable and often kept me going during tough times in my PhD. I'm sorry I could not attend the parade due to a conference, but I read every available article and flipped through images of the costumes and posters. You did me proud. I actually want to thank Cleveland sports fans in general. Your unwavering passion and blind hope despite all of the obstacles against our teams is a trait that genuinely got me through my PhD. In a lot of ways, my PhD experience mirrors my time as a Cleveland sports fan. I will never forget the fateful trip back to Ohio for my post-proposal vacation that also happened to be Game 7 of the 2016 NBA finals. Interestingly, the Cavs 2015 and 2017 losses lined up with a failed grant and a job rejection, respectively. Nor will I forget the 2016 historic World Series loss, which is one of the best games I have every witnessed, but coincided with my R01 grant rejection. Then there's the 2017 Indians-Yankees game that was rained out when I got stuck in lab finishing an experiment, but fortunately rescheduled for a double header on a day I could skip work. There is no feeling

like being the only 20-something female (wearing a Cleveland baseball cap and nursing the largest beer available for purchase) sitting alone in a sea of old, cranky male Yankees fans, watching the Indians hit banger after banger into the cloudless sky. The Indian's 2017 ALDS loss coincided with a grant rejection, but the apologetic note from our liquid nitrogen delivery tech and Yankee fan, Noah, made me feel better. There is no real correlation with the Browns other than they secured a perfect preseason record shortly before I submit my written thesis for review, and ended their perfect season right before I submit my final thesis for publication. You could also say we've both been quite consistent in terms of work produced, except I'm crushing it. Regardless, Manny's on 2nd will always be my favorite place to watch Browns games and I am lucky to have had a place to mourn and celebrate with fellow Cleveland fans. Thank you, Justin Michel(s), for introducing me to this gem and the wonderful people there. It is literally the reason I continue to be a steadfast Browns fan today.

Finally, I owe so much of this work to my supportive, encouraging, and talented labmates: Milos Spasic, Michael Duffy, and Michael Sutton. The work environment we cultivated together is second to none and enabled me to thrive as a researcher, mentor, and coworker. I thank them for troubleshooting protocols, providing insight on research strategies, collaborating on grant writing, editing manuscripts, and putting up with me on days when I drank too much coffee. I will miss our Friday drink tradition, late night grant writing parties, sports smack talk (especially fantasy football, Indians/Cubs, and Cavs/Warriors), throwing dry ice against the fire door to watch it explode, exchanging food-based souvenirs from our trips, staying up too late playing cards on conference nights, and many other things I'm sure to remember later. They have become dear friends to me throughout our time together and I have no doubt our paths will continue to cross in the future. PEW PEW PEW!

Chapter 1: Introduction

Due to advances in other areas of human disease and health, older generations are increasingly suffering from skeletal deficiencies and abnormalities. One of the most prevalent bone diseases in older populations is osteoporosis, whereby bones become brittle and weak due to loss of tissue. Osteoporosis is characterized by low bone mineral density (BMD) and affects a significant portion of adults in the United States. In fact, the Centers for Disease Control and Prevention (CDC) National Center for Health Statistics (NCHS) report that between 2005 and 2010, 5.1% of men and a staggering 24.5% of women in the U.S. the age of 65 and older suffered from osteoporosis of the hip and/ or spine[1]. Additionally, the NCHS found that 44.0% of men and 52.3% of women had low bone mass as defined by the World Health Organization's (WHO) diagnostic criteria[1]. Collectively, it is estimated that 44 million people over the age of 50 have low bone mass or osteoporosis and represent 55% of the U.S. population[2].

Osteoporosis is the most common cause of bone fractures, which pose a major public health concern and place significant financial strain on the U.S. economy[2]. 300,000 people in the U.S. over the age of 65 are hospitalized each year for hip fractures alone[3] and 30% of these cases are expected to result in death[4]. In general, fractures are associated with high rates of mortality and decreased quality of life[5,6]. Over 1 million surgeries performed each year in the US involve fracture repair, partial excision of bone, and grafting[7,8]. The average hospital cost associated with fractures is $13,000 per patient[9] and $2.5 billion are currently spent on bone grafts[10]. The number of procedures is expected to double within 25 years[11], resulting in sharp increases in patient and surgical costs.

Although notable strides have been made in understanding bone diseases, current therapeutics are far from effectively treating osteoporosis and fractures. Bisphosphonates are known to inhibit resorption of bone tissue and are frequently administered orally or intravenously to increase BMD and prevent fractures. They have displayed some clinical success[12] but their effectiveness is limited due to poor patient compliance and failures in persistence of therapy[13]. Additionally, a variety of health complications associated with bisphosphonate treatment have emerged[12], such as hypocalcemia[14], atypical fractures[15–21], and impaired fracture healing[22]. In 2001, sclerostin protein was found to increase bone resorption in order to suppress bone formation[23] and recent studies suggest sclerostin antibody treatment has extreme promise in enhancing bone mass, strength, and formation[24–26] without sacrificing bone quality[27]. However, clinical studies are very preliminary and adverse effects, such as osteonecrosis of the jaw and atypical fracture[28], have already been identified. This is perhaps not surprising since atypical fracture is associated with antiresorptive treatments[29]. In fracture repair, 50% of bone grafts used in surgical procedures fail due to limited availability, donor site morbidity, and insufficient mechanical properties[30–32]. The most successful advances in bone regeneration involve a substrate that harbors cells capable of differentiating into bone-forming cells[33,34]; however, extracting cells from patients can be very painful and the acquired cells require complex *in vitro* guidance to an osteogenic lineage[33]. Thus, generating bone and enhancing bone quality in patients is a significant unmet need.

An attractive target for enhancing bone formation is the primary cilium, a solitary antenna-like sensory organelle that projects from the cell surface. The primary cilium is present on signaling cells embedded in bone (osteocytes), bone-forming cells (osteoblasts), and stem and progenitor cells that are known to differentiate into osteoblasts. Our lab's previous work

indicates the cilium is critical for osteocytes[35,36] and osteoblasts[37,38] to respond to mechanical stimulation in an osteogenic manner. Additionally, stem cells with osteogenic potential require primary cilia to guide their differentiation into osteoblasts[39,40] and subsequently form bone[41]. Recently, we discovered that an FDA-approved treatment for hypertension is capable of enhancing osteocyte-mediated osteogenesis by lengthening, and therefore sensitizing, the primary cilium[42]. These studies suggest that the primary cilium may be an effective tool for treating osteoporosis in a pro-osteogenic manner, as opposed to an antiresorptive strategy, and therefore minimize adverse therapeutic effects, such as atypical fracture.

Bone tissue is a dynamic, self-repairing organ and its growth and adaptation can be studied in order to recapitulate natural skeletal phenomena in regenerative therapeutics. The skeleton was once believed to be an inert structure solely responsible for support, but has since been found to continuously regenerate itself through the process of bone remodeling and further plays a role in locomotion, calcium balance, and endocrine signaling[43]. In fact, cortical bone turns over at a rate of 2-3% each year and the rate is even higher in trabecular bone[44]. One commonly studied natural occurrence in bone physiology is development, which involves the initial formation and growth of the skeleton via intramembranous and endochondral ossification. Osteoblasts are directly recruited to lay down appositional layers of bone in intramembranous ossification, whereas cartilage cells (chondrocytes) undergo a program of differentiation before undergoing apoptosis or differentiating into osteoblasts[45,46] to produce bone via endochondral ossification. Both forms are prevalent in embryonic and juvenile development and the primary cilium is known to be critical for embryonic skeletogenesis[47]. A second natural skeletal phenomenon is adult bone adaptation, whereby the mature skeleton generates more bone in response to heightened exposure to physical forces. Our lab has demonstrated that the primary

cilium and its associated proteins are necessary for normal adult bone formation[37,41,48]. A third mechanism of naturally occurring bone generation is fracture healing. In response to trauma, inflammatory cells, bone cells, stem cells, and osteogenic precursors (osteochondroprogenitors) from periosteal tissue surrounding bone coordinate the repair of broken bone into a fully integrated, ossified segment of new tissue with comparable mechanical properties. It has been suggested that the primary cilium is important in bone healing[49], but this sensory organelle's role is yet to be concretely established in the context of fracture repair. Overall, it is known that bone is inherently capable of generating more tissue but further research must be done to reveal the underlying mechanisms that trigger osteogenesis. It is believed that these insights are critical to developing truly regenerative techniques that produce fully integrated, mechanically suitable bone in patients with insufficient BMD and poor bone quality. Furthermore, the primary cilium appears to play an important role at all stages of skeletal growth and adaptation, making it a potential therapeutic target for *in vivo* bone regeneration.

Due to the potential importance of osteogenic precursors and cilia in the normal program of bone development, adaptation, and repair, we chose to examine the role of an understudied progenitor source and its cilia, as well as a potentially unique signaling mechanism in the osteocyte primary cilium. In Chapter 1 of this thesis, we track the fate of progenitor cells initially residing in the periosteum and perichondrium, a thin coating surrounding bone and cartilage, respectively, during juvenile skeletal development. Furthermore, we assess the effects of cilium disruption on this progenitor source's contribution to postnatal skeletogenesis. In Chapter 2, we determine the role of the aforementioned periosteal progenitors in adult bone formation and characterize their response to mechanical stimulation. In Chapter 3, we establish a relationship between two signaling cascades in the cilium and identify strategies to enhance osteocyte

osteogenesis by adjusting cilium-associated protein levels. The goal of this research is to motivate pro-osteogenic approaches to combat the debilitating effects of osteoporosis. Specifically, we seek to encourage the use of an underappreciated pool of progenitor cells for surgical grafting in the immediate future and *in vivo* regenerative therapeutics on a long-term scale. Additionally, we propose a molecular mechanism that may eventually be pharmacologically manipulated to sensitive osteocyte cilia and encourage bone formation.

Background and Terms

1.1 Bone Cells

The following cells play an important role in the development and maintenance of bone. It is also important to note that these cell types often communicate with each other to holistically maintain the structure and function of bone. Furthermore, they all possess primary cilia (Section 1.4) and are thought to be mechanosensitive (Section 1.2).

Osteoblasts: bone-forming cells. These cells produce and secrete matrix proteins that ultimately become mineralized bone. A population of quiescent osteoblast-like cells line the cortical bone surface and are believed to facilitate signaling between other bone cells to ensure proper bone maintenance[50]. These "old osteoblasts" are referred to as *bone lining cells* and they are hypothesized to be first responders when the adult skeleton requires new cortical bone[51]. Specifically, it is believed that bone lining cells are triggered to deposit new bone matrix or differentiate into active osteoblasts in immediate response to mechanical stimulation.

Osteoclasts: bone-resorbing cells. These multinucleated cells secrete digestive enzymes that break down mineralized bone tissue, usually making way for osteoblasts to form new bone. Osteoporosis is perhaps a result of overactive osteoclasts, which resorb more bone than the

body's osteoblasts can replace. Current osteoporosis therapies, such as bisphosphonates and sclerostin antibody, attempt to restrict osteoclast activity in order to increase bone mineral density and are therefore called *antiresorptives*.

Osteocytes: bone-signaling cells. Osteocytes are embedded in cortical bone and reside in fluid-filled pockets called *lacunae*. Lacunae are connected via *canaliculi*. This lacunar-canalicular system allows for osteocytes to efficiently communicate with each other and other bone cells to coordinate formation, resorption, and overall skeletal maintenance. For example, osteocytes are known to directly activate osteoblast-mediated bone formation and osteoclast-mediated resorption.

Chondrocytes: cells that secrete cartilage matrix and embed themselves in cartilaginous tissue. These cells create structural templates during skeletal development and fracture repair, and make up the growth plate (Section 1.5), which is responsible for limb elongation during development. Furthermore, hypertrophic chondrocytes in the growth plate are known to become osteoblasts[46].

Mesenchymal stem cells: multipotent cells that can differentiate into a wide variety of cell types. Mesenchymal stem cells (MSCs) are generally associated with bone marrow but can also be found in adipose tissue, bone, lung, and peripheral blood in adults, as well as umbilical cord blood, placenta, and fetal tissues[52]. Due to their differentiation potential, many current strategies employ MSCs to regenerate a wide array of tissues, including bone.

Periosteal osteochondroprogenitors: cells residing in the periosteum that are capable of differentiating into osteoblasts and chondrocytes. Similar to MSCs, progenitors are able to differentiate into another cell type; however, progenitors are already committed to a more specific lineage. The periosteum is a thin covering surrounding cortical bone and has two distinct

layers. The outer *fibrous layer* primarily contains fibroblast-like cells that secrete matrix to give the periosteum its structure. The inner *cambium layer*, or "osteogenic layer", contains progenitor cells that readily differentiate into osteoblasts to generate new bone. A subset of progenitors in the cambium layer are also known to form the fracture callus and bone in response to fracture[53,54]. These cells can differentiate into both osteoblasts and chondrocytes and are therefore called *osteochondroprogenitors* (OCPs).

1.2 Mechanotransduction

Mechanotransduction is the process by which cells sense physical stimuli and convert these mechanical signals into biochemical changes within the cell. Mechanical forces are critical to normal cell function and directly influence the formation and behavior of almost all tissues, spanning every stage of life and length scale. In fact, changes in tissue mechanical properties and the cell's inability to engage in mechanotransduction are known to cause osteoporosis[55], cancer[56], cilium-specific diseases called ciliopathies[57], and a variety of other diseases. Anything that responds to physical stimuli is called a *mechanosensor* or is known to be *mechanosensitive*. Cells that generate a measurable response to mechanotransduction are termed *mechanotransducers*.

1.3 Second Messengers

Second messengers are molecules that relay chemical and mechanical signals received at the cell surface and trigger signaling cascades within the cell. Two second messengers that are commonly studied in the context of mechanotransduction are *calcium* (Ca^{2+}) and *cyclic adenosine monophosphate* (cAMP). Ca^{2+} is an extremely versatile molecule involved in a variety

of intracellular signaling pathways that encourage cell proliferation, transcription activation, and self-regulation of Ca^{2+} signalling[58]. Ca^{2+} may enter the cell due to changes in chemical gradients across the plasma membrane, as well as opening of stretch activated ion channels. The endoplasmic reticulum in the cell is also known to release internal stores of Ca^{2+} in response to mechanical and chemical stimulation. Studies from our lab and others suggest Ca^{2+} enters the primary cilium in response to fluid shear[36,59,60] and is critical to its role in mechanosensation[36,60–63]. Cyclic AMP is catalyzed from adenosine triphosphate (ATP)—which is commonly referred to as the "energy currency of the cell"[64]—by members of the adenylyl cyclase family. cAMP triggers intracellular signaling by activating protein kinase A (PKA), a phosphorylating enzyme known to be involved in osteogenesis[65], and exchange proteins independent of the PKA pathway[66]. Our lab recently determined that fluid flow-induced changes in cAMP production are crucial to the osteocyte's osteogenic response to physical stimulation[35].

Both Ca^{2+} and cAMP are tightly regulated spatially and temporally to effectively initiate intracellular signaling. The ability to tune the spatial and temporal release of these second messengers is critical to understanding how cell behavior can be manipulated on the molecular level and has become a popular topic of study. We propose that Ca^{2+}/ cAMP dynamics are intimately coordinated in bone signaling cells (osteocytes) and study a potential mechanism that links them together in Chapter 4 of this thesis.

1.4 Primary Cilia

Structure and function

The primary cilium is a solitary, non-motile organelle that is found in nearly all mammalian cell types. The ciliary base anchors the structure to the cell membrane and is

responsible for providing support, as well as managing entry of proteins and molecules into the cilium body. The portion of the cilium that projects from the cell surface is known as the *axoneme* and is composed of nine microtubule doublets (Figure 1.1) surrounded by a ciliary membrane, which is distinct from and not continuous with the plasma membrane. Cilia are approximately 250 nm in diameter and generally 1-4 μm long[67], and therefore very small compared to the cell body. The axoneme is formed and maintained via intraflagellar transport (IFT), a process that requires the motor complex protein, IFT88, and KIF3A, an essential component of the anterograde motor protein, Kinesin-2[68]. In the absence of IFT88 and KIF3A, the cilium cannot form[69] or is unable to engage in mechanotransduction[35,37,68]. Murine animal models have been developed to disrupt primary cilia and study its effects *in vivo*. In fact, mice containing osteoblasts that lack KIF3A form significantly less bone in response to mechanical stimulation[37] and some of our recent work shows a similar trend in mice lacking IFT88 in osteocytes/ osteoblasts.

Once believed to be a vestigial structure, the primary cilium has since been identified as a crucial sensory organelle involved in chemosensing and mechanotransduction. In fact, a series of health complications spanning multiple tissues are directly associated with defects in the formation and function of cilia and its associated components. These diseases and disorders are called *ciliopathies* and result in skeletal deficiencies, developmental abnormalities, and cyst formation, among a variety of other issues[57]. The cilium possesses an extracellular component (axoneme), channels for transduction, and an intracellular connection, which are three general features associated with mechanotransduction[70]. Specifically, the cilium's axoneme serves as the extracellular component, projecting from the cell surface to receive chemical signals and exposure to physical stimuli. The axoneme and base of the cilium contain ion channels and

transmembrane proteins that further engage in mechanotransduction. Physical bending of the cilium results in an influx of Ca^{2+}[36,71] and changes in cAMP[35], which trigger intracellular signaling cascades. Due to its sensory nature, the cilium has been referred to as an antenna-like, amplifying signaling nexus[72]; however, the exact mechanisms for cilium mechanotransduction have yet to be uncovered, particularly in the context of bone.

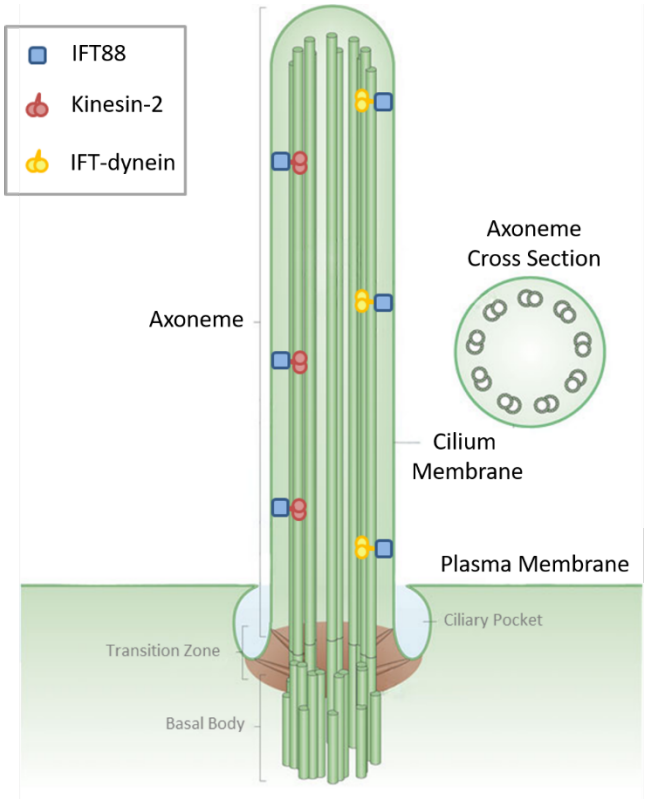

Figure 1.1: Structure of the primary cilium
The primary cilium is composed of nine microtubule doublets in a 9+0 configuration depicted in the axoneme cross section. The axoneme is anchored to the cell via the basal body and surrounded by a distinct ciliary membrane. The ciliary membrane is not continuous with the cell's plasma membrane, creating a ciliary pocket. The transition zone in the ciliary pocket functions as a filter, allowing only certain ciliary proteins to enter the axoneme. The axoneme is assembled and maintained via intraflagellar transport (IFT), whereby Kinesin-2 delivers IFT cargo, including IFT88, via anterograde transport and IFT-dynein removes cargo through retrograde transport. *Modified from Moore et al.*[72].

Proteins associated with the cilium

In addition to serving as a mechanosensing organelle, the primary cilium is associated with a variety of proteins that further enhance mechanotransduction. These proteins consist of stretch-activated ion channels, receptors, and transmembrane proteins that can directly interact with external stimuli. Although some proteins are unique to the primary cilium, many are expressed elsewhere in the cell but concentrated in the cilium. Disruptions in some of these proteins alone have been directly tied to ciliopathies[73,74]. One hypothesis is that many of these proteins localize at the base of the cilium such that bending easily triggers their activation[72]. For this reason, it is believed that the cilium acts as a signal amplifier since it can convert small physical movements into large scale intracellular signaling cascades[72]. We highlight two of the ciliary proteins important for mechanotransduction below.

TRPV4

One ion channel believed to be associated with osteocytes is Transient Receptor Potential Vanilloid 4 (TRPV4). This Ca^{2+} ion channel is believed to open from chemical gradients, heat, physical stretching of the cell membrane, and binding of external Ca^{2+}[75,76]. TRPV4 was first proposed to be involved in osteocyte cilium-mediated mechanotransduction when the Polycystin 1 and Polycystin 2 complex (PC1/PC2)—known to be responsible for Ca^{2+} influx in kidney cells[63]—was not influential in osteocytes[36]. Specifically, an siRNA-mediated knockdown of TRPV4 hindered osteocyte mechanotransduction *in vitro*, whereas there was no effect with a PC2 knockdown[36]. Furthermore, disrupting TRPV4's ability to bind Ca^{2+} disables the subsequent Ca^{2+} influx[76] and attenuates osteoclast activation and differentiation[77,78]. For these reasons, we investigate the effects of overexpressing TRPV4 and eliminating its ability to bind Ca^{2+} in the context of osteocyte mechanotransduction in Chapter 4.

Adenylyl Cyclase

There are 10 isoforms of adenylyl cyclase (AC), which catalyze the conversion of ATP to cAMP, an aforementioned important second messenger for mechanotransduction. The first nine isoforms (AC1 - AC9) are transmembrane proteins, while AC10 is soluble[79]. All isoforms are activated by Forskolin to produce cAMP, but others bind Ca^{2+} to modify their behavior. Specifically, AC5 and AC6 are inhibited and AC1, AC3, and AC8 are activated when bound to Ca^{2+}[80]. AC6 was discovered in the osteocyte cilium almost a decade ago and in vitro studies suggest the osteocyte's mechanically-induced osteogenic response is hindered when AC6 is knocked down[35]. Furthermore, mice containing a global knockout of AC6 form significantly less bone in response to mechanical stimulation[48]. Recent unpublished work in our lab suggests AC3 is also present in the cilium, but its role in osteocyte mechanotransduction has yet to be explored. Furthermore, it is unknown whether AC6 and AC3 binding to Ca^{2+}, a critical second messenger in mechanotransduction, serves as a link between osteocyte ciliary Ca^{2+} influx[36] and subsequent changes in cytosolic cAMP[35]. Consequently, we seek to identify a Ca^{2+}/cAMP complex that is mediated by ACs and potentially unique to the osteocyte primary cilium in Chapter 4.

1.5 Postnatal growth plate

The growth plate is a cartilaginous structure densely populated with chondrocytes that undergo a program of activation and differentiation to generate bone via endochondral ossification. The growth plates form shortly after birth in the epiphyses and are responsible for lengthening of the arm and leg bones. The growth plate contains four distinct regions termed *zones* that are determined by observing chondrocyte morphology: resting, proliferation, hypertrophic, and ossification zones (Figure 1.2). The resting zone is characterized by round

chondrocytes, which then flatten and align into vertical columns as they rapidly undergo mitosis in the proliferation zone. The hypertrophic zone contains expanded, cuboidal chondrocytes that express type X collagen. These cells then undergo apoptosis or become osteoblasts[46] to aid in forming mineralized matrix and, eventually, bone in the ossification zone. The size of the growth plate, proliferation zone, and hypertrophic zone are critical to the rate and extent of longitudinal bone growth[81]. Additionally, the onset and rate of hypertrophic differentiation is particularly critical for chondrocytes to undergo the normal program of endochondral ossification. The primary cilium protein IFT88 has been implicated in chondrocyte proliferation and differentiation during skeletal development [47,82], so we study the role of the primary cilium itself in postnatal limb development in Chapter 3.

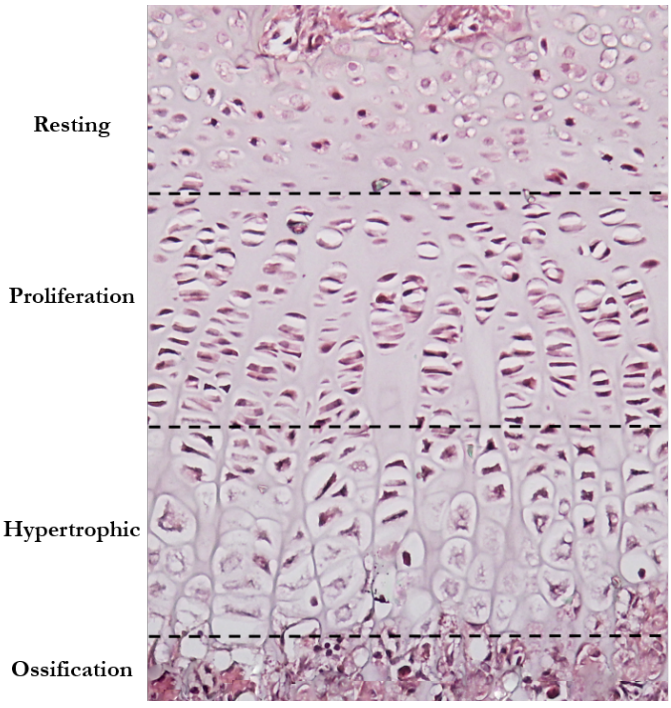

Figure 1.2: Structure of the postnatal growth plate
Hematoxylin and eosin stain of a murine ulnar growth plate at postnatal day 21 (P21). The growth plate is organized into four specific zones from the distal (top) to proximal end: resting zone, proliferation zone, hypertrophic zone, and ossification zone. In some instances, the region where proliferating cells begin to undergo hypertrophy is referred to as the pre-hypertrophic zone. Micrograph was collected with an inverted microscope (Olympus CKX41) at 20X.

Chapter 2: Periosteal osteochondroprogenitors are mechanosensitive and necessary for adult bone formation

Abstract

The fully developed adult skeleton adapts to mechanical forces by generating more bone, usually at the periosteal surface. Progenitor cells in the periosteum are believed to differentiate into bone-forming osteoblasts that contribute to load-induced adult bone formation, but *in vivo* evidence does not yet exist. Furthermore, the mechanism by which periosteal progenitors might sense physical loading and trigger differentiation is unknown. We propose that periosteal progenitors directly sense mechanical load and differentiate into bone-forming osteoblasts via their primary cilia, mechanosensory organelles known to be involved in osteogenic differentiation. We generated an ablation model to quantify the contribution of periosteal osteochondroprogenitors (OCPs) in adult bone formation *in vivo*. Indeed, mice lacking periosteal OCPs had severely attenuated mechanically induced bone formation and lacked mineralization necessary for daily skeletal maintenance. We also generated a cilium knockout model to study the primary cilium's role in periosteal OCP mechanosensing *in vitro*. Our results demonstrate that periosteal OCPs directly sense fluid shear and exhibit an upregulation in osteogenic markers; however, this response is essentially lost when the primary cilium is absent. Combined, our data show that periosteal progenitors are a mechanosensitive cell source that significantly contributes to load-induced adult bone formation. More importantly, this population persists in the adult skeleton and these cells, as well as their cilia, are promising targets for bone regeneration strategies.

Introduction

One way the skeleton structurally adapts to its mechanical environment is by generating new bone to alter its geometry and density to better withstand higher forces. Bone formation in response to mechanical loading involves multiple cell types and requires a sequence of events to occur. Specifically, mechanosensitive osteocytes sense physical loading and secrete paracrine factors that recruit cells to the bone surface[83]. These cells eventually transform into matrix-producing osteoblasts and, potentially, embedded osteocytes. With innovative regenerative bone therapies rapidly emerging, it is more important than ever to determine the origin of cells recruited to the bone surface. Bone-forming cells have long been thought to originate from progenitors, so approaches were developed to extract osteoblast precursors from bone marrow; however, these procedures are very invasive and the acquired progenitors require further treatment to encourage differentiation. An appealing alternative is to harvest periosteum, which surrounds bones and is rich in progenitor cells known to preferentially differentiate toward the osteogenic lineage[53,84,85].

Intriguingly, previous *in vitro* studies suggest that progenitor cells directly sense physical stimulation, which in turn enhances differentiation towards the osteogenic lineage[39,86]. In addition, mechanical forces on the periosteum are also known to enhance osteogenic lineage commitment *in vivo* and *in vitro*. Henderson et al. observed localization of cells with osteogenic gene expression to areas of tension on the outer edges of embryonic mouse rudiment tissues[87] and Kanno et al. found osteogenic markers were upregulated when mechanical strain was applied to human periosteal cells[88]. Although these *in vitro* studies are promising, it remains unknown whether progenitors within the periosteum directly sense mechanical stimulation and/ or respond in an osteogenic manner.

Many *in vivo* studies have successfully used a loading regimen to quantify how quickly new bone is laid down by osteoblasts[37,89,90], but fail to characterize the roles of progenitor cells in the normal program of adult bone formation. Furthermore, these studies typically report bone formation rates for only the periosteal region, which, due to geometry, experiences amplified mechanical signals compared to the endocortical region. A recent study suggests the periosteal surface is less mechanoresponsive than the endocortical surface and that the load-induced periosteal response decreases with age[91]. This contradicts prior claims that periosteal progenitor activity does not vary with age[33]. Thus, it is important to determine the extent to which periosteal progenitors contribute to adult bone formation and identify how they might sense and respond to mechanical cues *in vivo*. For these reasons, we quantify the amount of bone formed in skeletally mature mice without periosteal progenitors and investigate the mechanism by which these progenitors recognize and respond to mechanical loading.

One potential mechanism by which progenitor cells may become mechanically activated is through the primary cilium. Primary cilia are antenna-like organelles that extend from the cell surface and serve as amplifying microdomains to enhance interactions between external stimuli and intracellular signaling molecules. Impairment of primary cilia formation and signaling is known to influence bone development and formation[37,48,92,93]. A prior study conducted in our lab revealed that load-induced bone formation was attenuated when an intraflagellar retrograde transport protein important for primary cilia function (Kif3a) was deleted in osteoblasts and osteocytes[37]. Our previous work also suggests cilia are critical to osteogenic differentiation of periosteal progenitors[84,86], as well as human mesenchymal stem cells[39,94], *in vitro*. Furthermore, we recently determined that mechanical loading activates progenitors to form bone in adults but this response is attenuated when their cilia are disrupted[167]. Despite the clear implications, how

periosteal progenitor cell primary cilia mediate the *in vivo* bone formation response to mechanical stimulation has yet to be investigated.

Prx1 is expressed in the inner layer of the periosteum in close association with cortical bone and is deemed a marker for osteochondroprogenitors (OCPs), or cells that preferentially differentiate into osteoblast and chondrocytes[53]. In adult animals, Prx1-expressing cells are restricted to the appendicular skeleton and populate the fracture callus[53] and cortical bone[167]. Our prior work suggests that Prx1-expressing cells found embedded in bone in response to mechanical loading are perhaps periosteum-derived; however, Prx1's specific expression patterns have yet to be determined in the skeletally mature adult. Progenitor cells generally demonstrate upregulation in osteogenic markers when subjected to physical stimuli *in vitro*[39,40,88], so it is possible that progenitors residing in the cambium layer generate bone in response to mechanical cues *in vivo*[33,95–97]. This hypothesis has yet to be tested since ubiquitous ablation of Prx1-expressing cells is embryonic lethal[98]. A recent tamoxifen-inducible Prx1CreER-GFP model[53] has made it possible to study Prx1-expressing OCP ablation after birth and at specific timepoints of interest. Thus, this conditional transgenic model is perhaps a novel method for studying the unknown role of periosteal OCPs in normal adult physiology.

The objectives of this study are three-fold. First, to determine Prx1 expression in the skeletally mature adult mouse using the GFP tag associated with our Prx1CreER-GFP model. Second, to quantify the contribution of Prx1-expressing OCPs in load-induced bone formation using a conditional diphtheria toxin A (DTA) ablation model. Finally, we seek to determine the mechanism by which primary cilia mediate the periosteal OCP's potential osteogenic response to mechanical loading through *in vitro* fluid shear studies.

Materials and Methods

Animal models

All mouse models are on a C57BL6 background. Prx1CreER-GFP males were bred with Rosa26^{tdTomato} females acquired from Jackson Laboratories to generate our Prx1CreER-GFP; Rosa26$^{tdTomato(-/+)}$ fluorescent reporter model. Prx1CreER-GFP females were bred with Rosa26^{DTA} males acquired from Jackson Laboratories to generate Rosa26$^{DTA(-/+)}$ control and Prx1CreER-GFP; Rosa26$^{DTA(-/+)}$ experimental offspring. Animals used for the ulnar loading experiments did not participate in breeding. Prx1CreER-GFP males were bred with Ift88$^{fl/fl}$ females to generate Prx1CreER-GFP; Ift88$^{fl/fl}$ offspring for primary cell isolations. Genotype was determined using PCR and agarose gel electrophoresis. Primer sequences are available upon request. Animals were housed, maintained, and evaluated for health complications in accordance with IACUC standards. The Institute of Comparative Medicine at Columbia University approved all experiments.

Tamoxifen injections

Tamoxifen (Sigma Aldrich) was dissolved in corn oil (Sigma Aldrich) in a shaking incubator at 37°C to create a 25 mg/mL stock solution stored at 4°C and protected from light. Tamoxifen solution was prepared fresh for each series of loading experiments. Skeletally mature 16 week-old adult Prx1CreER-GFP; Rosa26^{tdTomato} mice received a single intraperitoneal injection of 100 mg/kg body weight tamoxifen. Adult Prx1CreER-GFP; Rosa26^{DTA} experimental and Rosa26^{DTA} controls received daily intraperitoneal injections of 75 mg/kg tamoxifen solution for five days prior to loading, concurrent with the 3 days of loading, and concurrent with fluorochrome label injections after loading.

In vivo ulnar loading

Skeletally mature 16-week-old mice were placed under isofluorane anesthesia and the right forelimbs were anchored between 2 platens attached to an electromagnetic loading system with feedback control (Bose Enduratec ELF 3220). Following an initial 0.1 N load, a peak compressive axial load of 3 N was applied with a 2 Hz sine wave for 120 cycles/day for 3 consecutive days. The non-loaded left forelimbs served as internal controls. Body weight was measured each time an injection or ulnar loading was administered and cage activity and anesthesia recovery time were observed to monitor animal health. Mice received subcutaneous injections of 10 mg/kg calcein (Sigma Aldrich) and 70 mg/kg alizarin red (Sigma-Aldrich) 5 and 9 days following initiation of loading, respectively. All animals were euthanized 15 days after the initiation of loading and prepared for analysis.

Micro-computed tomography (microCT) and dynamic histomorphometric analysis

Upon sacrifice, loaded and non-loaded ulnae were dissected and stored in 70% ethanol for up to a week. The non-loaded limb of each specimen was imaged by microCT (Scanco vivaCT 80, Scanco Medical AG) at 10.4 μm isotropic resolution using scan settings of 55 kV, 145 μA, and 300 ms integration time. Bone lengths were determined from scout views. Cortical bone analyses were performed at the mid diaphysis of each ulna and Scanco analysis software was used to determine total bone area, the ratio of bone volume to total volume (BV/TV), bone mineral density (BMD), cortical thickness, the polar moment of inertia (pMOI), and the minimum and maximum second moments of inertia (I_{min} and I_{max}).

Following the microCT scan, ulnae were gradually dehydrated in a tissue processor (Leica ASP300S), infiltrated with methyl methacrylate, and embedded in methyl methacrylate

and benzoyl peroxide (Sigma Aldrich), as described previously[37]. Embedded specimens were sectioned at the ulnar midshaft using a diamond-tip blade and saw (Isomet) and transverse sections were imaged on a confocal microscope (Olympus Fluoview). The bone surface, single label, and double label perimeters and double label area were quantified in ImageJ in order to calculate mineralizing surface/bone surface (MS/BS), mineral apposition rate (MAR), and bone formation rate/bone surface (BFR/BS)[37,99]. All measurements were taken from the periosteal surface. Non-loaded ulnae values were subtracted from loaded values to determine relative measurements of rMS/BS, rMAR, and rBFR/BS, which represent changes due to mechanical loading.

Histology

Upon sacrifice, ulnae were dissected and fixed overnight at 4°C. For histological analysis, specimens were fixed in 10% formalin (Sigma Aldrich), decalcified, embedded in paraffin, sectioned in 5 μm increments, and stained with Hematoxylin and Eosin (Sigma Aldrich) for 10 minutes and 30 seconds, respectively. Micrographs were collected with an inverted microscope (Olympus CKX41) at 20X magnification. To determine whether our ablation model was successful, ulnae were fixed in 4% paraformaldehyde (Sigma Aldrich), decalcified, and cryosectioned in 5 μm increments. Micrographs were collected with a confocal microscope (Olympus Fluoview) at 100X magnification.

Primary periosteal OCP isolation

Prx1CreER-GFP and Prx1CreER-GFP; Ift88$^{fl/fl}$ juveniles were sacrificed between 3 and 4 weeks of age and their fore and hindlimbs were collected for dissections. The skin, fascia, connective tissue, and majority of the muscle surrounding the periosteum were removed using a

scalpel and the specimens were placed in sterile PBS (Life Technologies) on ice. The epiphyses were then cut off, the remaining muscle surrounding the periosteum was removed, and the specimens were transferred to fresh cold PBS. In a sterile culture hood, the periosteum was scored with a scalpel, peeled off the bone, cut into 1 mm^2 sections, and placed into fibronectin (Sigma Aldrich) coated tissue culture dishes containing MEMα (Life Technologies) supplemented with 10% FBS and 1% P/S (Life Technologies). Tissue sections were incubated at 37°C for 7 – 10 days and the resulting primary periosteal cells were passaged onto fresh fibronectin coated tissue culture dishes and cultured until reaching 80% confluence.

Immunocytochemistry

To visualize cilia, cells were rinsed with cold PBS and fixed in 10% formalin solution (Sigma) for 10 min, then blocked in 10% goat serum for 1 hour at room temperature. Blocked cells were incubated in a 1:10 dilution of primary anti-acetylated α-tubulin antibody isolated from a C3B9 hybridoma line (Sigma), followed by a 1:500 dilution of the fluorescent secondary antibody AlexaFluor 568. Both incubations were for 1 hour at room temperature. Nuclei were detected using NucBlue ReadyProbes (Life). Fluorescent images were collected using an Olympus Fluoview FV1000 confocal microscope and software.

Cell culture and sorting

Primary periosteal cells were cultured on fibronectin coated dishes in MEMα supplemented with 10% FBS and 1% P/S at 37°C. An Influx cell sorter (BD Biosciences) was used to separate cambium layer osteochondroprogenitors (GFP+) from other cells of the periosteum (GFP-). Sorted cells were cultured for 1 – 2 weeks until a sufficient number of cells were available for flow studies. Passages P2 – P4 were used for all *in vitro* experiments.

Oscillatory fluid flow (OFF)

To test the effects of direct mechanical stimulation on periosteal cells, Prx1-expressing osteochondroprogenitors (GFP+) and other cells of the periosteum (GFP-) were seeded on fibronectin coated glass slides (Fisher Scientific; 75 x 38 x 1 mm) and cultured in reduced serum media (MEMα supplemented with 2.5% FBS, 2.5% CS, and 0.5% P/S) 48 hours prior to fluid flow. To disrupt primary cilia, cells were treated with (Z)-4-Hydroxytamoxifen (Sigma Aldrich) diluted to 5 μg/mL in 95% ethanol or vehicle control 24 hours prior to flow. Upon reaching 80% confluence, cells were placed in parallel-plate flow chambers (56 × 24 × 0.28 mm), incubated at 37°C for 30 minutes at rest, and exposed to 60 minutes of oscillatory fluid flow (OFF) at 1 Hz with a peak shear stress of 10 dyn/cm^2. Slides were removed from the chambers and lysed immediately with TriReagent (Sigma Aldrich) to isolate RNA. RT-qPCR was performed to quantify flow-induced changes in Cyclooxygenase-2 (COX-2), Osteopontin (OPN), and GAPDH using fluorescent primers (Life Technologies) and an ABI PRISM 7900 (Applied Biosystems). Samples were performed in triplicate and COX-2 and OPN were normalized to GAPDH expression levels. OFF samples were normalized to static controls.

Statistics

No sex-dependent differences were identified in our dynamic histomorphometric analysis according to a 2-way ANOVA, so males and females were grouped together for the ulnar loading experiment results. All data were analyzed with a two-tailed student's t-test and values are reported as mean ± SEM, with $p < 0.05$ considered statistically significant. Sample size was selected in order to achieve a power of at least 80%.

Results

Successful generation of mouse models

PCR and gel electrophoresis confirmed that we generated Prx1CreER-GFP; Rosa26^{DTA} and Rosa26^{DTA} littermates, as well as Prx1CreER-GFP; Rosa26^{tdTomato} reporter mice (Figure 2.2). When Prx1CreER-GFP; Rosa26^{DTA} animals are injected with tamoxifen, Prx1-expressing cells will produce diphtheria toxin A, causing periosteal OCPs to be ablated. Similarly, Prx1-expressing cells and their progeny will produce red fluorescent protein in Prx1CreER-GFP; Rosa26^{tdTomato} mice.

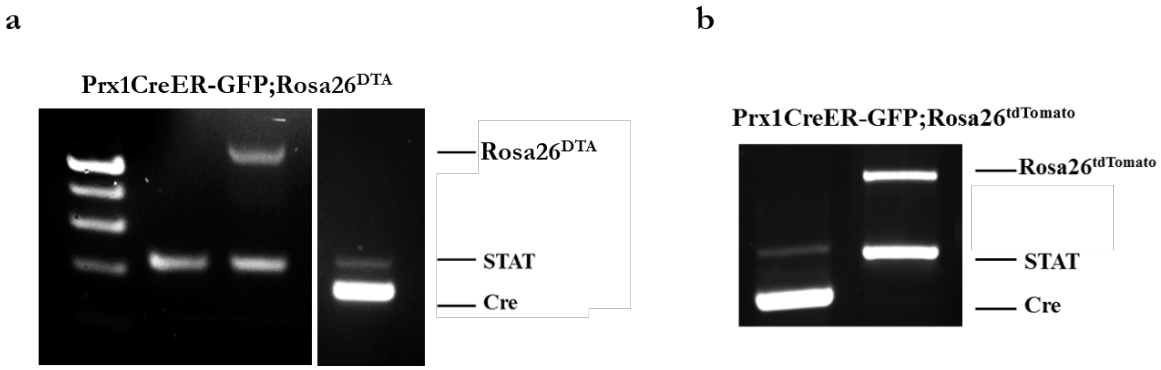

Figure 2.1: Prx1-driven OCP ablation and red fluorescent reporter models were generated
Gel electrophoresis confirmed Prx1CreER-GFP animals were successfully crossed with (a) Rosa26^{DTA} mice to generate a conditional periosteal osteochondroprogenitor ablation model (Prx1CreER-GFP; Rosa26^{DTA}) and (b) Rosa26^{tdTomato} animals to produce a Prx1CreER-GFP; Rosa26tdTomato fluorescent reporter model.

Prx1 expression is restricted to the periosteum in adult ulnae

Skeletally mature 16-week old fluorescent reporter mice (Prx1CreER-GFP; Rosa26^{tdTomato}) were injected with a single dose of tamoxifen to determine the location of Prx1-expressing cells and confirm Cre activity. Indeed, red fluorescent cells were present, indicating successful Cre recombination. We found recombined cells in the ulnar periosteum (Figure 2.1) and perichondrium (not pictured), but these cells were absent from cortical bone, trabecular

bone, muscle, and marrow. We therefore conclude the Prx1CreER-GFP model is an appropriate tool for determining the effects of periosteal OCP ablation on load-induced adult bone formation.

Tamoxifen treatment ablates periosteal OCPs *in vivo* and disrupts their cilia *in vitro*

We visualized GFP expression to determine whether Prx1-expressing OCPs were present in the periosteal tissue of Prx1CreER-GFP; Rosa26^{DTA} mutants and Prx1CreER-GFP controls injected with tamoxifen. Indeed, mutants (Figure 2.3b) lacked the green fluorescent Prx1-expressing cells observed in control periosteum (Figure 2.3a), indicating tamoxifen-induced Cre recombination successfully ablated the periosteal OCP population of interest *in vivo*. Primary periosteal OCPs obtained from Prx1CreER-GFP; Ift88$^{fl/fl}$ animals were sorted via GFP and treated with 4-hydroxytamoxifen, the active compound of tamoxifen that is generated when

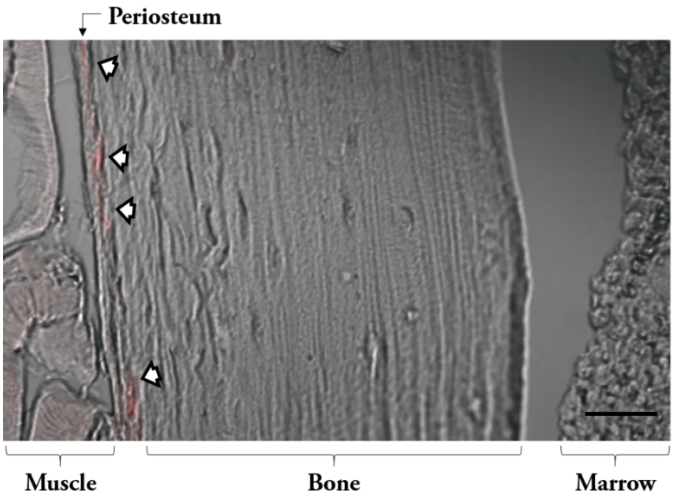

Figure 2.2: Prx1 expression is restricted to the periosteum in the adult ulnae
Skeletally mature 16-week-old Prx1CreER-GFP; Rosa26^{tdTomato}mice received a single dose of tamoxifen to induce Cre recombination and, subsequently, red fluorescent protein production, and were sacrificed a week later. Recombined cells were found in the periosteal tissue but were absent from cortical bone, trabecular bone, muscle, and bone marrow. Micrographs were captured with a confocal microscope at 20X. Black scale bar represents 50 μm.

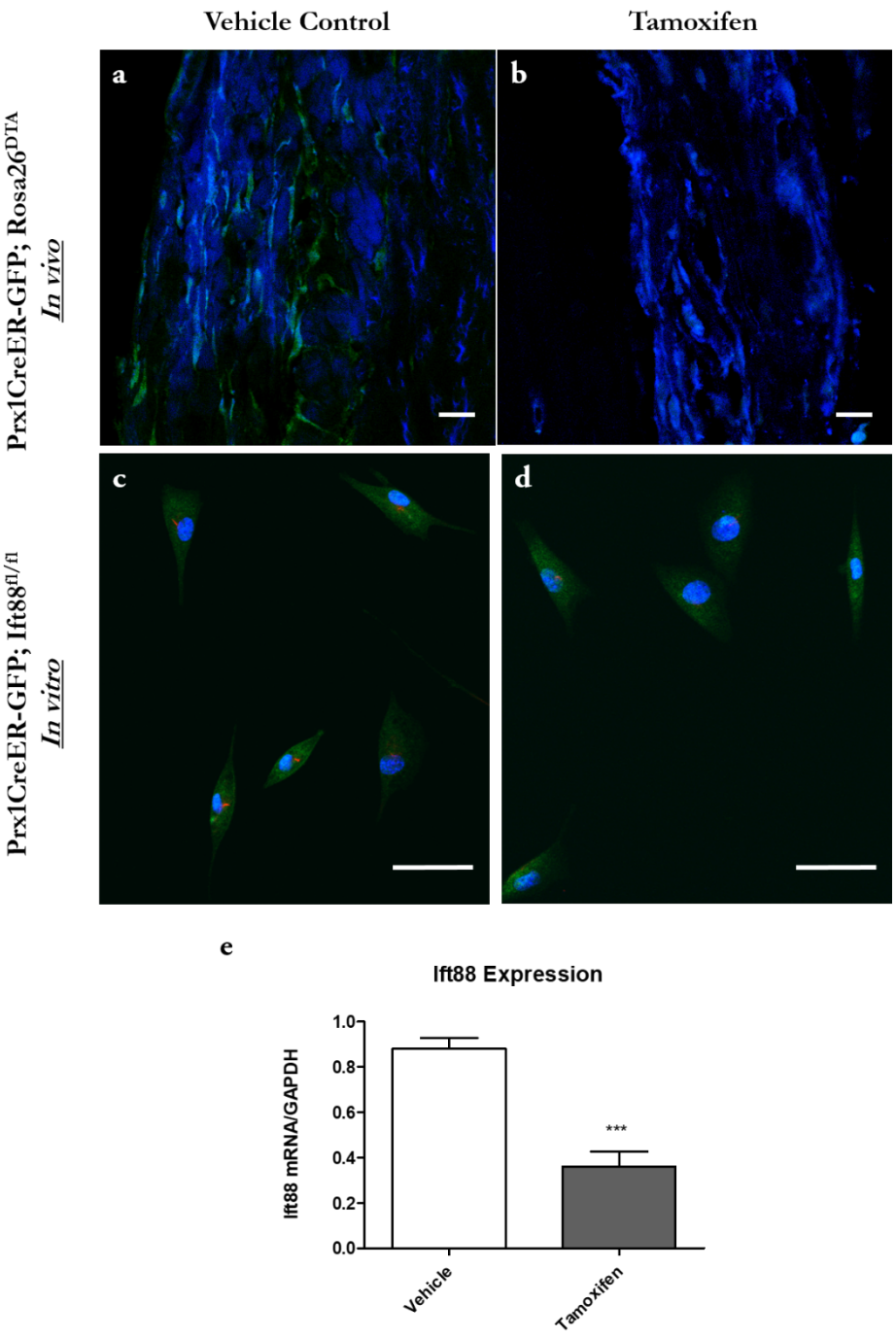

Figure 2.3: Tamoxifen successfully activates Cre recombination in our animal models *in vivo* and *in vitro*

Prx1-expressing cells (green) were observed in the periosteum of Prx1CreER-GFP; Rosa26^{DTA} animals not exposed to tamoxifen (a). Prx1CreER-GFP; Rosa26^{DTA} animals injected with 100 mg/kg tamoxifen (b) no longer contain these periosteal OCPs. Primary OCPs obtained from Prx1CreER-GFP; Ift88$^{fl/fl}$ animals (c) normally contain primary cilia (red); however, the presence and length of these cilia are diminished when exposed to 5 μM 4-hydroxytamoxifen (d). Indeed, cells treated with tamoxifen have decreased Ift88 mRNA expression (e). Micrographs of the periosteum and isolated cells were collected at 20X and 40X, respectively. Nuclei are displayed in blue. Scale bars indicate 50 μm. Data reported as mean and standard error. n = 4 for each group, ***$p < 0.0001$.

tamoxifen is introduced into animals *in vivo*. Cells treated with 4-hydroxytamoxifen (Figure 2.3d) demonstrated shorter and fewer cilia compared to vehicle controls (Figure 2.3c), confirming that this treatment successfully disrupted primary *in vitro*.

Table 2.1 Ulna cortical bone properties

	Female		Male	
Parameter	**Control**	**Prx1 Ablation**	**Control**	**Prx1 Ablation**
n	5	5	8	5
Bone Area (mm^2)	0.281 ± 0.012	0.263 ± 0.018	0.294 ± 0.005	0.295 ± 0.006
Cortical Thickness (mm)	0.172 ± 0.001	0.169 ± 0.004	0.169 ± 0.004	0.175 ± 0.002
BV/TV	0.867 ± 0.002	0.864 ± 0.003	0.863 ± 0.002	0.863 ± 0.001
BMD (mg HA/ ccm)	1293 ± 5.3	1289 ± 5.2	1282 ± 3.3	1288 ± 7.0
pMOI (mm^4)	0.024 ± 0.003	0.020 ± 0.003	0.027 ± 0.001	0.027 ± 0.001
I_{max} (mm^4)	0.019 ± 0.003	0.016 ± 0.003	0.022 ± 0.001	0.023 ± 0.001
I_{min} (mm^4)	0.0043 ± 0.0004	0.0040 ± 0.0005	0.0048 ± 0.0004	0.0040 ± 0.0002

Data are presented as the mean ± standard error

Mice lacking periosteal osteochondroprogenitors have severely attenuated load-induced bone formation

Genetic modifications may alter bone structure in transgenic animals, resulting in changes that influence the skeleton's response to load. To ensure that our ablation model did not alter bone properties, which would introduce a confounding variable in our compressive ulnar loading studies, we first assessed bone microstructure in our Prx1CreER-GFP; $Rosa26^{DTA}$ and

Rosa26^{DTA} animals using micro-computed tomography (μCT). We did not identify any differences in bone microstructure (Table 2.1); therefore, all of our loading experiment results are specifically due to periosteal OCP ablation.

H&E stains were then performed to visualize bone tissue in the loaded ulna of animals with and without periosteal OCPs (Figure 2.4). Interestingly, the periosteum was often thinner in the ablation model, perhaps due to loss of progenitors in the cambium layer. We initially noticed this trend when we observed GFP expression following ablation (Figure 2.3a,b) and noted that the periosteum was often thinner when GFP+ cells were absent. We also identified periosteal cells differentiating into osteoblasts to lay down new matrix in response to load (Figure 2.4c) but this behavior was lost entirely in the ablation animals.

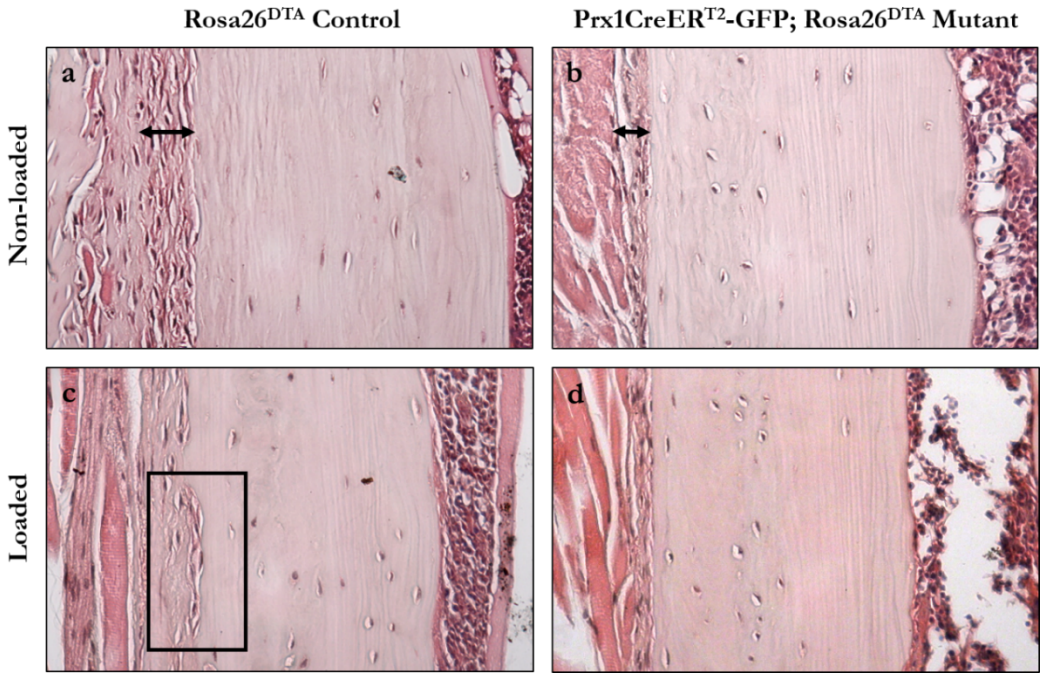

Figure 2.4: OCP ablation results in a thinner periosteum and a lack of load-induced osteoblast differentiation

Hematoxylin and eosin stains of tissue sections from control (a,c) and experimental animals (b,d). Loaded ulnae (c,d) were compared to non-loaded contralateral controls (a,b). Periosteum thickness is denoted with black arrows. The black box in (c) highlights periosteal cells differentiating into osteoblasts. Micrographs were collected at 20X magnification.

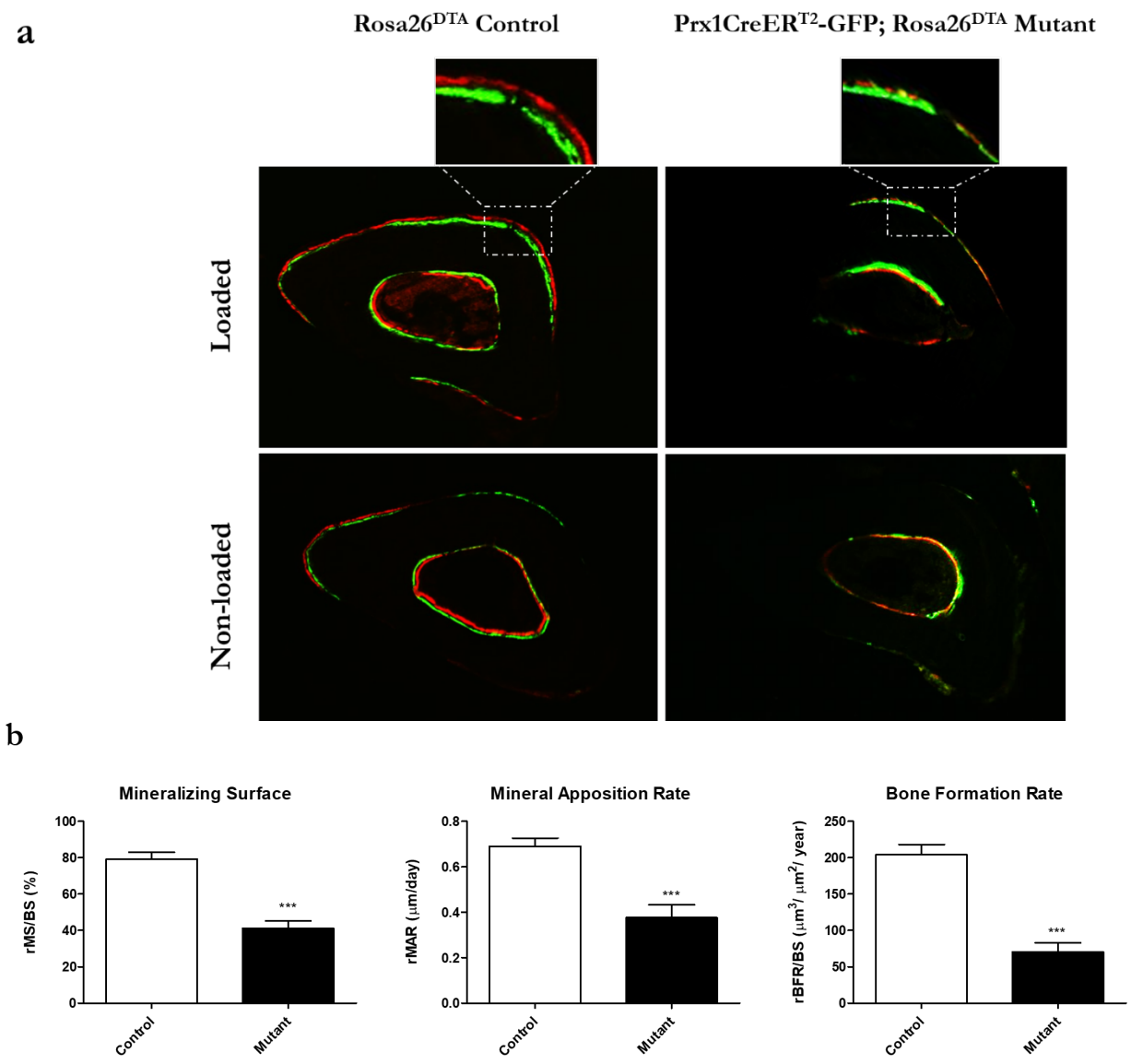

Figure 2.5: Mineralization and load-induced bone formation are severely attenuated in mice lacking OCPs

Dynamic histomorphometry of Rosa26^{DTA} control and Prx1CreER-GFP; Rosa26^{DTA} ablation animals. Mice lacking periosteal OCPs demonstrate poor mineralization, indicated by calcein (green) and alizarin (red) fluorochrome labels (a), and attenuated bone formation due to a limited mineralizing surface and mineral apposition rate (b). Loaded ulnae were normalized to non-loaded limbs. Data reported as mean and standard error. n = 16, ***$p < 0.0001$. Micrographs collected at 10X.

We visualized calcein and alizarin fluorochrome labels to assess mineralization with standard cage activity and in response to load. Control animals demonstrated some

mineralization in the non-loaded limb and, as expected, the mineralizing surface was greater in response to load (Figure 2.5a). We also observed a distinct gap between the alizarin and calcein labels in loaded control animals, indicating newly formed bone. In contrast, ablation animals demonstrated almost no mineralization under non-loaded conditions and a weak increase in response to load, suggesting very little bone was formed under static and loaded conditions. We quantified our observations via dynamic histomorphometry and, indeed, mutants lacking OCPs have severely attenuated bone formation rate (Figure 2.5b), making this the most severe disruption our lab has witnessed in our history of dynamic histomorphometry studies[37,48].

Periosteal OCPs respond to mechanical stimulation in a primary cilium-dependent manner

Although periosteal tissue[100] and calvaria periosteal osteoprogenitors[101] respond to physical stimulation, it is unknown whether osteochondroprogenitors in long bone periosteal tissue are mechanoresponsive. We therefore isolated cells from murine tibial periosteum and exposed them to oscillatory fluid flow (OFF) to determine if these cells respond to mechanical stimulation. Furthermore, we separated periosteal Prx1-expressing OCPs from the other cells of the periosteum to evaluate whether this population has a greater osteogenic response to physical stimuli. Indeed, both the sorted OCPs and other cells of the periosteum exposed to OFF exhibited increased Cyclooxygenase-2 (COX-2) mRNA production compared to static controls (Figure 2.6a), indicating an inflammatory response that signifies a cellular reaction to stimulation. Interestingly, only Prx1-expressing OCPs demonstrated a flow-induced increase in Osteopontin (OPN), a marker for osteogenesis (Figure 2.6b). In fact, Prx1-expressing OCPs had significantly higher levels of OPN than other cells of the periosteum under static conditions, suggesting this periosteal OCP population is inherently more osteogenic. Periosteal OCPs also exhibited

significantly greater fold changes in COX-2 and OPN expression compared to other cells of the periosteum (Figure 2.6c), indicating OCPs are more responsive to mechanical stimulation.

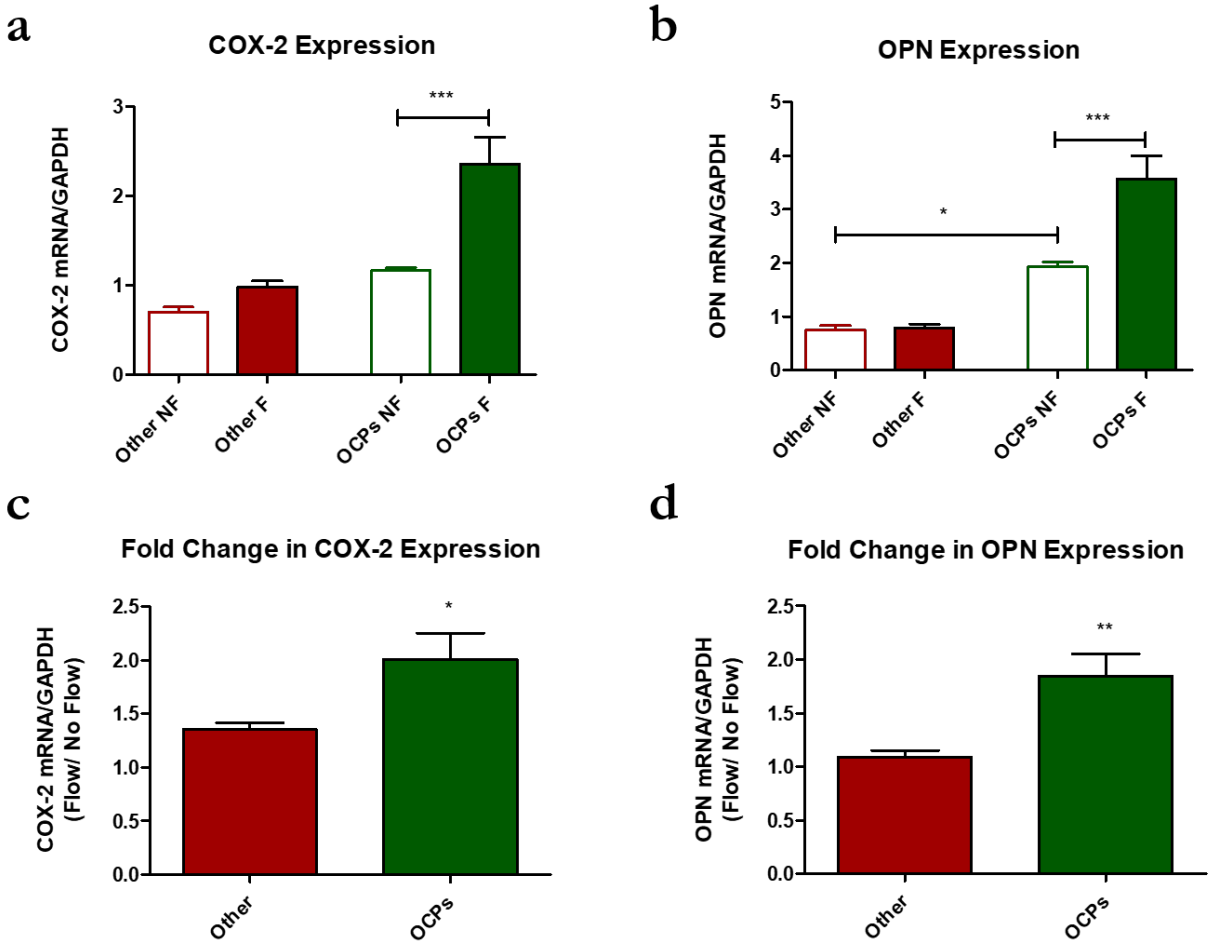

Figure 2.6 Periosteal OCPs uniquely respond to mechanical stimulation in an osteogenic manner

Periosteal cells isolated from 3-week-old Prx1CreER-GFP mice were exposed to 1 hour of oscillatory fluid flow (OFF) and changes in mRNA expression were quantified via RT-qPCR. Prx1-expressing osteochondroprogenitors (OCPs, green) demonstrated flow-induced increases in COX-2 (a) and OPN expression (b), whereas other cells of the periosteum (red) were nonresponsive. Additionally, the fold changes in COX-2 (c) and OPN (d) expression were significantly higher for OCPs compared to other cells of the periosteum. Data reported as mean and standard error. Other NF n = 5, Other F n = 7, OCPs NF and F n = 6, *$p < 0.01$, ***$p < 0.0001$.

We then examined whether this osteogenic response to flow was mediated by the primary cilium. Indeed, primary periosteal OCPs isolated from Prx1CreER-GFP; Ift88$^{fl/fl}$ animals that

were treated with tamoxifen had an abrogated response to OFF. Specifically, periosteal OCPs containing a tamoxifen-induced Ift88 knockout to disrupt primary cilia formation demonstrated significantly lower flow-induced increases in COX-2 and OPN expression compared to vehicle controls (Figure 2.7). This suggests that primary cilia are necessary for CLOPs to a) sense mechanical stimulation and b) respond to fluid shear in an osteogenic fashion.

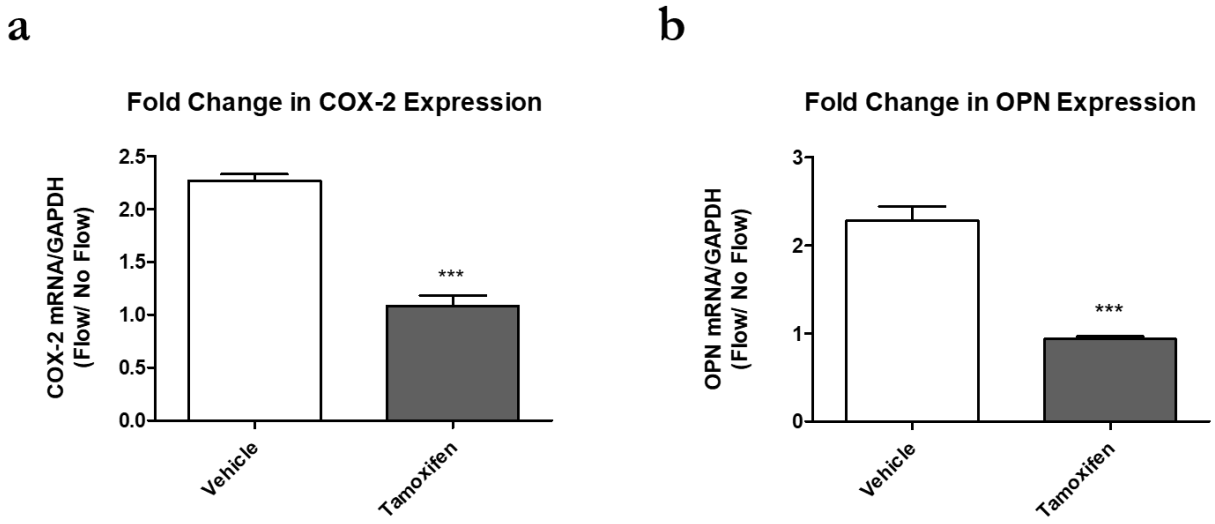

Figure 2.7 OCP primary cilia are necessary for the flow-induced osteogenic response
Periosteal OCPs isolated from 3-week-old Prx1CreER-GFP; Ift88$^{fl/fl}$ mice were exposed to 1 hour of oscillatory fluid flow (OFF) and changes in mRNA expression were quantified via RT-qPCR. Vehicle control OCPs (white bars) demonstrated flow-induced increases in the fold changes of COX-2 (a) and OPN expression (b). This effect was lost in OCPs treated with tamoxifen (gray bars) to disrupt primary cilia formation. Data reported as mean and standard error. Vehicle n = 6, Tamoxifen n = 5, ***$p < 0.0001$.

Discussion

Despite its ubiquity in embryonic development, Prx1 expression is restricted to a unique osteochondroprogenitor cell population in the adult forelimb. Prx1 expression is rampant in the mesenchymal limb bud and has been incompletely characterized after birth[53], so we utilized our Prx1CreER-GFP; Rosa26t^{dTomato} reporter to identify cells that express Prx1 in the forelimbs of

skeletally mature adults. The vast majority of labeled cells were found in the periosteum, with some present in the perichondrium and shoulder tendon. Furthermore, these cells were only present in the inner cambium layer of the periosteum, which is known to readily provide osteogenic precursors that participate in osteogenesis. The perichondrial expression may be unique to mice since their epiphyseal growth plates do not seal like those in other animals and humans. Due to physical distance alone, it is highly unlikely that cells from the perichondrium or shoulder tendon would contribute to bone formation in the midshaft of the diaphysis; thus, we are confident that our Prx1 model is an excellent tool for studying the role of periosteal OCPs in load-induced bone formation. Additionally, the presence of Prx1 in adults is an exciting finding because it indicates this OCP population remains active with age. Kawanami et al. previously determined that Prx1-expressing cells populate the fracture callus in response to trauma[53], but it was previously unknown whether this population existed under static physiological conditions. Progenitor activity and presence is often negatively correlated with increasing age, but these common drawbacks perhaps do not apply to the periosteal Prx1-expressing OCP population. Prx1-expressing cells isolated from the periosteum readily and specifically differentiate into osteoblasts and chondrocytes *in vitro* and therefore have been characterized as osteochondroprogenitors[53,54]. Thus, this Prx1 promoter can be used to study a unique adult periosteal OCP cell population.

Periosteal cells have long been thought to participate in load-induced bone formation, but our work is the first to demonstrate and quantify this contribution. Our dynamic histomorphometry reveals that Prx1-expressing OCPs in the periosteum not only contribute to bone formation, but they are perhaps the primary source of osteoblasts in load-induced adaptation. The complete ablation of Prx1-expressing periosteal OCPs is the most severe

disruption our lab has witnessed in the history of our dynamic histomorphometry work[37,48]. This is potentially because former disruptions were cilium-specific, but we initially had suspicions that ciliary disruptions could result in more severe attenuation. To clarify, cilium disruption affects only the cell's ability to sense mechanical stimulation, whereas ablation eliminates the entire cell. When the entire cell is absent, repopulation or compensation from other progenitor sources are possible[102,103], but these options are not available when cells lacking cilia persist. The nearly complete lack of mineralization in the non-loaded limbs suggests this progenitor source is required for daily skeletal maintenance, in addition to load-induced bone formation. The mineralization that does occur is likely due to bone lining cells, which are mature osteoblasts that line the periosteal surface and are a continuous source of osteoblasts in cortical bone[50,51]. Another possibility is that some OCPs remain due to incomplete Cre recombination, but we found that Prx1-expressing cells were totally ablated *in vivo* in our model (Figure 2.3b). With these observations, we now have a complete characterization of the Prx1-expressing cell population from embryonic development to adult adaptation. Specifically, Prx1-expressing progenitors contribute to the initial formation of the limbs[98], postnatal endochondral and intramembranous ossification to completely develop the skeleton (Chapter 1), static and load-induced adult periosteal bone formation, and fracture repair[53].

Periosteal progenitors have long been thought to be mechanosensitive, but this study demonstrates, for the first time, that periosteal Prx1-expressing OCPs directly sense loading. Periosteal cells are believed to differentiate into osteoblasts *in vivo* in response to physical stimulation. Indeed, *in vitro* studies demonstrate that primary periosteal cells readily differentiate into osteoblasts when conditioned media is applied[84]. We isolated the population of primary periosteal OCPs that was ablated in our ulnar loading studies and found that these cells not only

directly sense fluid shear, but upregulate mRNA expression of typical markers for osteogenesis. Interestingly, this osteogenic response to fluid shear is not present in other cells of the periosteum, suggesting this characteristic is unique to Prx1-expressing OCPs. Given that adult bone formation is severely attenuated when this mechanosensitive population is absent, we finally confirm a long-standing hypothesis that Prx1-expressing OCPs in the periosteum directly sense mechanical stimulation and differentiate into bone-forming osteoblasts during adult bone formation.

Furthermore, we speculate that the primary cilium is the mechanism by which these progenitors participate in adult bone formation. We previously identified that load-induced bone formation was attenuated in animals lacking Prx1-expressing cell primary cilia[167]. Although we identified that the rate of mineralization was attenuated in mutant animals, the periosteal OCP primary cilium's exact role during bone formation remains unclear. One possibility is that periosteal OCPs directly sense mechanical stimulation via their primary cilia and consequently differentiate into bone-forming osteoblasts. Indeed, we found that periosteal OCPs have an osteogenic response to physical stimulation that is abrogated when primary cilia are absent. We therefore propose that, during load-induced bone formation, periosteal OCP primary cilia directly sense loading and differentiate into osteoblasts that actively lay down new bone matrix.

Primary OCPs are easily extracted from periosteal tissue and grown up in culture, suggesting they are an attractive source for tissue regeneration strategies. A typical isolation was performed with 6 – 8 mice and periosteal tissue was extracted from only the ulnae and tibiae. Cells adhered to the dish surface within 3 – 5 days and continued to migrate from tissue for as long as 2 weeks after the dissection. Within 3 weeks of the initial dissection, approximately 8 million cells were available for sorting and, on average, only 3.3 ± 0.8% of those cells were

GFP+ Prx1-expressing OCPs. It is interesting that Prx1-expressing cells make up such a small percentage of the total cells in the periosteum, yet have such a drastic impact on adult bone formation and fracture repair. Despite the low percentage and some cell death due to sorting, these cells rapidly proliferate within 24 hours and we were able to generate enough cells for a typical fluid flow study (about 500k) in a matter of days. These cells continued to proliferate at the same rate and were passaged up to 10 times spanning 2 months after sorting. It is possible that the cells can be cultured for longer, but this was the maximum duration we tested due to available time and resources. The percentage of Prx1-expressing cells increased when given more time in culture before sorting, suggesting these cells proliferate at a higher rate than other cells of the periosteum. This extraction is faster or similar to the amount of time it takes to isolate primary mesenchymal stem cells (MSCs)[104] and proliferation rates are comparable. MSCs require further guidance *in vitro* to differentiate into osteoblasts, whereas periosteal OCPs are pre-programmed towards an osteoblastic or chondrogenic lineage and therefore require less culture time[53,54]. Further work must be done to compare human periosteal OCPs and MSCs to get a definitive answer, but our results suggest that the periosteum is a promising source for osteogenic precursors in tissue regeneration applications.

Collectively, our results motivate the use of periosteal Prx1-expressing OCPs and manipulation of their primary cilia for TERM applications. The field of Tissue Engineering and Regenerative Medicine involves using cells to restore damaged or unhealthy tissue, usually in combination with an engineered scaffold to deliver the cells to a region of interest. The current preferred method for bone regeneration is to seed MSCs that have been extracted and guided to an osteoblastic lineage *in vitro*[33]. However, periosteal progenitors are a promising candidate for bone tissue regeneration because they preferentially provide both osteoblasts and chondrocytes[95].

Our studies demonstrate that periosteal OCPs are still prevalent and active in skeletally mature adults and can therefore be useful when extracted in older patients. This finding is consistent with studies that suggest periosteal progenitors consistently proliferate and function independent of age[105–107]. More importantly, we identified that periosteal OCPs are not only inherently involved in normal and load-induced adult bone formation, but are by far the main contributors to these phenomena. Similarly, Colnot et al. demonstrated that periosteum-derived progenitors are the most prevalent cell source in the fracture callus[95]. This suggests periosteal OCPs have a surprising ability to proliferate and generate new bone *in vivo*, even though they represent a mere 3% of cells found in the periosteum. Additionally, OCPs are easier to extract and take less time to culture *in vitro* compared to MSCs. We also found that primary cilia are critical to the osteogenic nature of OCPs. These sensory organelles can be manipulated *in vitro* to enhance osteogenesis[42] and preliminary work in our lab suggests this work can be translated *in vivo*. Overall, periosteal OCPs are perhaps the optimal source for bone TERM strategies since they are easy to extract and culture, supply osteoblasts and chondrocytes for both forms of ossification, function independent of age, and contain primary cilia that can be tuned to enhance OCP-mediated osteogenesis.

Chapter 3: Osteochondroprogenitors populate the postnatal skeleton and require primary cilia to participate in ossification

Abstract

Although Prx1-expressing osteochondroprogenitor cells and their primary cilia are critical for embryonic development, they have yet to be studied in the context of postnatal skeletogenesis due to the lethality of previous mouse models. A tamoxifen-inducible Prx1 model has since become available and we determined that expression directed by this promoter is highly restricted to the cambium layers in the periosteum and perichondrium after birth. To determine the postnatal role of these cambium layer osteochondroprogenitors (CLOPs) and their primary cilia, we developed models to track the fate of CLOPs (Prx1CreER-GFP; $Rosa26^{tdTomato}$) and selectively disrupt their cilia (Prx1CreER-GFP; $Ift88^{fl/fl}$). Our tracking studies revealed that CLOPs populate cortical and trabecular bone, the growth plate, and secondary ossification centers during the normal program of postnatal skeletogenesis. Furthermore, animals that lack CLOP cilia exhibit stunted limb lengthening and thickening due to disruptions in endochondral and intramembranous ossification, respectively. Histological examination indicates ossification is stunted due to limited differentiation, proliferation, and/ or abnormal hypertrophic differentiation in the growth plate. Collectively, our results suggest that CLOPs are programmed to rapidly produce bone tissue *in vivo* in a primary cilium-mediated mechanism.

Introduction

Embryonic and juvenile skeletal development occurs via intramembranous and endochondral ossification to provide an important foundation for adult bone health. Embryos

undergo mesenchymal condensation to produce cartilaginous structures surrounded by a thin layer of fibrous tissue, known as the perichondrium. These skeletal templates eventually become mineralized bone via intramembranous and endochondral ossification. In the appendicular skeleton, the surrounding perichondrium provides precursors that form the bone collar, a cuff of spongy bone around the cartilaginous diaphysis, which supports and preserves the proper shape as the limbs develop. Blood vessels penetrate the bone collar, enabling perichondrial progenitors to form a primary ossification center in the diaphysis. After birth, secondary ossification centers appear in the epiphyses such that cartilaginous sections separate the secondary and primary ossification centers. These areas are known as the epiphyseal plates, or growth plates, and are responsible for postnatal lengthening of the limbs. The periosteum surrounds the diaphysis as it is converted into bone and provides osteoblasts that deposit appositional layers of bone via intramembranous ossification to thicken the postnatal skeleton.

The periosteum and perichondrium contain progenitors capable of differentiating into various cell types that populate skeletal tissues. A portion of cells in the inner cambium layers of the periosteum and perichondrium express Prx1, a homeobox protein whose expression is highly restricted in the postnatal skeleton[53]. These Prx1-expressing cells are deemed osteochondro-progenitors (OCPs) because they preferentially commit to a chondrogenic and/ or osteogenic fate[53,54]. Cells in the periosteum have long been known to possess osteogenic characteristics *in vitro*[53,84,108–110] and form cartilage and bone *in vivo*[49,95,111–113], but only recently have Prx1-expressing cells in the cambium layer been proposed as the periosteum's main source of OCPs[114].

Prx1-expressing cells are critical for embryonic skeletal development and survival, but have not yet been studied in the context of postnatal development. Prx1 is expressed throughout

the embryonic limb bud mesenchyme and a subset of the craniofacial mesenchyme as early as 9.5 days post coitum. By 10.5 dpc, essentially all of the mesenchymal cells in the limb express Prx[115 115]. Not surprisingly, these Prx1-expressing cells contribute to formation of the growth plate, the bone collar, and secondary ossification centers and, subsequently, impact endochondral ossification[47,116]. In fact, this cell population is so critical that Prx1 mutants do not survive birth[47,54,117]. Prx1-expressing cells have not been studied during postnatal development, when skeletal growth is most rapid[118–120], partially due to the embryonic lethality associated with current models. Recently, Kawanami et al. developed an inducible model and found that Prx1 expression is more restricted in the limbs after birth[53]. This group suggests Prx1 expression is primarily in the periosteum and perichondrium, but the full postnatal expression profile is incomplete.

Periosteal progenitors populate adult skeletal tissues in response to mechanical stimulation or fracture. Progenitor cells generally demonstrate upregulation in osteogenic markers when subjected to physical stimuli *in vitro*[39,40,88], so it is perhaps not surprising that cambium-derived cells generate bone in response to mechanical cues *in vivo*[33,95–97]. Fracture studies suggest periosteal progenitors significantly contribute to callus formation[114], and a considerable portion of these cells are derived from a Prx1-expressing population[53,54]. Interestingly, Colnot et al. determined that bone marrow and periosteum both supply osteoblasts to facilitate skeletal repair, but only the periosteum provides chondrocytes. Compared to marrow, the periosteum is therefore the primary contributor to post-fracture repair, which is dominated by endochondral ossification[95]. Collectively, these studies suggest the adult periosteum contains a Prx1-expressing population that continues to populate skeletal tissues due to its osteochondrogenic nature.

A mechanism by which osteochondroprogenitors may mediate differentiation is through their primary cilia, solitary sensory organelles that project from the cell membrane and are found in almost every mammalian cell. The cilium is an established mechanosensor and is known to be instrumental in progenitor osteochondrogenesis[39,121]. The primary cilium is also a potent chemosensor that directs left-right patterning and functions as a nexus for signaling pathways during embryonic vertebrate development[122,123]. Haycraft et al. disrupted primary cilia in Prx1-expressing cells and observed severe defects in embryonic development of the appendicular skeleton, including dwarfism, polydactyly, an inability to form the bone collar or secondary ossification centers, and abnormal growth plate structure. This knockout was so severe that mutants did not survive birth due to malformed ribcages[98] and, consequently, the role of Prx1-expressing cell primary cilia is yet to be examined after birth. However, it is likely that these cells and their cilia are also critical for postnatal development, given the extent to which they contribute to embryonic skeletogenesis and adult bone formation.

Progenitors in the cambium layers and their cilia are promising candidates for intramembranous and endochondral ossification, but are surprisingly understudied. The postnatal appendicular skeleton thickens via intramembranous ossification, whereby osteoblasts are directly recruited from the periosteum to lay down appositional layers of new bone. Additionally, in endochondral ossification, chondrocytes of undetermined origin populate the growth plate, proliferate, and undergo hypertrophy to lengthen the limbs. Yang et al. proposed a model whereby periosteal and perichondrial progenitors differentiate into growth plate chondrocytes, some of which further differentiate into osteoblasts, but studies have yet to confirm whether these progenitors are indeed a source of chondrocyte and osteoblast progeny[124]. Furthermore, there are no current studies on periosteal or perichondrial primary cilia in postnatal development.

Rosa Serra's group has extensively studied the role of chondrocyte cilia in the growth plate and found that deletion of a key ciliary gene, *Ift88*, results in decreased proliferation and accelerated chondrocyte hypertrophy, due to disruption of many cilium-mediated signaling pathways[82,125]. They also determined cilia orientation is critical to chondrocyte proliferation, consistent with work from other groups that suggest a function for cilia polarity[47,126–129]. In an *in vivo* overloading model, Rais et al. determined that chondrocyte cilia sense mechanical loading of the growth plate and accelerate chondrocyte hypertrophy in response to increased loads[130]. In fact, chondrogenesis is highly dependent on chondrocyte mechanosensing, which is mediated through the cilium[121,131]. Overall, it is possible that Prx1-expressing cells reside in the cambium layers and contribute to postnatal ossification through a cilium-dependent mechanism, but this is yet to be confirmed due to the lack of an *in vivo* model.

Due to the osteochondrogenic nature of Prx1-expressing cells and extent to which chondrocyte cilia regulate endochondral ossification, we seek to determine the role of cambium-derived progenitors in postnatal skeletogenesis as mediated by their primary cilia *in vivo*. We developed a model that allows us to disrupt primary cilia to test our hypothesis that cambium-layer OCPs require cilia to participate in postnatal skeletogenesis. Additionally, we developed a mouse model to track Prx1-expressing cells as they differentiate and become incorporated in new juvenile skeletal tissues *in vivo*. We anticipate that the knowledge gained from studying postnatal development will provide insights on how to recapitulate skeletogenesis *in vivo* and more effectively utilize cambium-derived progenitors for bone regeneration therapies.

Materials and Methods

Animal models

All mouse models are on a C57BL6 background. Prx1CreER-GFP mice were bred with Kif3a$^{fl/fl}$, Ift88$^{fl/fl}$, or Rosa26^{tdTomato} mice to generate Prx1CreER-GFP; Kif3a$^{fl/fl}$, Prx1CreER-GFP; Ift88$^{fl/fl}$, and Prx1CreER-GFP; Rosa26^{tdTomato} offspring, respectively. Kif3a$^{fl/fl}$ and Ift88$^{fl/fl}$ females were bred with Prx1CreER-GFP; Kif3a$^{fl/fl}$ and Prx1CreER-GFP; Ift88$^{fl/fl}$ males to generate Prx1CreER-GFP; Kif3a$^{fl/fl}$ and Prx1CreER-GFP; Ift88$^{fl/fl}$ experimental pups and Kif3a$^{fl/fl}$ and Ift88$^{fl/fl}$ littermate controls that received tamoxifen injections (Figure 3.1). To avoid embryonic recombination, mothers were isolated for one month after any potential exposure to tamoxifen before breeding again. We also intentionally selected controls so all mice receive tamoxifen since there are reports of cross contamination between animals housed together or that use the same experimental equipment. Genotype was determined using PCR and agarose gel electrophoresis. Animals were housed, maintained, and evaluated for health complications in accordance with IACUC standards. The Institute of Comparative Medicine at Columbia University approved all experiments.

Tamoxifen injections

Tamoxifen (Sigma Aldrich, T5648) was dissolved in corn oil (Sigma Aldrich, C8267) in a shaking incubator at 37°C to create a 20 mg/mL stock solution stored at 4°C and protected from light. Injection solution was prepared fresh daily by diluting the stock solution to 10 mg/mL and adding 10% ethanol to prevent infection. Prx1CreER-GFP; Kif3a$^{fl/fl}$ and Prx1CreER-GFP; Ift88$^{fl/fl}$ experimental pups and Kif3a$^{fl/fl}$ and Ift88$^{fl/fl}$ littermate controls received daily intraperitoneal injections of 33 mg/kg tamoxifen solution until sacrifice. Prx1CreER-GFP;

Rosa26^{tdTomato} pups either received a single dose of 100 mg/kg or daily injections of 33 mg/kg tamoxifen solution until sacrifice. Pups were injected as early as postnatal day 7 (P7) depending on the group to which they were randomly assigned (Figure 3.1). Prx1CreER-GFP; Kif3a$^{fl/fl}$ and Kif3a$^{fl/fl}$ pups were injected daily with 33 mg/kg tamoxifen solution from P7 – P30 since they were solely used to initially assess the safety of our injection protocol. The injection site was swabbed with 70% ethanol and animals were weighed with an electronic scale immediately prior to each injection.

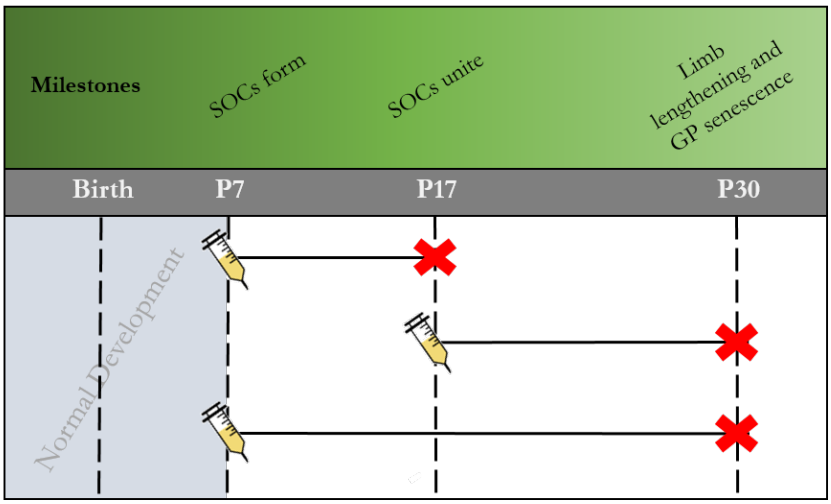

Figure 3.1: Experimental groups selected to evaluate juvenile skeletal development
Following normal embryonic development, postnatal transgenic mice received injections of tamoxifen to induce Cre recombination-mediated tdTomato expression or primary cilia deletion exclusively in CLOPs. The earliest injections were administered at postnatal day 7 (P7) in order to allow secondary ossification centers (SOCs) in the ulnae to develop normally[132]. SOCs in the ulnae generally unite by P17 and our preliminary injection trials suggested P30 was optimal to observe significant increases in limb length and growth plate (GP) senescence. The group injected at P7 and sacrificed (red X) at P17 serves to evaluate the role of CLOPs and their cilia in SOC unification, while the P17 – P30 group functions to determine their behavior if SOCs are already united. The P7 – P30 group was selected to observe the overall contribution of CLOPs and their cilia to juvenile skeletal development. Animals received a single or daily injections until sacrifice depending on the experiment.

Histology

Upon sacrifice, ulnae were dissected and fixed overnight at 4°C. Prx1CreER-GFP; Ift88$^{fl/fl}$ and control specimens were fixed in 10% formalin (Sigma Aldrich, HT5011),

decalcified, embedded in paraffin, and sectioned in 5 μm increments. Prx1CreER-GFP; Rosa26^{tdTomato} ulnae were fixed in 4% paraformaldehyde (Sigma Aldrich, P6148), decalcified, and cryosectioned in 5 μm increments. Prior to decalcification, the midpoint along the length of each ulna was measured and marked with tissue stain to ensure transverse sections were collected at the same region.

Staining and immunohistochemistry

Cryosections were placed in distilled water upon removal from the freezer, incubated in mounting media containing a nuclear stain (Electron Microscopy Sciences) for 5 minutes, washed with PBS, mounted, and sealed. Paraffin embedded specimens were deparaffinized and rehydrated in a tissue processor (Leica ASP300S). Toluidine solution was prepared by diluting 0.05% w/v Toluidine Blue-O (Sigma Aldrich, T3260) in 100 mM sodium acetate buffer, pH 6. Slides were submerged in Hematoxylin solution (Sigma Aldrich, MHS1) for 10 minutes followed by 30 seconds in Eosin solution (Sigma Aldrich, HT110216), or submerged in Toluidine solution for 10 minutes. To identify proliferating cells in the growth plate, slides were incubated in 2 mg/mL hyaluronidase (Sigma Aldrich, H3884) for 1 hour at 37°C, blocked with 15% goat serum (abcam, ab7481) for 20 minutes at room temperature, and incubated in a PCNA primary (abcam, ab29) 1:10,000 in 15% goat serum for 1 hour at 37°C, followed by overnight incubation at 4°C. To detect hypertrophic cells in the growth plate, slides were incubated in 2 mg/mL hyaluronidase for 1 hour at 37°C, blocked with 15% goat serum and 0.3% Triton-X 100 (Sigma Aldrich, T9284) in PBS, and incubated in a Type X Collagen primary antibody (abcam, ab58632) 1:250 in 3% goat serum and 0.3% Triton-X 100 overnight at 4°C. Both PCNA and Type X slides were incubated in a fluorescent secondary antibody, Alexa Fluor 488 (Life Technologies, A11029 and ab150077) 1:500 in PBS, for 1 hour at room temperature. All slides

were washed with PBS then distilled water, mounted, and sealed. Toluidine and H&E stains were visualized on an Olympus CKX41 inverted microscope and micrographs were captured with a Canon EOS60D 18.0 MP digital SLR camera. All fluorescent images were collected using an Olympus Fluoview FV1000 confocal microscope and software.

Quantifying length, area, and cell count

Ulnar length and area were quantified from H&E images using Image J software. Proliferating cells were counted and normalized to growth plate area from PCNA IHC slides using Image J. At least four consecutive sections per specimen were analyzed and averaged when assessing differences in phenotype and quantifying ulnar length, cortical or marrow area, and number of proliferating cells. Investigators were blinded to the groups during the experiment, specimen generation, image acquisition, and post-imaging analysis steps. Quantifications were performed by two separate investigators to assess repeatability and ensure accuracy of reported results.

Statistics

No sex-dependent differences were identified according to a 2-way ANOVA so males and females were grouped together for all experiments. All data were analyzed with a two-tailed student's t-test and values are reported as mean ±SEM, with $p < 0.05$ considered statistically significant. Sample size was determined in order to achieve a power of at least 80%.

Results

Successful generation of mouse models

PCR and gel electrophoresis confirmed that we generated Prx1CreER-GFP; Ift88$^{fl/fl}$ and Ift88$^{fl/fl}$ littermates, as well as Prx1CreER-GFP; Rosa26^{tdTomato} reporter mice (Figure 3.2). We utilized the same procedure to confirm genotypes in our previously established Prx1CreER-GFP; Kif3a$^{fl/fl}$ and Kif3a$^{fl/fl}$ colonies (data not shown).

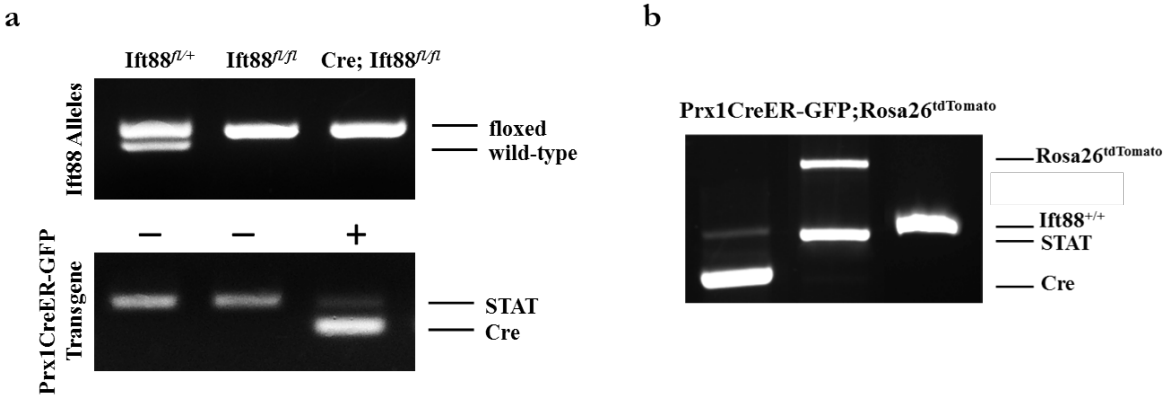

Figure 3.2: Prx1-driven cilia knockout and fluorescent reporter models were generated
Gel electrophoresis confirmed Prx1CreER-GFP animals were successfully crossed with (a) Ift88$^{fl/fl}$ mice to generate a conditional cilium knockout (Prx1CreER-GFP; Ift88$^{fl/fl}$) and (b) Rosa26^{tdTomato} animals to produce a Prx1CreER-GFP; Rosa26^{tdTomato} fluorescent reporter model.

Creation of tamoxifen injection protocol

Since there are no published reports of long-term tamoxifen injections in young pups, we sought to determine a safe, yet effective dosing regimen to induce genetic recombination without compromising animal health. Due to off-target effects of Kif3a, deletion of Ift88 has since been shown to be a more appropriate tool for specifically disrupting the primary cilium[68]. During the process of generating Prx1CreER-GFP; Ift88$^{fl/fl}$ animals, we tested our injection protocol on our available Prx1CreER-GFP; Kif3a$^{fl/fl}$ stock. We administered 33 mg/kg tamoxifen via intraperitoneal injection each day from P7 – P30 based on a published week-long regimen in P0 – P10 pups[133]. At P30, Prx1CreER-GFP; Kif3a$^{fl/fl}$ experimental animals did not exhibit

noticeable changes in ambulation, diet, weight, or cage activity compared to Kif3a$^{fl/fl}$ controls as a result of the injections. Injected animals consistently weighed less than non-injected controls from P10 – P15, but all animals were a similar weight by P20. One study reports that a single injection of tamoxifen killed over 90% of gastric cells in normal mice 3 days after administration, but gastric histology eventually returned to normal[134]. This timeline is similar to the phenomena we observed and explains the temporary weight loss. This protocol produced identical results in our Prx1CreER-GFP; Ift88$^{fl/fl}$ animals.

Prx1 expression is restricted to the cambium layers in the appendicular skeleton after birth

The vast majority of limb bud mesenchymal cells express Prx1 during embryonic development; however, recent studies indicate Prx1 expression is highly restricted to the calvaria and specific regions of the appendicular skeleton after birth[53,54]. In order to fully characterize postnatal Prx1 expression in the forelimbs at our chosen experimental time points (Figure 3.1), we injected Prx1CreER-GFP; Rosa26^{tdTomato} pups with a single dose of 100 mg/kg tamoxifen at P7, P17, or P28. Pups were sacrificed two days following injection and we visualized GFP to identify cells that currently express Prx1, as well as tdTomato—which denotes CreER recombination—to track cells that expressed Prx1 at the time of injection. At every time point, Prx1 expression was observed in the cambium layers of the perichondrium (Figure 3.3a) and periosteum (Figure 3.3b). In mice injected at P7, Prx1-expressing cells were found in the ulnar growth plate near the Groove of Ranvier, where progenitors are believed to be rapidly recruited to supply chondrocytes to the growth plate[135]. Very few Prx1-expressing cells were identified in the Groove of Ranvier in mice injected at P17 and P30 juvenile growth plates had none. In the four P30 specimens, a total of three osteocytes located near the periosteal edge expressed Prx1. All Prx1-expressing cells found in the growth plate and cortical bone also expressed tdTomato

(Figure 3.3a), indicating Cre recombination had occurred. At every time point examined, cells that solely expressed tdTomato were found in the periosteum, perichondrium, cortical bone, and both the resting zone and Groove of Ranvier in the growth plate. Cre recombination was absent from all other tissues, other than a negligible number of cells in the epiphyseal growth plate in one P7 specimen.

Overall, Prx1 expression was highly restricted to the cambium layers of the periosteum and perichondrium, had a trivial presence in the growth plate and cortical bone, and was completely absent from epiphyseal centers, trabecular bone, marrow, muscle, connective tissue, and cartilage in the juvenile forelimbs. For this reason, we refer to the cell population examined in this study as **C**ambium **L**ayer **O**steochondro**P**rogenitors, or CLOPs.

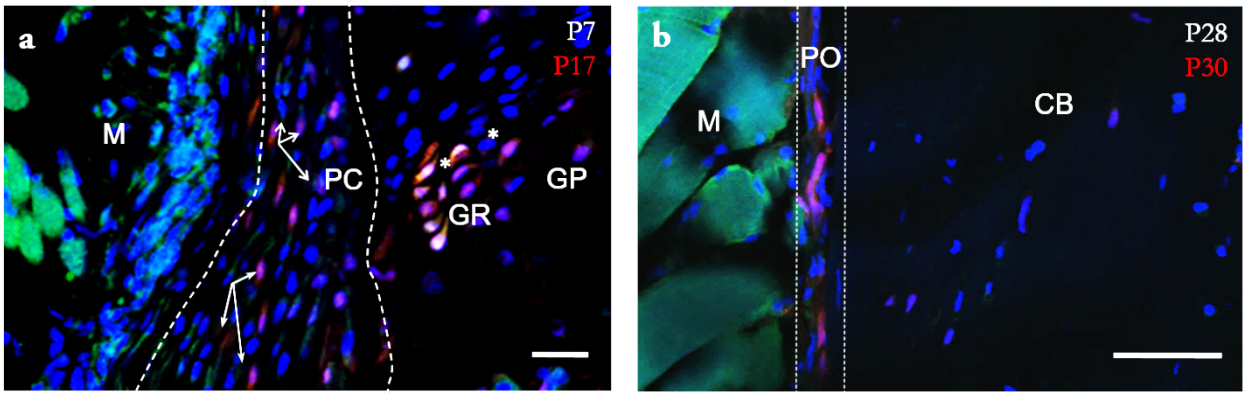

Figure 3.3: Prx1 expression is highly restricted to the cambium layers of the periosteum and perichondrium in the forelimbs after birth
Cells currently expressing Prx1 (green), cells that expressed Prx1 at the time of injection two days prior (red), and nuclei (blue) in a Prx1CreER-GFP; Rosa26^{tdTomato} reporter model. Cells expressing Prx1 at P7 (closed arrows) were identified in the perichondrium (PC), periosteum (PO), Groove of Ranvier (GR) in the growth plate (GP), and cortical bone (CB) at P9 (a). All Prx1-expressing cells located outside the cambium layers also expressed tdTomato (a, asterisks). Cells that underwent Cre recombination (open arrows) were observed in the perichondrium and growth plate. At P30, Prx1-expressing cells were found in the periosteum, which also contained more recombined cells than the earlier time points (b). Soft tissues, such as muscle (M), and bone marrow exhibited autofluorescence but lacked tdTomato-expressing cells or GFP signal that would indicate Prx1 expression. Injection period (white) and day of sacrifice (red) are noted in the upper right corner of each image. Scale bars represent 50 μm.

Progenitors initially in the cambium layers populate a number of juvenile skeletal tissues

We then utilized our reporter model to histologically track the fate of CLOPs as they differentiate and populate tissues outside the cambium layers. Prx1CreER-GFP; Rosa26td^{Tomato} mice received a single tamoxifen injection at either P7 or P17 to activate tdTomato expression in CLOPs and their progeny until sacrifice at P17 or P30. CLOPs residing in the cambium layers at P7 were found in the growth plate, proximal ulnar head, styloid processes, trabecular and cortical bone, and the endocortical surface at P17 and P30 (Figure 3.4). CLOPs initially in the cambium layers at P17 populated the same areas at P30 but were fewer in number compared to those tracked at P7. P7 activated cells were absent from the cambium layers by P17 (Figure 3.4c), but P17 activated cells were still present in the periosteum and perichondrium at P30 (Figure 3.4d). In the growth plate, both P7 and P17 activated cells were primarily found in the resting zone or trabecular bone beneath the growth plate, suggesting CLOPs rapidly proliferate and undergo hypertrophy to form ossified bone. We then injected Prx1CreER-GFP; Rosa26^{tdTomato} mice daily to determine the overall CLOP contribution to skeletal development from P7 – P30 (Figure 3.4e). Indeed, CLOPs make up a significant portion of cells in the aforementioned regions. In fact, the majority of osteocytes and osteoblasts in cortical and trabecular bone, respectively, originated from the cambium layers, and the styloid and coronoid processes were almost entirely composed of CLOPs. In the growth plate, CLOPs were found in the proliferation and hypertrophic zones in addition to the resting zone, indicating these progenitor cells participate in the normal program of endochondral ossification. Overall, the CLOP presence in ossified and cartilaginous tissues further confirms their osteochondrogenic nature[53,54], and the extent to which their progeny participate in skeletogenesis implies they serve an important role in juvenile development.

Mice lacking CLOP primary cilia have stunted intramembranous ossification

The primary cilium is critical to osteogenic differentiation of progenitors[39,40] so we investigated the role of CLOP cilia in juvenile skeletogenesis. Progenitors in the inner cambium layer of the periosteum are known to differentiate into bone-forming osteoblasts that deposit appositional layers of bone matrix to thicken the limbs. To determine whether CLOP primary

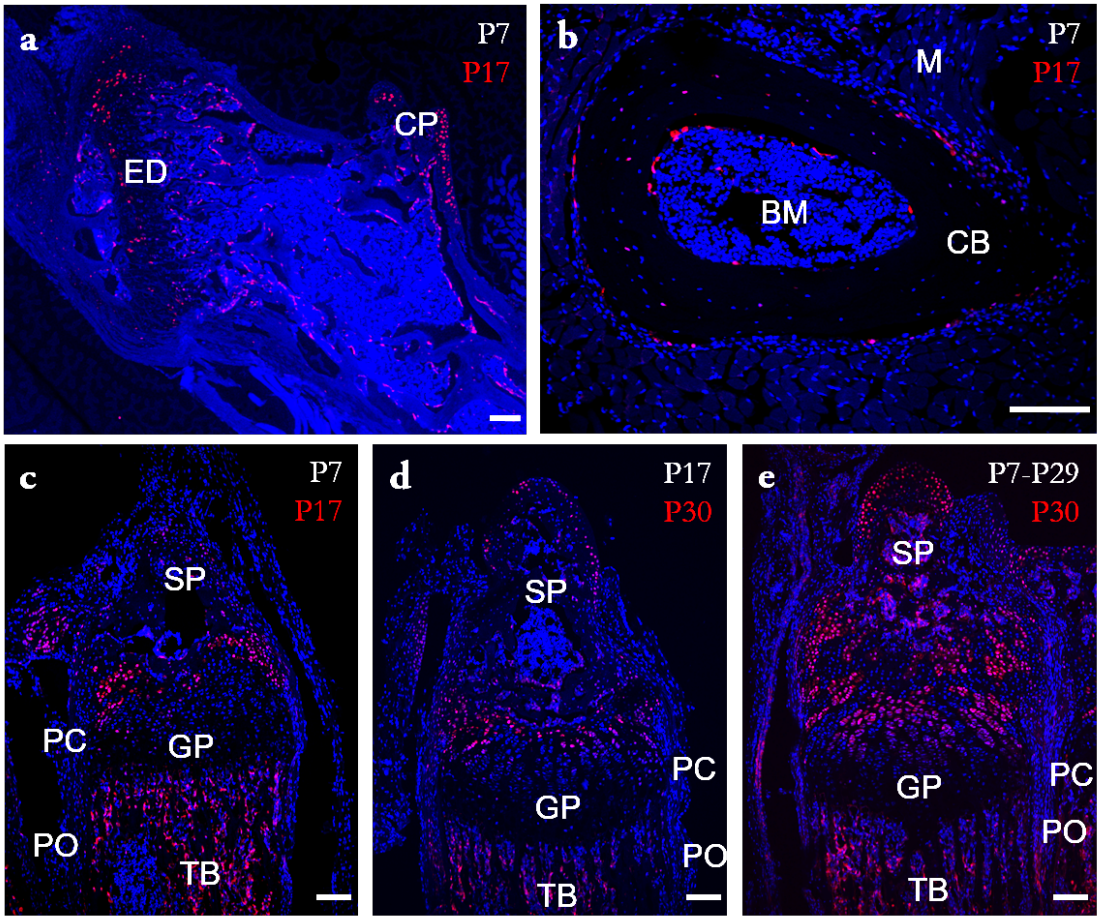

Figure 3.4: CLOPs initially in the cambium layers populate cartilage and bone tissue throughout the limb

At P30, CLOPs initially residing in the periosteum and perichondrium at P7 and their progeny (red) were found in the epiphyseal disk (ED) and coronoid process (CP) in the proximal head of the ulna (a) and cortical bone (CB), but absent from bone marrow (BM), and muscle (M) (b). These progenitors were also observed in the ulnar growth plate (GP), styloid process (SP), and trabecular bone (TB). At P17, these progenitors were found in the GP, SP, and TB, but absent from the periosteum (PO) and perichondrium (PC) (c). CLOPs initially in the cambium layers at P17 populated the PO, PC, GP, SP, and TB (d). CLOPs in the cambium layers from P7 until sacrifice at P30 and their progeny were found in the GP, SP, TB, PO, and PC (e). Nuclei are displayed in blue. Injection period (white) and day of sacrifice (red) are noted in the upper right corner of each image. White scale bars represent 100 μm.

cilia mediate this mechanism of intramembranous ossification, Prx1CreER-GFP; Ift88$^{fl/fl}$ pups were injected daily with tamoxifen to eliminate production of a protein critical to cilia formation and maintenance (IFT88) in order to disrupt CLOP primary cilia. We quantified cortical area and found that mutants developed significantly less cortical bone than their respective controls in all of the injection groups (Figure 3.5a). Surprisingly, knockouts initiated at P7 also had wider marrow canals (Figure 3.5b). This effect was not seen in knockouts initiated at P17, suggesting that progenitor disruption has a greater impact in the earlier stages of juvenile skeletogenesis.

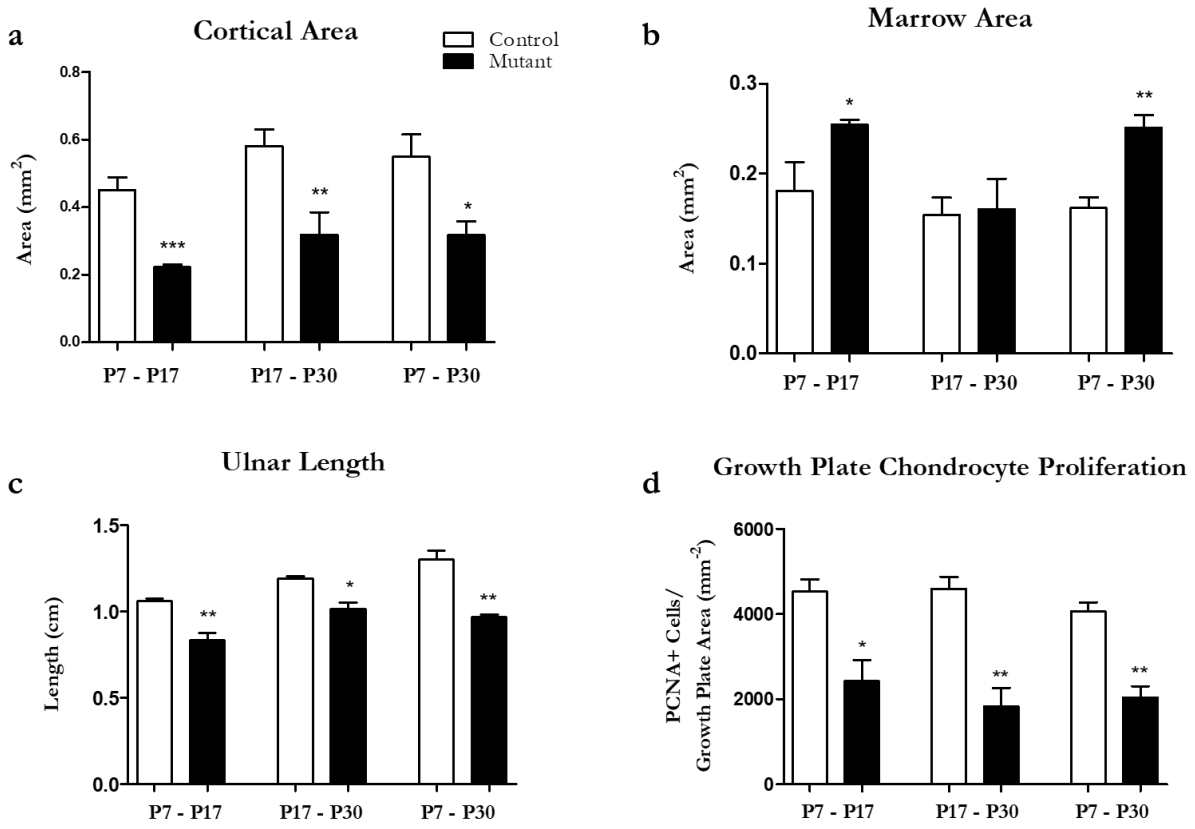

Figure 3.5: Mice lacking CLOP primary cilia exhibit stunted limb development and growth plate chondrocyte proliferation

Juvenile transgenic mice lacking primary cilia (Prx1CreER-GFP; Ift88$^{fl/fl}$) developed less cortical bone compared to controls (Ift88$^{fl/fl}$) at all developmental stages examined (a). Additionally, the cortical marrow lumen area was greater in knockouts initiated at P7 (b). This phenotype was absent in the P17 – P30 mutants, which had similar areas compared to controls. Mutants also had attenuated limb lengthening (c) and significantly fewer proliferating growth plate chondrocytes (d). n = 5 per group, * $p < 0.05$, ** $p < 0.01$, *** $p < 0.001$.

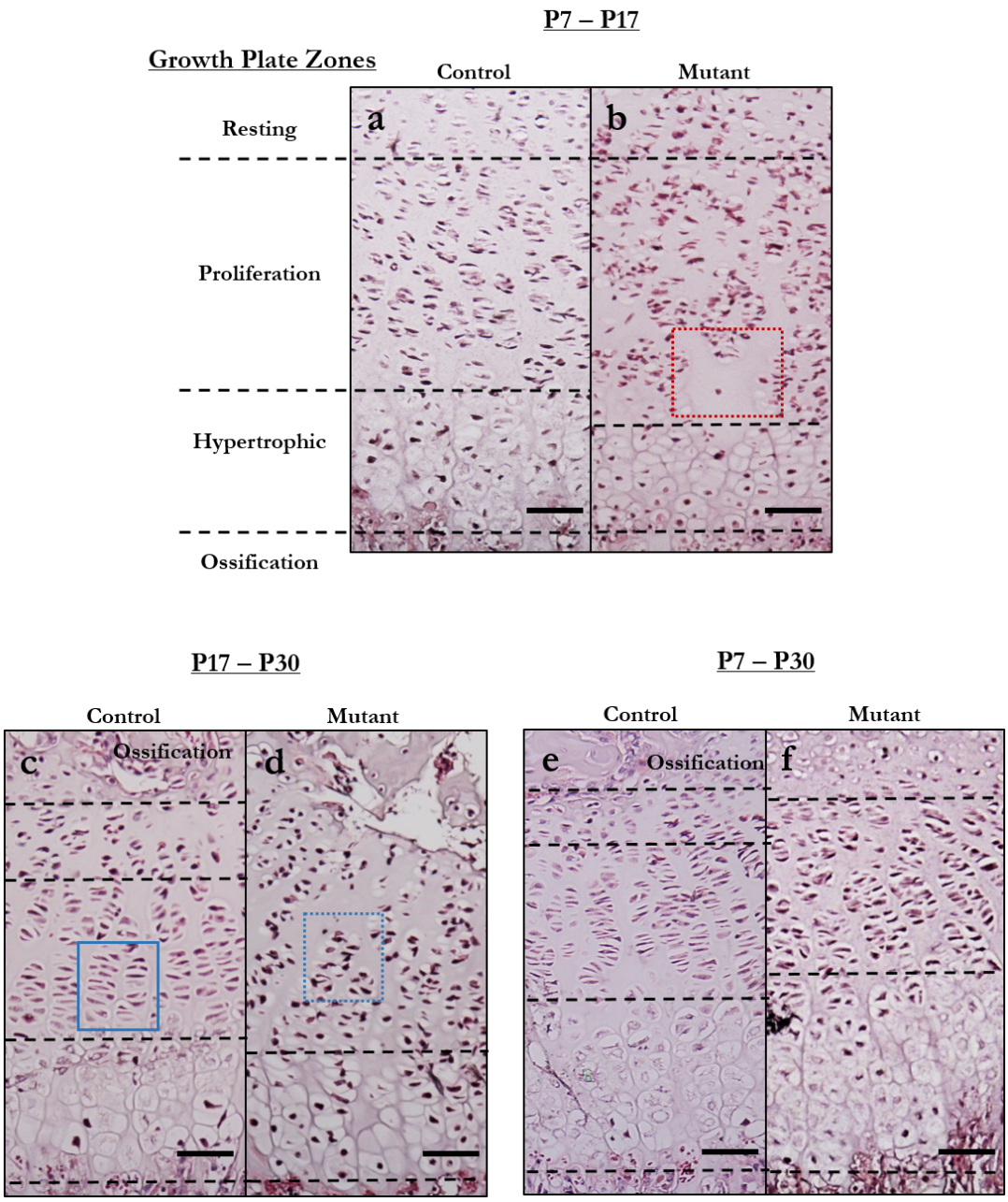

Figure 3.6: Juveniles lacking CLOP cilia demonstrate abnormal growth plate morphology
H&E stains were performed to discern ulnar growth plate zones (black dashed lines). The proliferating zones in P7 – P17 mutants contained noticeable cartilaginous sections lacking cells (b, red dashed box). These non-cellularized regions were not present in controls (a), which were densely populated with cells. Chondrocytes in the P17 – P30 control proliferation zones were neatly arranged in vertical columns (c, solid blue box); however, this structure was much less organized or completely absent in mutants (d, blue dashed box). The lack of columnar organization and flatter morphology normally associated with proliferating cells also made it difficult to distinguish the resting and proliferation zones in P17 – P30 mutants (d). Ossified bone normally present in the styloid processes above the growth plate (c, e) was lacking in P17 – P30 (d) and P7 – P30 (f) mutant growth plates. Although the growth plate zones were distinguishable in the P7 – P30 group, mutants appeared to have larger hypertrophic zones compared to controls (e, f). Black scale bars represent 50 µm.

Endochondral ossification is attenuated in mutants

Embryos lacking primary cilia in Prx1-expressing cells have severely shortened limbs[47] so we also examined ulnar length in juveniles with and without CLOP cilia. At each time point, mutants had significantly shorter ulnae compared to their respective controls (Figure 3.5c). In fact, mutants assessed at P30 had shorter ulnae than P17 controls. Mutants disrupted beginning at P7 had shorter average lengths at P30 compared to those injected at P17.

Because limb lengthening occurs via endochondral ossification, which depends on proper growth plate chondrocyte differentiation and proliferation, we investigated differences in growth plate morphology. At all stages, mutants demonstrated abnormal phenotypes but the characteristics and severity varied. Growth plate zones (Figure 3.6, black dashed lines) can be roughly determined by observing cell morphology. Chondrocytes in the resting zone are round with spherical nuclei but eventually flatten and align in vertical columns to rapidly proliferate, until they finally expand into cuboidal hypertrophic cells. P7 – P17 knockouts contained noticeable patches in the proliferation zone that lacked chondrocytes (Figure 3.6b, red dashed box), suggesting fewer cells populated the growth plate (Figure 3.6b). The boundary between the resting and proliferation zones was less distinct in P7 – P17 and P17 – P30 mutants. Columnar stacking was prevalent in P17 – P30 controls (Figure 3.6c, blue solid box); however, this behavior was almost entirely lost in mutants (Figure 3.6bd, blue dashed box). The hypertrophic zone in P7 – P30 mutants appeared to be much larger than controls (Figure 3.6e,f). Finally, controls evaluated at P30 exhibited ossification in the styloid processes (Figure 3.6c,e), which is correlated with growth plate senescence; however, this phenomenon was drastically less pronounced in mutants (Figure 3.6d,f). Overall, the phenotypic variation with timing of

disruption suggests the predominant role of CLOP primary cilia, or CLOPs themselves, may change with each successive stage of juvenile development.

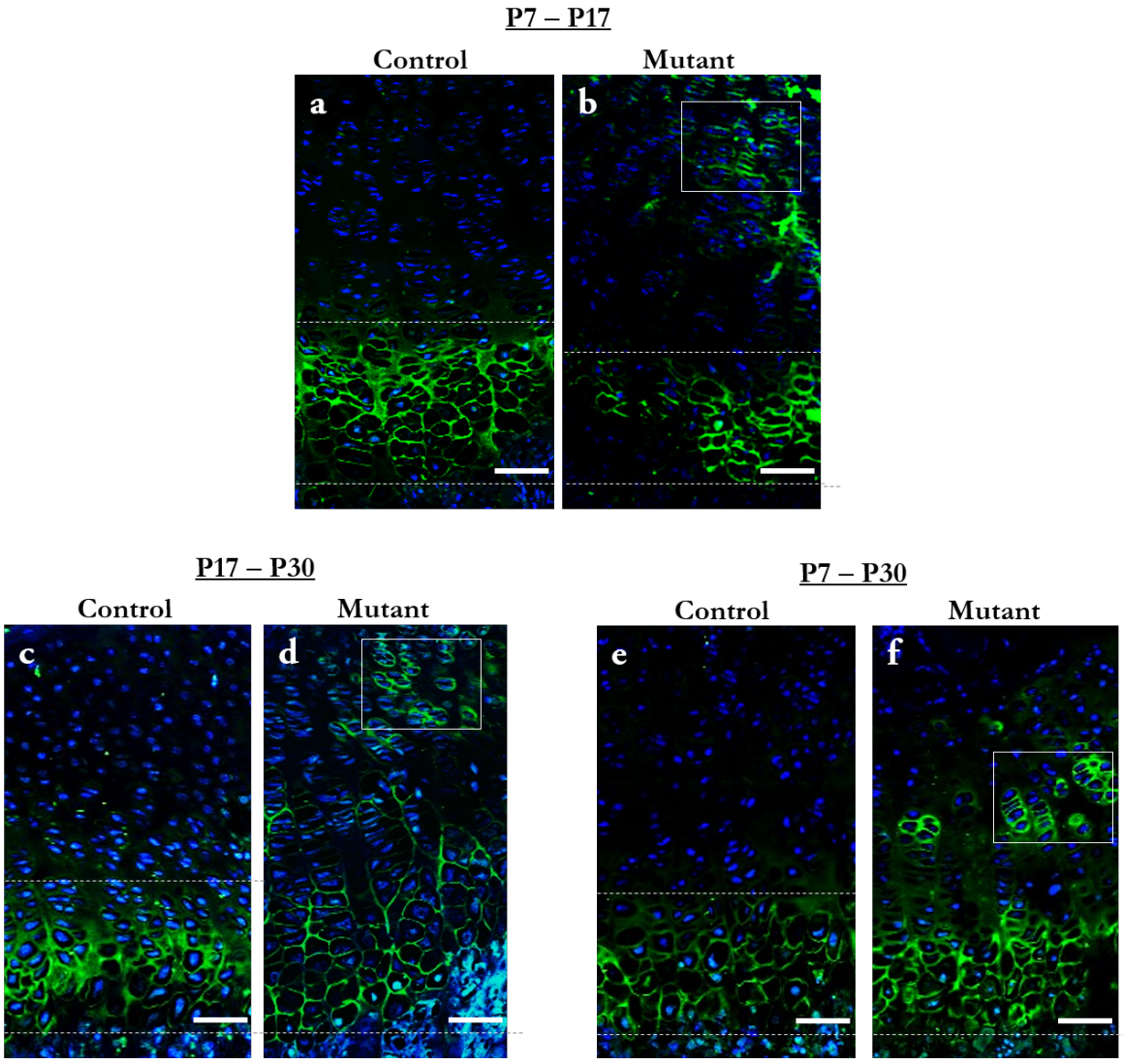

Figure 3.7: Mice lacking CLOP cilia exhibit ectopic hypertrophy in the growth plate
Type X Collagen stains were performed to identify growth plate chondrocytes undergoing hypertrophy (green). In all control groups (a, c, e), hypertrophic cells were found exclusively at the proximal end of the growth plate, where the hypertrophic zone is normally present (white dashed lines). Mutants examined at P17 had smaller hypertrophic zones compared to controls and contained hypertrophic cells in the resting/ proliferation zones (b, white box). Mutants examined at P30 also contained hypertrophic cells in the resting/ proliferation zones (d, f, white boxes). Nuclei are displayed in blue. White scale bars represent 50 μm.

In order to evaluate these observed differences in growth plate morphology, we performed immunohistochemistry for markers of growth plate chondrocyte proliferation (PCNA) and hypertrophy (Type X Collagen). Indeed, mutants had fewer cells in the proliferation zone compared to controls (Figure 3.5d) regardless of when progenitor primary cilia were disrupted. P7 – P17 mutants generally had smaller hypertrophic zones (Figure 3.7a,b) that were easily distinguishable from corresponding proliferation zones. In contrast, the P17 – P30 (Figure 3.7d) and P7 – P30 (Figure 3.7f) mutants did not have distinct hypertrophic and proliferation zones. Ectopic hypertrophy was present near the border between resting and proliferation zones in all mutant groups (Figure 3.7b,d,f); however, these chondrocytes were primarily found near the Groove of Ranvier in P7 – P17 mutants, but present throughout the entire growth plate in groups evaluated at P30.

Secondary ossification centers are underdeveloped in mutant juveniles

Prx1-expressing cells are known to form ossification centers during embryonic development[47,136], and our tracking studies reveal CLOPs continue to populate ossification centers in juvenile skeletogenesis (Figure 3.4). We therefore performed Toluidine Blue-O stains to examine ossification in the epiphyses and trabecular bone proximal to the ulnar growth plate. At P30, mice lacking primary cilia (Figure 3.8b,d) had less bone and vasculature in the proximal head compared to controls (Figure 3.8a,c). Mutant epiphyseal disks stained a lighter purple than their respective controls, suggesting they have lower proteoglycan contents. Furthermore, mutant epiphyseal disk cartilage also contained ectopic hypertrophic chondrocytes similar to those examined in the distal ulnar growth plates (Figure 3.7). These phenotypic differences were slightly more severe when the knockout was initiated at P7 (Figure 3.8b) compared to P17 (Figure 3.8d). In the trabecular space, controls examined at P30 (Figure 3.8e) had fewer cartilage

nodules and more bone with increasing distance from the growth plate. Although mutants exhibited a similar pattern proximal to the growth plate, they contained more retained cartilage and less bone compared to controls (Figure 3.8f). The phenotypic differences in the trabecular space were equally severe whether the knockout was initiated at P7 or P17. Interestingly, ossification in the aforementioned regions was comparable between mutants and controls in the P7 – P17 group.

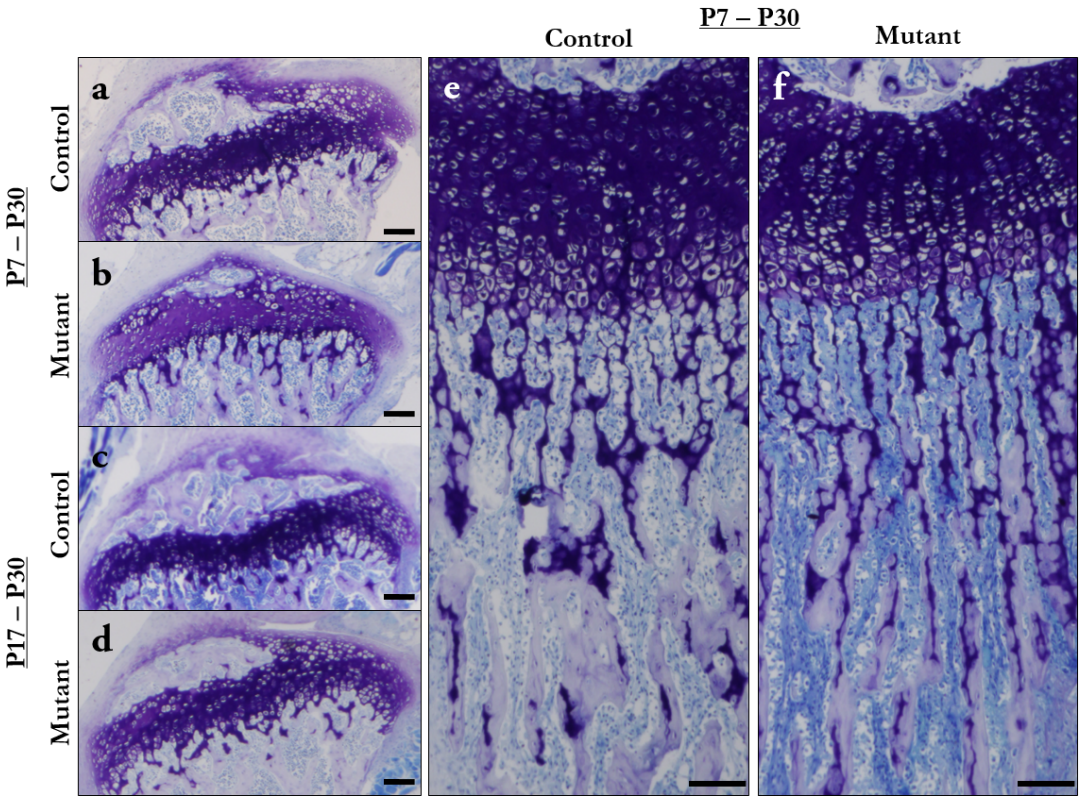

Figure 3.8: General ossification is stunted in juveniles when CLOP cilia are deleted
Toluidine Blue-O stains were performed to identify cartilage (purple), mineralized bone (off-white), and marrow (light blue) in the limbs of mice with and without CLOP primary cilia. The epiphyseal disk in P7 – P30 mutants (b) contained more cartilage and less bone than controls (a). This phenotype was also present in P17 – P30 controls (c) and mutants (d) but not as pronounced. All mutants (f) examined at P30 had a greater presence of cartilage nodules and mineralized cartilage in the trabecular space proximal to the growth plate, while controls (e) contained more bone (P7 – P30 group pictured). Nuclei are displayed in blue. Black scale bars represent 100 µm.

Discussion

Despite its ubiquity in the embryonic limb bud, Prx1 expression is highly restricted to the cambium layers after birth. When the Prx1CreER-GFP model was first developed, Kawanami et al. injected a Rosa26^{lacZ} reporter at postnatal day 19 (P19) and assessed Cre recombination at P23 to report the presence of Prx1-expressing cells[53]. However, observing Cre activity 96 hours later may not accurately represent Prx1 expression at the time recombination was triggered since skeletal development occurs rapidly in mice, especially in the first 3 weeks after birth[118–120]. In fact, it takes only 48 hours for chondrocytes to transition through the hypertrophic zone and become bone-forming osteoblasts in the primary spongiosa[124]. Another study of the murine forelimb suggests the entire hypertrophic zone turns over once every 24 hours[132]. For this reason, it is perhaps more appropriate to evaluate the presence of GFP, which is dependent on Prx1 expression, instead of Cre recombination. Furthermore, their group did not fully characterize Prx1 expression in the early days after birth, when important developmental milestones occur that are of interest when studying postnatal skeletogenesis.

We therefore crossed the Prx1CreER-GFP model with a Rosa26^{tdTomato} reporter and visualized GFP to detect Prx1 expression in the forelimb, as well as tdTomato to evaluate Cre activity 48 hours after recombination was induced. Kawanami et al. identified the vast majority of recombined cells in the cambium layers, with some in tendon, the epiphyses, and articular cartilage, and very few at the endocortical surface and in bone marrow[53]. In agreement with Kawanami et al., we found Prx1-expressing cells were primarily in the cambium layers of the periosteum and perichondrium and to a lesser degree in tendon. Since postnatal development is so rapid, the Prx1-expressing chondrocytes we found in the growth plates of P7 activated mice are likely recently differentiated progenitors recruited via the Groove of Ranvier[135]. Indeed,

Kawanami et al. no longer detected recombined cells in epiphyseal chondrocytes at P26, merely 96 hours after they observed them in P23 mice[53]. Additionally, because it takes 26 hours for GFP to turn over[137], these cells may not express Prx1 but still contain residual GFP protein. Using our red fluorescent reporter to trace cells with activated Cre, we found recombined cells in the same locations Kawanami identified, but did not detect accompanying Prx1 expression in the marrow space, articular cartilage, epiphyses, or endosteum. This indicates postnatal Prx1 expression is much more restricted to the cambium layers than previously believed and that these progenitors possess a surprising ability to rapidly populate skeletal tissues. We therefore conclude that this Prx1CreER-GFP model is a valuable tool for studying cambium layer osteochondroprogenitors (CLOPs), especially 3 weeks after birth when the most rapid developmental stage has ended.

Periosteal progenitors have long been thought to participate in intramembranous ossification; however, our tracking studies show for the first time that CLOPs are incorporated in the postnatal growth plate and engage in endochondral ossification. Prx1-expressing progenitors are known to differentiate into cells that contribute to intramembranous and endochondral ossification during adult fracture healing[53,138], but it is unknown whether these cells operate similarly in the normal program of juvenile skeletogenesis. A number of studies indicate osteoblasts are recruited from the cambium layer of the periosteum to lay down appositional layers of bone via intramembranous ossification[139], so perhaps it is not surprising that we found differentiated CLOPs embedded in cortical bone near the periosteal surface. Ono and Kronenberg determined that cells within the perichondrium and growth plate eventually become osteoblasts in the primary spongiosa[140]. Furthermore, Yang et al. recently discovered that hypertrophic chondrocytes become osteoblasts and osteocytes during juvenile development, and proposed that progenitors from the periosteum and perichondrium contribute to the osteogenic

pool responsible for bone growth[124]. Our reporter studies provide direct evidence to support this hypothesis because we show that progenitors within the cambium layers of the periosteum and perichondrium naturally populate the growth plate, cortical bone, trabecular bone, and secondary ossification centers. Additionally, our results provide further support that hypertrophic chondrocytes can become bone-forming osteoblasts. Hypertrophic chondrocyte fate has been a topic of controversy since it was first suggested they do not simply undergo apoptosis[141], so it is important to highlight any evidence of their osteogenic potential. Finally, our tracking studies importantly build on embryonic studies demonstrating that Prx1-expressing cells contribute to both forms of ossification[98,142]. Although Prx1 expression patterns become more restricted with age, our results indicate this cell population's participation in skeletogenesis spans multiple stages of development. Moreover, it is now reasonable to suggest CLOPs play a role in adult skeletal adaptation, especially since they populate the callus[53,95] in response to fracture.

Primary cilia are known to be critical for embryonic skeletal development, but our results suggest their participation in skeletogenesis extends beyond birth. Embryos lacking cilia in Prx1-expressing cells exhibit severely shortened limbs and loss of bone collar[98], a segment of bone that forms around the diaphysis to provide structure and support for further endochondral bone formation. Although ossification is prevalent in juvenile growth, it was previously unknown whether primary cilia in Prx1-expressing cells play a continued role since mutants did not survive birth. We generated an inducible knockout to study a postnatal deletion of CLOP primary cilia and found that juvenile mutants had disrupted endochondral and intramembranous ossification, resulting in shorter and thinner forelimbs. Our immunohistochemistry suggests the disruption in endochondral ossification is a combination of attenuated chondrocyte proliferation and abnormal hypertrophy in the growth plate. This phenotype is similar to juvenile mice with a

conditional chondrocyte cilia knockout[82] and suggests for the first time that CLOPs and their progeny comprise an appreciable number of the cells present in the growth plate. In their embryonic studies, Haycraft et al. determined that Prx1-expressing cells in the perichondrium normally differentiate into osteoblasts that form the bone collar, but those lacking cilia tend to follow a chondrogenic lineage[47]. It is therefore likely that Prx1-expressing progenitors in the periosteum/ perichondrium lacking cilia are unable to differentiate directly into osteoblasts or chondrocytes that eventually become osteoblasts. Overall, our results suggest this cell population and their primary cilia are attractive targets for osteoporosis prevention research, since the amount of bone accrued during postnatal development is an important factor in determining the risk for osteoporosis[120] and a variety of skeletal abnormalities are directly tied to the cilium[57].

Although we observed differences in phenotype with each developmental time point, all mutants consistently displayed a delayed program of osteogenesis. Juvenile mutants had shorter ulnae, fewer proliferating cells in the growth plate, ectopic hypertrophic chondrocytes in uncharacteristic zones of the growth plate, and less cortical area regardless of when CLOP primary cilia were disrupted. Interestingly, P17 – P30 mutants did not exhibit an increase in marrow area like the other groups, suggesting CLOPs influence development of the marrow space primarily within the first 2-3 weeks of birth. The marrow space typically widens with age as more cortical bone is laid down via intramembranous ossification and osteoclasts subsequently resorb bone at the endocortical surface. Our previous work suggests the primary cilium mediates formation and resorption to maintain adult bone homeostasis[38], so it is possible that this disruption also creates an imbalance in juveniles. Although all mutant growth plates contained fewer proliferating cells, P7 – P17 mutants suffered from low recruitment of resting zone cells, whereas P17 – P30 and P7 – P30 mutants displayed poor columnar stacking and

accelerated hypertrophy. Interestingly, the P7 – P30 mutant growth plates regained some columnar structure and the boundary between the resting and proliferation zones was more distinct compared to the phenotype in P17 – P30 mutants. This recovery implies CLOP cilium disruption delays rather than prevents endochondral ossification in juveniles. Indeed, conditions that hinder growth plate activity are known to encourage catch-up growth, whereby growth occurs more rapidly than normal at a particular age because the growth plate continues to operate in the absence of senescence[143]. Studies suggest growth plate senescence is dictated by the progress of growth, rather than age itself[143–145], so it is possible that CLOP cilium disruption delays senescence and temporarily stunts endochondral ossification. Regardless of whether catch-up growth can occur, we did not find evidence that the negative effects of CLOP cilium disruption on ossification are recoverable. Lastly, our Toluidine Blue-O stains revealed that P7 – P17 mutants did not display the attenuated ossification observed in the other groups. This is perhaps expected since secondary ossification centers are not formed until P7 and may not undergo detectable changes by P17.

The phenotypic abnormalities in mutants are potentially due to disruptions in ciliary signaling pathways that are known to coordinate intramembranous and endochondral ossification (i.e. Ihh, PTHrP, TGFβ, and BMP). Perhaps the most recognized signaling pathway in the growth plate is the interplay between Indian hedgehog (Ihh) and parathyroid hormone-related protein (PTHrP), which coordinate with the perichondrium to control the timing and rate of hypertrophy. The primary cilium has long been known to mediate hedgehog signaling during development[146], and juvenile mutants lacking chondrocyte primary cilia exhibit disrupted Ihh signaling[125] and accelerated hypertrophic differentiation[82]. Although transforming growth factor beta (TGFβ) and bone morphogenic protein (BMP) have established roles in skeletal

development, only recent studies show that the TGFβ/BMP signaling pathway is directly influenced by the primary cilium[147,148]. Prx1Cre embryos containing a knockout of TGFβ receptor 2 exhibit dwarfism and severely attenuated intramembranous ossification[149]. The deficiencies in endochondral ossification are perhaps not surprising since the Ihh/PTHrP pathway is believed to work intimately with TGFβ2 and BMP signaling to influence chondrocyte hypertrophy[150,151]. We therefore conclude that our CLOP cilia knockouts display attenuated intramembranous ossification in part due to disrupted BMP signaling and exhibit ectopic and accelerated hypertrophy as a result of interrupted Ihh, PTHrP, TGFβ, and BMP signaling.

Chondrocyte proliferation is also limited when primary cilia and their associated signaling pathways are disrupted. Chondrocytes in the proliferation zone are able to rapidly proliferate by dividing and rotating to stack themselves in tight vertical columns, a process known as *chondrocyte rotation*. Primary cilia are normally oriented along the long axis of the growth plate in the proliferation zone and this directionality is critical for rotation to occur[82,126–128]. For example, transgenic mice containing a chondrocyte-specific primary cilia knockout exhibit randomly oriented cilia in clusters of chondrocytes that fail to vertically align, resulting in severely attenuated proliferation[82]. We also confirmed in our model that the observed disorganized clusters in mutant proliferation zones had randomly oriented cilia, if any cilia at all, whereas control animals displayed perpendicularly oriented cilia in tight vertical columnar stacks (Figure 3.9). It has been suggested that the cilium mediates this process through noncanonical Wnt signaling[82,125] since chondrocyte rotation is tightly regulated by the planar cell polarity (Wnt/PCP) pathway[152]. In addition to their roles in chondrocyte hypertrophy, Ihh and BMP signaling also enhance chondrocyte proliferation. In fact, overexpression of Ihh alone is sufficient to enhance proliferation[153]. Another form of Hedgehog signaling, Sonic hedgehog

(Shh), and BMP signaling are believed to trigger resting zone chondrocytes to enter the proliferation zone[154,155]. Collectively, these prior studies suggest our primary cilium knockouts cannot adequately recruit cells from the resting zone and those cells that enter the proliferation zone fail to engage in chondrocyte rotation due to disruptions in ciliary signaling pathways.

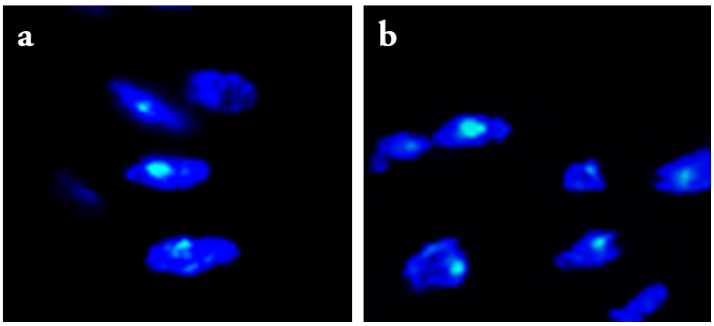

Figure 3.9: Orientation of growth plate chondrocyte primary cilia
In control growth plates (a), proliferating chondrocytes contain cilia (green) that are oriented along the longitudinal axis of the limb. In contrast, Prx1CreER-GFP; Ift88$^{fl/fl}$ mutant cilia were randomly oriented and their corresponding chondrocytes failed to stack in the tight, vertical columns demonstrated in control growth plates. Nuclei are pictured in blue. Micrographs were collected using a confocal microscope (Olympus FV1000) with a 100X oil objective.

In conclusion, our results suggest cambium layer osteochondroprogenitors have greater regenerative potential than previously envisioned and are perhaps the most suitable source for recapitulating bone regeneration *in vivo*. Mesenchymal cells are the leading cell type for regenerative applications since they self-renew, differentiate into a vast array of cell types, and can be extracted from many different tissues[33]. Bone marrow is a particularly attractive source since it contains osteogenic precursors; however, the periosteum has also been identified as a clinically useful progenitor source[156]. Prx1-expressing cells are critical to embryonic skeletogenesis[98] and the majority of cells in the adult fracture callus are derived from periosteal progenitors[95]. Additionally, periosteum derived progenitors demonstrate high proliferation rates *in vitro* and regenerative performance does not vary with age[33]. We demonstrated that Prx1-

expressing cells function as periosteal/perichondrial progenitors in the postnatal skeleton and populate a surprising number of nearby and distant skeletal tissues during juvenile development. Because of their continued existence after birth, regenerative potential, and pre-programmed fate towards an osteogenic lineage, CLOPs are potentially optimal for producing bone tissue *in vivo*. More importantly, we demonstrated that CLOPs differentiate into osteoblasts, hypertrophic chondrocytes, and osteocytes, providing a diverse source of progenitors for development, trauma response, and adult skeletal homeostasis[124]. Furthermore, we have shown that disrupting the primary cilium alone results in significant skeletal abnormalities, implicating this organelle as a potential mechanism to manipulate CLOP involvement in skeletogenesis and bone adaptation.

Chapter 4: TRPV4 and AC6 mediate calcium/ cAMP dynamics during osteocyte primary cilium mechanotransduction

Abstract

One mechanism by which osteocytes transduce mechanical stimuli is through the primary cilium, which contains a unique microdomain of proteins that facilitate mechanotransduction. Our lab recently found that a calcium (Ca^{2+}) channel, TRPV4, and transmembrane proteins that produce cAMP, AC3 and AC6, are present in the osteocyte primary cilium. TRPV4 opens via a calmodulin (CaM) domain and (Ca^{2+}) binds to AC3 and AC6 to activate and inhibit cAMP production, respectively. Osteocyte cAMP levels initially decrease when stimulated, so we hypothesize that Ca^{2+} enters via TRPV4 and inhibits production of cAMP through AC6. The objectives of this study are to determine whether 1) Ca^{2+}-mediated opening of TRPV4 is critical to osteogenesis and 2) AC6 mediates Ca^{2+}/ cAMP dynamics. AC3/6 overexpression (OE) plasmids were generated and their Ca^{2+} binding pockets were disrupted via site directed mutagenesis. Similarly, the calmodulin binding domain was removed from a TRPV4 OE plasmid. MLO-Y4 osteocytes were transfected with either the OE, mutant, or vector control plasmids via electroporation and either fixed for ICC or exposed to 2 or 30 minutes of oscillatory fluid flow (OFF). Protein expression was confirmed via ICC and treatment with forskolin, an AC agonist, confirmed the catalytic activity is comparable between OE and mutant plasmids, suggesting any detected changes in cAMP production are due to disruption of the binding pocket. After 2 min of OFF, cAMP production was drastically increased in AC3 OE and AC6 Mut OE compared to their respective counterparts. Osteogenesis was attenuated in AC3 OE and AC6 Mut OE, suggesting cAMP levels and osteogenesic response are negatively correlated in

the early stages of osteocyte mechanotransduction. Furthermore, TRPV4 OE had an enhanced osteogenic response compared to controls after 5 and 30 min of OFF, but this effect was lost in mutants. These studies demonstrate for the first time that Ca^{2+} and cAMP are perhaps coupled via ACs and influence osteogenesis. Additionally, our results further implicate TRPV4 as the mechanism by which Ca^{2+} enters the cilium during osteocyte mechanotransduction. These mechanisms could be targeted to generate therapeutics that promote bone formation to combat osteoporosis. We will next use our novel FRET biosensors to characterize Ca^{2+} influx and cAMP production specifically in the cilium with our intact and mutated overexpression plasmids.

Introduction

Osteocytes are the mechanosensory cells in bone that control modeling and remodeling of the skeleton by signaling to osteoblasts and osteoclasts. Adult skeletal maintenance and adaptation is dependent on the osteocyte's ability to sense physical stimulation and convert these signals into intracellular and extracellular processes that encourage bone formation or resorption. There are two predominant theories for how osteocytes embedded in cortical bone sense mechanical stimulation. First, some researchers suggest osteocytes respond to deformation of the bone matrix in the perilacunar space, or fluid-filled pockets in which osteocytes reside. Others postulate that fluid flow through the lacunar/canalicular system generates shear stresses that act on osteocytes. Our lab primarily explores the effects of fluid shear and the subsequently triggered mechanotransduction pathways that lead to osteogenic signaling from osteocytes.

One mechanism by which osteocytes transduce mechanical stimuli is through the primary cilium, which contains a unique microdomain of proteins and signaling molecules that enhance mechanotransduction. In response to fluid shear, kidney cilia bend and Ca^{2+} enters the cilium

through a transmembrane protein, polycystin 1 (PC1), interacting with a Ca^{2+} channel, polycystin 2 (PC2). Our lab recently found that osteocyte primary cilia experience a similar flow-induced Ca^{2+} influx and this behavior is critical to osteogenesis. However, the osteocyte ciliary Ca^{2+} influx does not occur through the PC1/PC2 complex[36]. We identified another Ca^{2+} channel, Transient Receptor Potential Vanilloid 4 (TRPV4), is present in the osteocyte cilium and an siRNA-mediated knockdown of TRPV4 attenuates flow-induced osteogenesis[36]. Thus, we speculate that, in response to fluid shear, the osteocyte primary cilium bends and Ca^{2+} enters the cilium through the opening of TRPV4 channels.

Our group has also identified adenylyl cyclases (ACs) in the osteocyte primary cilium that are not present in kidney cilia. There are nine transmembrane isoforms of adenylyl cyclase but AC3 and AC6 are the only isoforms that also localize to the osteocyte cilium. ACs convert ATP to cyclic AMP (cAMP), a signaling molecule that is downregulated in osteocytes at the onset of fluid shear[35]. We previously demonstrated that osteocytes containing siRNA-mediated knockdowns of AC6 and Ift88 maintain cytosolic levels of cAMP with fluid shear, resulting in attenuated osteogenesis[35]. Interestingly, the decrease in cAMP production occurs within 2 minutes but is lost after 30 minutes of applied flow[35]. This suggests that decreased cAMP levels are most important at the onset of flow or another mechanism is at play with increasing exposure to physical stimulation. Unpublished work in our lab suggests that an siRNA-mediated knockdown of AC3 in osteocytes enhances the osteogenic response to fluid shear after 30 minutes of applied fluid flow. Thus, we speculate that ciliary AC6 and AC3 play an antagonistic role in manipulating cAMP production to trigger osteogenesis.

TRPV4, AC3, and AC6 all contain Ca^{2+} binding domains that can be disrupted through genetic mutations. Extracellular Ca^{2+} binds to a calcium-modulated protein (calmodulin, CaM)

domain of TRPV4, causing this channel to open and allow Ca^{2+} to enter the cell[76]. This CaM domain can be removed by eliminating 17 residues beginning at position 814 in TRPV4's amino acid sequence[76]. The initial studies were performed in proteins in hypotonic solutions, but the removal of this TRPV4 CaM domain was later found to inhibit calcium influx in osteoclasts and ultimately prevent their activation[78]. The activity of some AC isoforms, such as AC3 and AC6, are modified by binding Ca^{2+}. Protein binding experiments revealed that AC5/6 competitively binds Ca^{2+} and its ability to produce cAMP is inhibited in the bound state[157]. Another group used x-ray crystallography to identify two aspartic acid residues that are critical for AC6 to fold and form the binding pocket[158]. Mutation of these two residues renders AC6 unable to bind calcium so it continues to catalyze the conversion of ATP to cAMP. This characteristic is conserved in AC5 and AC3; however, AC3 is activated by calcium to produce cAMP[80]. Therefore, in contrast to AC6, disrupting AC3's binding pocket prevents cAMP production. There is some evidence that Ca^{2+} binding alone does not activate AC3 and occurs after AC3 has already been activated to enhance cAMP production, but definitive proof is lacking[80].

We hypothesize that fluid flow in the lacunar/canalicular system bends osteocyte primary cilia, allowing calcium to enter through TRPV4 channels and bind to AC6 or AC3. We anticipate that in the early initiation of flow, calcium will bind to AC6 and inhibit production of cAMP, resulting in an upregulation of osteogenic markers in the osteocyte. The objectives of this study are to determine whether 1) Ca^{2+}-mediated opening of TRPV4 is critical to osteogenesis and 2) AC6 and AC3 mediate Ca^{2+}/ cAMP dynamics.

Materials and Methods

Plasmid Design

Entry clones for murine AC6 (MmCD00297230) and human AC3 (HsCD00505998) in pENTR223.1 vectors were obtained from the DNASU Plasmid Repository. AC6 and AC3 entry clones were inserted into a pcDNA3.2 mammalian expression destination vector (12489019, Life) using the Gateway LR Clonase System (Life) to generate pcDNA3.2 + AC6 (AC6 OE) and pcDNA3.2 + AC3 (AC3 OE) overexpression plasmids. This kit provides a reaction control entry clone, GWCAT, and the resulting pcDNA3.2 + GWCAT overexpression vector (Control OE) was used as the empty vector control for all transfection experiments. The pcDNA3.2 vector contains a V5 tag at the end of the inserted protein that we used to identify protein expression via immunocytochemistry.

The calcium binding pockets of AC3 and AC6 were disrupted using site directed mutagenesis. We identified the two charged aspartic (Asp) acid residues responsible for calcium binding and performed point mutations to convert them to neutral alanine (Ala) residues. These residues are located in the 324^{th} and 368^{th} positions for AC3 and the 382^{nd} and 426^{th} positions for AC6. PCR was performed on the AC3 and AC6 OE plasmids using custom designed mutation primers to convert the Asp residues to Ala (Table 4.1). Resulting PCR product was ligated and transformed into bacteria using the Q5 Site-Directed Mutagenesis Kit (New England Biolabs), which also contained reactants for the PCR. Transformed bacteria were placed onto agar (Sigma) plates containing 100 μg/mL Ampicillin for antibiotic selection and incubated at 37°C overnight. Individual bacteria colonies were swabbed and grown up in LB broth (Sigma) containing 100 μg/mL Ampicillin for 16 hours in a shaking incubator (225 rpm) at 37°C. Plasmids were isolated from bacteria using a QIAprep Spin Miniprep Kit (Qiagen) and re-suspended in 30 μL nuclease

free water (Promega). The resulting plasmids are pcDNA3.2 + $AC3^{Ala\ 324,\ 368}$ (AC3 Mut OE) and pcDNA3.2 + $AC6^{Ala\ 382,\ 426}$ (AC6 Mut OE) overexpression plasmids that contain AC3 and AC6, respectively, that cannot bind calcium.

The TRPV4 OE plasmid was gifted from Dr. Heinrich Brinkmeier at the University of Greifswald in Greifswald, Germany. This plasmid contains TRPV4 with a yellow fluorescent protein (YFP) tag in a pcDNA3.1 vector. The YFP tag can be used to determine transfection efficiency and protein expression in live or fixed cells. The CaM domain was removed using the aforementioned site directed mutagenesis protocol with published primer sequences (Table 4.1)[78]. The pcDNA3.1 and pcDNA3.2 backbones have negligible differences that will not affect this experiment; thus, pcDNA3.2 + GWCAT (Control OE) was also used as a vector control for all TRPV4 experiments.

All constructed plasmids and sequence mutations were confirmed using Genewiz's Sanger sequencing and custom designed primers (Table 4.1). Control GWCAT OE sequence was confirmed using primers provided in the Gateway Clonase kit. Primers were purchased from Integrated DNA Technologies and re-suspended in 1 mL nuclease-free water upon arrival (Promega), then aliquoted in 10 μM concentrations and stored at -20°C.

Cell Culture

MLO-Y4 osteocyte-like cells were passaged at least twice before used for experiments, seeded on Type I Collagen (Corning) coated dishes or glass slides, and cultured in MEMα (Life) supplemented with 5% FBS, 5% CS, and 1% PenStrep (Life). Cells were cultured in reduced serum media (MEMα supplemented with 2.5% FBS, 2.5% CS, and 0.5% P/S) 48 hours prior to fluid flow. MLO-Y4s did not reach over 60% confluence in standard passage, but were grown to

reach at least 80% confluence for fluid flow studies. Cells transfected with AC6 OE or AC6 Mut OE were cultured in MLO-Y4 media supplemented with 600 ug/mL Geneticin (Life) for 48 hours the day after electroporation, followed by 48 hours of reduced serum media. AC3 OE and AC3 Mut OE specimens received reduced serum media for 48 hours the day after electroporation. AC3 and AC6 plasmids were cultured for a total of 3 and 5 days, respectively, before experimentation since this is when each plasmid demonstrated peak protein expression. Passages 38 – 48 were used for all experiments.

Table 4.2 Mutation and sequencing primers for mutation plasmid design

Plasmid	Mutation Primers	Sequencing Primer
AC3 Mut OE	324 For: TCCTCTTTGCCGCCATCG 324 Rev: TGCTGACGTTCTCGTGACG 368 For: TTAAGATCCTGGGCGCCTGC 368 Rev: TCCGCAGCTGGTGGTATTTAGC	For: TCTATGACGGTGATGGTGTTCC
AC6 Mut OE	382 For: TTGAGGGCTTCACCAGCCTG 382 Rev: TGGCCGCAAACAGGATGCTG 426 For: TAGGAGCCTGTTACTACTGC 426 Rev: AGATCTTGATCCTCAGACAG	For: TGTCTGCACACACTACCCTG
TRPV4 Mut OE	For: CTTCTCCCTGAACAAGAACTCAAGC Rev: TTGTTCAGGGAGAAGCCATAGTACTG	For: TCTCTACCACTGACACCCGTTC

Transfections

For each transfection, 1.25 million MLO-Y4s were re-suspended in 250 µL of BTX Buffer (Harvard Apparatus). Plasmid DNA was added to the cells in BTX solution and gently flicked to mix, then transferred to a 4 mm gap cuvette for electroporation. The amount of plasmid DNA added was normalized to copy number; therefore, AC3 OE/ AC3 Mut OE/ AC6 OE/ AC6 Mut OE/ TRPV4 OE/ TRPV4 Mut OE specimens received 15 µg and GWCAT controls received 7 µg per transfection. Cells were transfected via electroporation using a BTX

ECM 360 Electro Cell Manipulator (Harvard Apparatus) to generate a single pulse with settings: 300 V, 100 Ω, 1000 μF. Cells remained in BTX buffer for no more than 10 minutes to minimize cell death. The resulting electroporation solution was split between 4 glass slides for fluid flow studies or 4 tissue culture dishes for Forskolin treatment. 10 μL of electroporation solution was seeded on 35 mm glass bottom dishes for immunocytochemistry. Cells were rinsed and media was changed the morning after a transfection to remove dead cells and facilitate cell recovery.

Forskolin treatment

MLO-Y4s transfected with AC6 OE, AC6 Mut OE, AC3 OE, AC3 Mut OE, and GWCAT vector control were split onto 4 tissue culture dishes (100 mm) immediately after the electroporation. Transfected cells were cultured to achieve peak protein expression and treated with 10 μM Forskolin (Sigma) dissolved in DMSO (Sigma) or vehicle control for 20 minutes at 37°C. After treatment, cells were rinsed with cold PBS, lysed with 1 mL of 0.1 M HCl (cAMP ELISA kit, Enzo) for 10 minutes at room temperature, scraped off the dish, centrifuged at 4°C for 15 min at 16 rcf. The resulting supernatant was transferred to a fresh microcentrifuge tube.

Immunocytochemistry (ICC)

To determine plasmid expression patterns and cilia incidence/ length, we performed double ICC to detect the V5 tag of the destination vector and primary cilia. Cells were fixed with 4% paraformaldehyde for 10 min at room temperature and blocked with 3% BSA + 2% goat serum + 0.1% TritonX-100 (Sigma) in PBS for 1 hour at room temperature. Cells were then incubated in primary antibodies against V5 (1:500, Life) and Arl13b (1:1000, Protein Tech), a protein localized to cilia, overnight on a rocker at 4°C. The fluorescent secondary antibodies, AlexaFluor 488 (1:500, Life) and AlexaFluor 568 (1:500, Life) were applied for 1 hour at room

temperature to detect V5 and Arl13b, respectively. Nuclei were detected using NucBlue ReadyProbes (Life). All fluorescent images were collected using an Olympus Fluoview FV1000 confocal microscope and software.

Quantifying cilium incidence and length

Cilium incidence and length were measured by hand from confocal stacks using Image J software. At least four images per dish were analyzed to determine the average incidence and length per trial. Each transfection was performed on 3 separate occasions to evaluate repeatability and consistency between trials. Investigators were blinded to the groups during the experiment, staining, image acquisition, and post-imaging analysis steps. Quantifications were performed by two investigators to assess repeatability and ensure accuracy of reported results.

Oscillatory fluid flow (OFF)

Transfected MLO-Y4s were seeded on glass slides (Fisher Scientific; 75 x 38 x 1 mm). Upon reaching 80% confluence, cells were placed in parallel-plate flow chambers (56 × 24 × 0.28 mm), incubated at 37°C for 30 minutes at rest, and exposed to 2, 5, or 30 minutes of OFF at 1 Hz with a peak shear stress of 10 dyn/cm^2. For RT-qPCR analysis, samples were incubated for an hour (2 and 5 min OFF studies) or 30 min (30 min OFF studies) post-flow and were removed from the chambers, rinsed in cold PBS, and lysed immediately with 1 mL TriReagent (Sigma Aldrich) to isolate RNA. For cAMP quantification studies, 0.5 mM of the phosphodiesterase inhibitor 3-isobutyl-1-methylxanthine (IBMX) (Sigma) was added to flow media to prevent cAMP degradation. At the conclusion of flow, samples were rinsed and lysed immediately with 500 μL of 0.1 M HCl (cAMP ELISA kit, Enzo) for 10 minutes. The resulting

lysate was centrifuged at 4°C for 15 minutes at 16 rcf and the supernatant was transferred to a fresh microcentrifuge tube.

mRNA quantification

RT-qPCR was performed to quantify flow-induced changes in Cyclooxygenase-2 (COX-2) and GAPDH using fluorescent primers (Life Technologies) and an ABI PRISM 7900 (Applied Biosystems). Samples were performed in triplicate and COX-2 was normalized to GAPDH expression levels. OFF samples were normalized to static controls.

cAMP ELISA

Cytosolic cAMP levels were quantified using a kit from Enzo Life Sciences (ADI-900-163). Samples were analyzed in triplicate and prepared according to the manufacturer's instructions for non-acetylated samples in hydrochloric acid lysis buffer. cAMP levels were normalized to total protein content of the lysate, which was determined by a Pierce BCA Protein Assay (Thermo Fisher). OFF samples were normalized to static controls.

Statistics

Data were analyzed using a one-way ANOVA followed by Bonferroni post-hoc correction, or a two-tailed student's t-test. Values are reported as mean ± SEM, with $p < 0.05$ considered statistically significant. Sample size was determined to achieve a power of at least 80%.

Results

Protein is overexpressed in transfected MLO-Y4s

We first determined whether our constructed plasmids would result in supranormal levels of AC3, AC6, and TRPV4 protein. Double ICC for V5 and AC6 revealed that only 20 – 30% of transfected cells overexpressed AC6 3 days post-transfection (PT). We therefore treated these cells with Geneticin to select cells that were successfully transfected. With 2 days of Geneticin treatment, followed by 2 days of culture in reduced serum media, we achieved 100% efficiency 5 days PT (Figure 4.1b). We repeated these stains on cells transfected with GWCAT OE, AC3 OE, or AC3 Mut OE. For AC3 plasmids, 80-90% of the cells overexpressed AC3 protein 3 days PT. Cells transfected with the GWCAT OE plasmid demonstrated > 90% efficiency 3 days PT (Figure 4.1) and maintained this behavior 5 days PT. For the TRPV4 plasmids, we visualized YFP in live cells and determined that more than 90% of cells overexpressed protein 3 days PT (Figure 4.1a). The mutation plasmids exhibited identical expression patterns as their non-

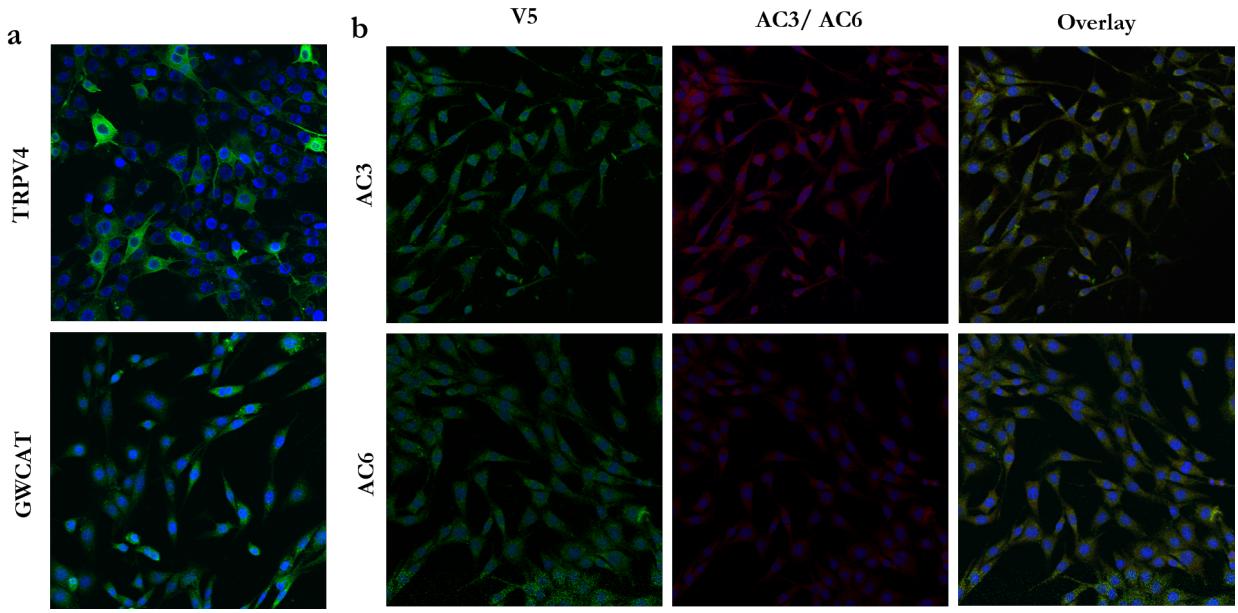

Figure 4.1: MLO-Y4s containing our plasmids demonstrate supranormal protein levels
ICC for V5 (green) revealed that MLO-Y4s transfected with GWCAT (A, bottom), AC3 OE (B, top), and AC6 OE (B, bottom) express proteins produced as a result of their respective plasmid. TRPV4 expression was confirmed by visualizing YFP (green) (A, top). AC3 and AC6 are pictured in red (B, middle). Nuclei are pictured in blue. Images were collected at 20X. This experiment was performed 3 times for each group.

mutated plasmids (data not shown). All protein was expressed in the cytosol of MLO-Y4s, which is typical for CMV-driven plasmids. For these reasons, AC3/ TRPV4 and AC6 experiments were performed 3 or 5 days PT, respectively, and the GWCAT OE plasmid was considered an acceptable empty vector control for both of these time points.

AC3 and AC6 catalytic activity is maintained when the calcium binding pocket is disrupted

AC3 and AC6 modify their catalytic activity by binding Ca^{2+}, but all ACs are activated by forskolin. This AC agonist binds at a separate site so ACs are able to produce cAMP independent of metal binding. We therefore treated transfected MLOY4s with forskolin to confirm that our mutations do not disrupt general AC activity. Indeed, AC3 Mut OE and AC6 Mut OE specimens had comparable increases in cAMP levels, and therefore similar AC activity (Figure 4.2). This result indicates that any changes in cAMP production are a direct consequence of disruption of the Ca^{2+} binding pocket. Furthermore, the activity is elevated compared to Control OE since cells transfected with AC OE plasmids simply contain more AC.

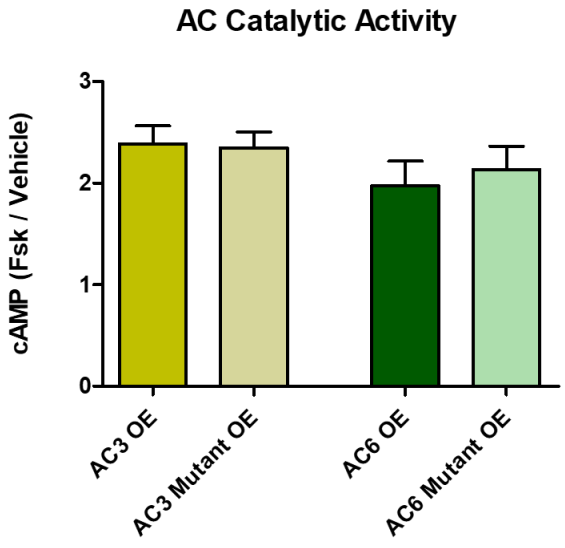

Figure 4.2: Ca^{2+} binding pocket disruption does not influence general AC catalytic activity

MLO-Y4s were transfected with AC3 (yellow) and AC6 (green) overexpression plasmids and treated with forskolin. Compared to vehicle controls, all specimens demonstrated at least an approximate 2-fold increase in cAMP production. This increase was comparable between OE plasmids and their Mut OE counterparts, as well as between AC3 and AC6 specimens. Data are normalized to vehicle controls and reported as the mean ± SEM. n = 5 for AC3 specimens, n = 6 for AC6 specimens.

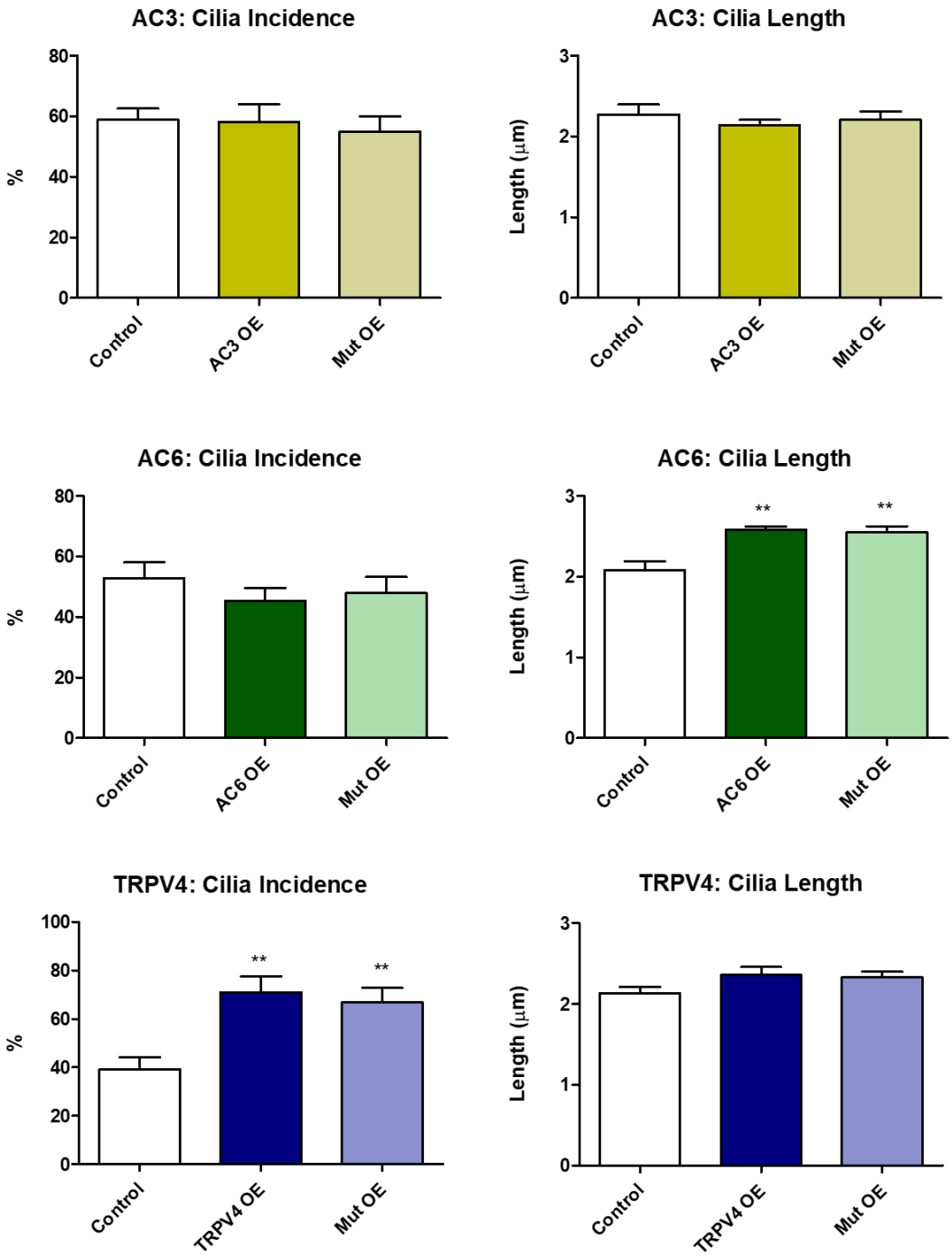

Figure 4.3: Increasing TRPV4 and AC6 protein expression enhances ciliogenesis
Cilia were identified in transfected MLO-Y4s using double ICC for V5 and Arl13b, a protein that localizes to cilia. A nuclear dye was used to detect nuclei. 3-D stacks were collected at 100X magnification using a confocal microscope. Cilia incidence and length were measured manually using Image J software. Data are presented as mean ± SEM, $^{**}p < 0.001$. AC3: Control n = 13, OE n = 15, Mut OE n = 14. AC6: Control n = 15, OE n = 12, Mut OE n = 12. TRPV4: Control n = 9, OE n = 8, Mut OE n = 6.

Cilium incidence and length increase with overexpression of TRPV4 and AC6, respectively

Recent work in our lab suggests enhanced ciliogenesis in MLOY4s increases their osteogenic response to fluid shear[42]. We therefore sought to determine whether cilium incidence or length increased when these osteocyte ciliary proteins were overexpressed. Interestingly, incidence and length increased only with TRPV4 and AC6 overexpression, respectively (Figure 4.3). AC3 overexpression elicited no change compared to vector controls. This behavior was consistent for the mutation plasmids.

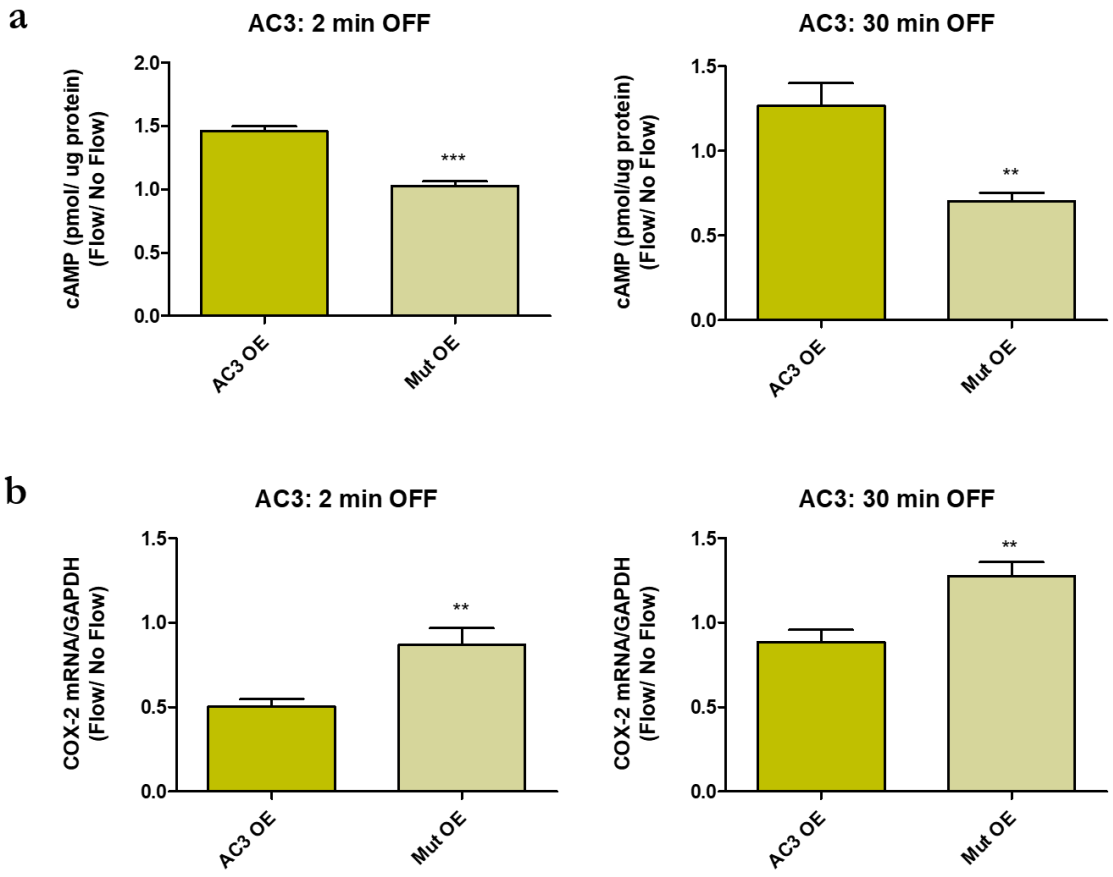

Figure 4.4: Flow-induced changes in cAMP levels and COX-2 expression in osteocytes overexpressing intact and mutated AC3

MLO-Y4s were transfected with AC3 OE, AC3 Mut OE, or Control OE plasmids and exposed to 2 or 30 min OFF. The AC3 Mut OE group exhibits decreased cAMP levels and enhanced osteogenesis compared to AC3 OE samples. Bar graphs represented fold changes with OFF compared to static controls. AC3 OE and AC3 Mut OE data are normalized to Control OE data. Data are presented as mean ± SEM. n = 6 for all groups, $^{**}p < 0.001$, $^{***}p < 0.0001$.

Disrupting the Ca^{2+} binding pocket of AC3 and AC6 alters flow-induced cAMP production

We then sought to determine how cytosolic cAMP levels change when the Ca^{2+} binding pockets of AC3 and AC6 are disrupted. Transfected cells were exposed to 2 min and 30 min of fluid shear in order to compare our results to previous work[35]. Normally, osteocytes exhibit decreased levels of cAMP production after 2 min of flow. With 2 min OFF, cells transfected with AC3 Mut OE produced less cAMP than those containing AC3 OE (Figure 4.4a), whereas the AC6 Mut OE group exhibited increased levels compared to AC6 OE (Figure 4.5a) We have previously shown that cAMP levels actually increase after 30 min of flow[35]. Interestingly, at this examined time point, there was no significant difference between AC6 OE and AC6 Mut OE samples. The relationship between AC3 OE and AC3 Mut OE persisted with the increase in flow duration.

Osteogenesis is attenuated when cAMP production is altered

We then evaluated changes in flow-induced osteogenesis to identify how cAMP production may influence the osteocyte's response to fluid shear. Specifically, we quantified expression of COX-2 under the same conditions as in our cAMP experiments. Osteocytes normally demonstrate an increase in COX-2, and therefore increased osteogenesis, with fluid shear. Cells transfected with AC3 Mut OE demonstrated enhanced osteogenesis compared to AC3 OE at both timepoints examined (Figure 4.4b). AC6 Mut OE had an attenuated osteogenic response compared to AC6 OE, but only when flow was applied for 2 min (Figure 4.5b). There was no significant difference between AC6 OE and AC6 Mut OE groups after 30 min of flow. Overall, the data indicate there is a negative correlation between cytosolic cAMP levels and flow-induced osteogenesis.

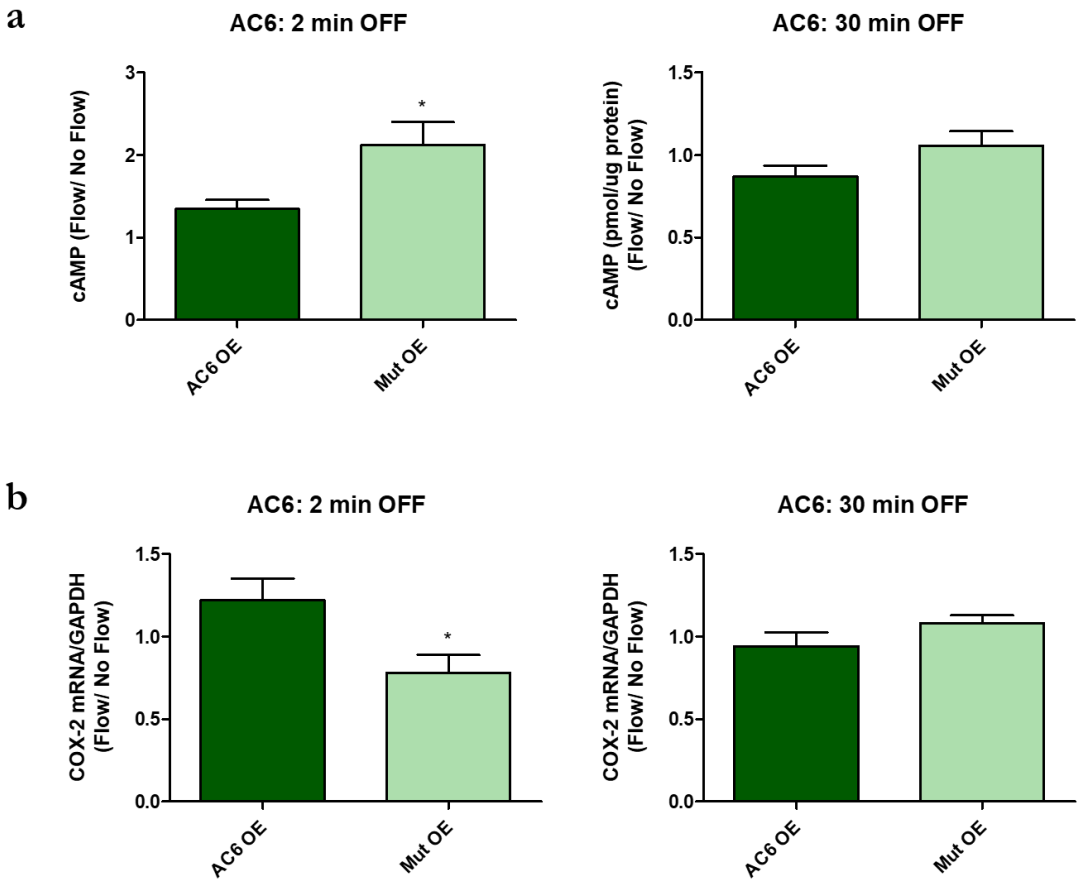

Figure 4.5: Flow-induced changes in cAMP levels and COX-2 expression in osteocytes overexpressing intact and mutated AC6

MLO-Y4s were transfected with AC6 OE, AC6 Mut OE, or Control OE plasmids and exposed to 2 or 30 min OFF. After 2 min of OFF, the AC6 Mut OE group exhibits an increase in cAMP production and decreased osteogenic response compared to the AC6 OE group. There is no difference in cAMP production or COX-2 expression between the groups with 30 min of OFF. Bar graphs represented fold changes with OFF compared to static controls. AC6 OE and AC6 Mut OE are normalized to Control OE. Data are presented as mean ± SEM. n = 6 for all groups, *$p < 0.01$.

Osteogenesis is attenuated when the TRPV4 CaM domain is removed

Finally, we investigated changes in flow-induced osteogenesis when intact and mutated TRPV4 are overexpressed. We exposed cells transfected with TRPV4 OE and TRPV4 Mut OE to 5 and 30 min of flow to remain consistent with time points examined in our initial studies[35,36]. Regardless of flow duration, cells overexpressing TRPV4 Mut OE had an attenuated response to flow compared to the TRPV4 OE group. However, TRPV4 OE had significantly higher COX-2

levels compared to Control OE ($p < 0.01$), suggesting TRPV4 overexpression enhances osteogenesis.

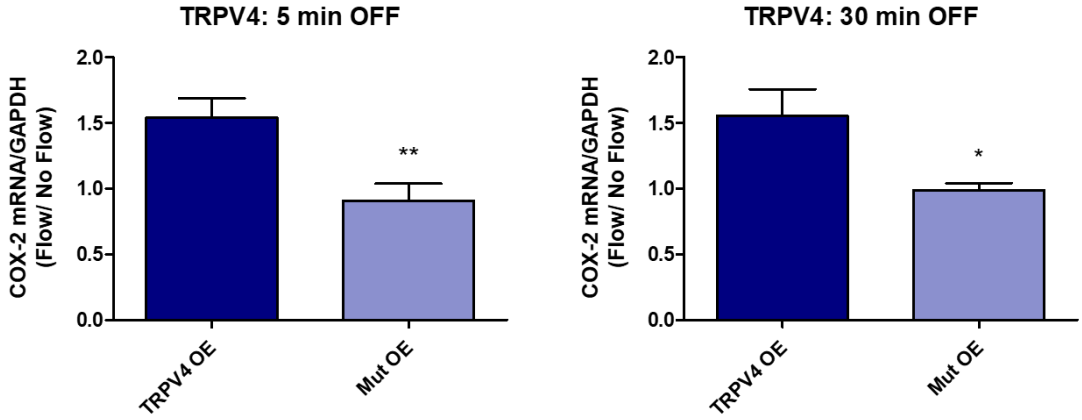

Figure 4.6: Osteocytes demonstrate attenuated flow-induced osteogenesis when the CaM domain of TRPV4 is removed

MLO-Y4s were transfected with TRPV4 OE, TRPV4 Mut OE, or Control OE plasmids and exposed to 5 or 30 min OFF. The TRPV4 Mut OE group has attenuated osteogenesis compared to the TRPV4 OE group. Bar graphs represented fold changes with OFF compared to static controls. TRPV4 OE and TRPV4 Mut OE data are normalized to Control OE data. Data are presented as mean ± SEM. n = 6 for all groups, *$p < 0.01$, **$p < 0.001$.

Discussion

These studies demonstrate, for the first time, that Ca^{2+} and cAMP are coupled via AC3 and AC6 in osteocytes. AC3 and AC6 have long been known to bind Ca^{2+} to enhance and inhibit cAMP production[80], respectively, but the purpose of this relationship remains poorly characterized in the context of cell behavior. AC5/6 expression and activity are important for proper heart development and function[159,160] and AC5, which is also inhibited by Ca^{2+}, is critical to Ca^{2+}-mediated cardiac regulation[161]. AC3 is present in many tissue types and known to bind free Ca^{2+} to stimulate cAMP production[162], but the cellular function of this phenomena remains unknown. Our lab identified that cAMP levels decrease in MLOY4 osteocytes exposed to flow and their fluid shear-induced osteogenic response is lost when AC6 or IFT88 is downregulated[35]. We further demonstrated that fluid flow-induced osteocyte mechanotransduction is initiated

when Ca^{2+} enters the cilium[36], and mice containing a global knockout of AC6 exhibit attenuated load-induced bone formation[48]. We therefore suspected that ACs mediate Ca^{2+} entry and subsequent cAMP production, and found that AC3 and AC6[35] are present in MLOY4 cilia. To determine whether ciliary ACs mediate Ca^{2+}/ cAMP dynamics during osteocyte mechano-transduction, we disrupted the Ca^{2+} binding pocket of AC3/6 and evaluated flow-induced cAMP production and osteogenesis in MLO-Y4s *in vitro*. Indeed, osteocytes containing disrupted forms of AC3/6 demonstrated conflicting cAMP production compared to their functional counterparts. Furthermore, osteocytes that demonstrated higher levels of cAMP (AC3 OE and AC6 Mut OE) exhibited attenuated flow-induced osteogenesis. These results support our hypothesis that AC3/6 bind Ca^{2+} to mediate cAMP production and this behavior is important for osteocyte mechanotransduction.

This work also further implicates TRPV4 as the mechanism by which Ca^{2+} enters the cilium during osteocyte mechanotransduction. A prior study conducted by our lab found that an siRNA-mediated knockdown of TRPV4 uniquely resulted in attenuated osteogenesis in MLO-Y4s[36]. We also determined that knockdown of PC2, the predominant Ca^{2+} channel in kidney cilia, does not influence osteocyte mechanotransduction. Interestingly, we show in this study that MLO-Y4s with supranormal TRPV4 protein levels had an enhanced osteogenic response to fluid shear. However, when these cells overexpressed TRPV4 that could not open to allow Ca^{2+} entry into the cell or cilium, the enhanced osteogenic response was lost. This is perhaps not surprising since this phenomena has also been observed in osteoclasts, which require the same TRPV4 CaM domain to be activated for bone resorption[78]. Collectively, these results suggest that bone maintenance relies on TRPV4-mediated activation of osteocytes and osteoclasts, which promote and undermine bone formation, respectively.

AC6 is an attractive therapeutic target for bone regeneration since it can be easily manipulated and is potentially unique to osteocyte cilia. In this study, we demonstrated that MLO-Y4s overexpressing AC6 had longer cilia and an enhanced osteogenic response to fluid flow. This is consistent with our previous work that demonstrates cilia lengthening via Fenoldopam treatment promotes osteogenesis in MLO-Y4s[42]. Fenoldopam, an FDA-approved treatment for hypertension, has been proposed to enhance mechanotransduction by lengthening cilia via an AC/cAMP-mediated mechanism[163,164]. Our prior work implicates AC6 is perhaps the key AC in enhancing mechanotransduction via lengthening[42], and this study lends further support. Our group also determined that AC6 is present in the osteocyte primary cilium, but not in kidney cilia[35]. More cell types must be examined, especially cardiac cells, to truly determine whether AC6 is unique to the osteocyte cilium. It is important to note that AC6 is expressed in the cell body of many cell types, including osteocytes, so therapeutic strategies would be most effective if targeted to the primary cilium. Although we also identified that TRPV4 is perhaps the predominant Ca^{2+} channel in osteocytes, TRPV4 is also important for osteoclast activation[77,78]. Thus, therapeutic strategies that manipulate TRPV4 to enhance osteogenesis absolutely have to be targeted to the osteocyte primary cilium. Similarly, AC3 is present in many cell types so any manipulation would need to be targeted to avoid negative side effects. Additionally, the effects of AC6 overexpression only affected the onset of mechanotransduction, whereas AC3 overexpression continued to promote osteogenesis with longer durations of fluid flow. The primary cilium tunes its response to physical stimuli in order to prevent overstimulation[165]. This is an important negative-feedback mechanism inherent to cilium function, so therapeutic strategies should not interfere with this adaptation.

Our lab recently developed novel cilium-targeted biosensors that we will next use to specifically characterize Ca^{2+}/ cAMP dynamics in the cilium. One limitation with our studies is that we utilize overexpression plasmids and measure cytosolic readouts. CMV-driven mammalian expression plasmids typically result in supranormal protein levels in the cell body, and are difficult to direct to a specific organelle like the primary cilium. Our ICC results suggest protein is also overexpressed in the primary cilium, as well as the cell body, so we have currently measured the impact of higher protein levels throughout the entire osteocyte. Fortunately, we have developed cilium-targeted genetically encoded FRET sensors that measure changes in Ca^{2+} and cAMP levels in the cilium alone[36]. Furthermore, we can simultaneously and distinctly measure changes in ciliary and cytosolic Ca^{2+} or cAMP. In order to specifically measure the effects of overexpressing TRPV4/ AC3/ AC6 in the cilium, as well as the consequences of disrupting their ability to bind Ca^{2+}, we intend to measure changes in Ca^{2+} influx and cAMP production using our targeted biosensors. Indeed, our preliminary work indicates we can successfully transfect both our OE plasmids and our biosensor into the same cell. We are currently troubleshooting flow studies and live imaging to collect the final data. Another option is to utilize CRISPR to specifically overexpress, eliminate, or mutate ciliary AC3, AC6, and TRPV4. Unfortunately, this technology was not widely available at the time we generated our plasmids but would have been a superior approach. Despite this limitation, general overexpression of these ciliary proteins did enhance overall osteogenesis and we were still able to determine that these Ca^{2+} binding mechanisms are important to osteocyte mechanotransduction.

Combined, our results suggest that AC6 and TRPV4 are important for the immediate onset of flow-induced osteocyte mechanotransduction. Specifically, we speculate that, when

exposed to flow, the osteocyte cilium bends and extracellular Ca^{2+} binds to the CaM domain of TRPV4 (Figure 4.7). TRPV4 then opens and Ca^{2+} enters the cilium, most likely in the direction from the ciliary base to the axoneme tip[36]. Ciliary Ca^{2+} binds to AC6, which is then unable to catalyze the conversion of ATP to cAMP. Consequently, cytosolic cAMP levels decrease since existing cAMP is recruited for flow-induced intracellular signaling and AC6 is inhibited from replenishing cAMP.

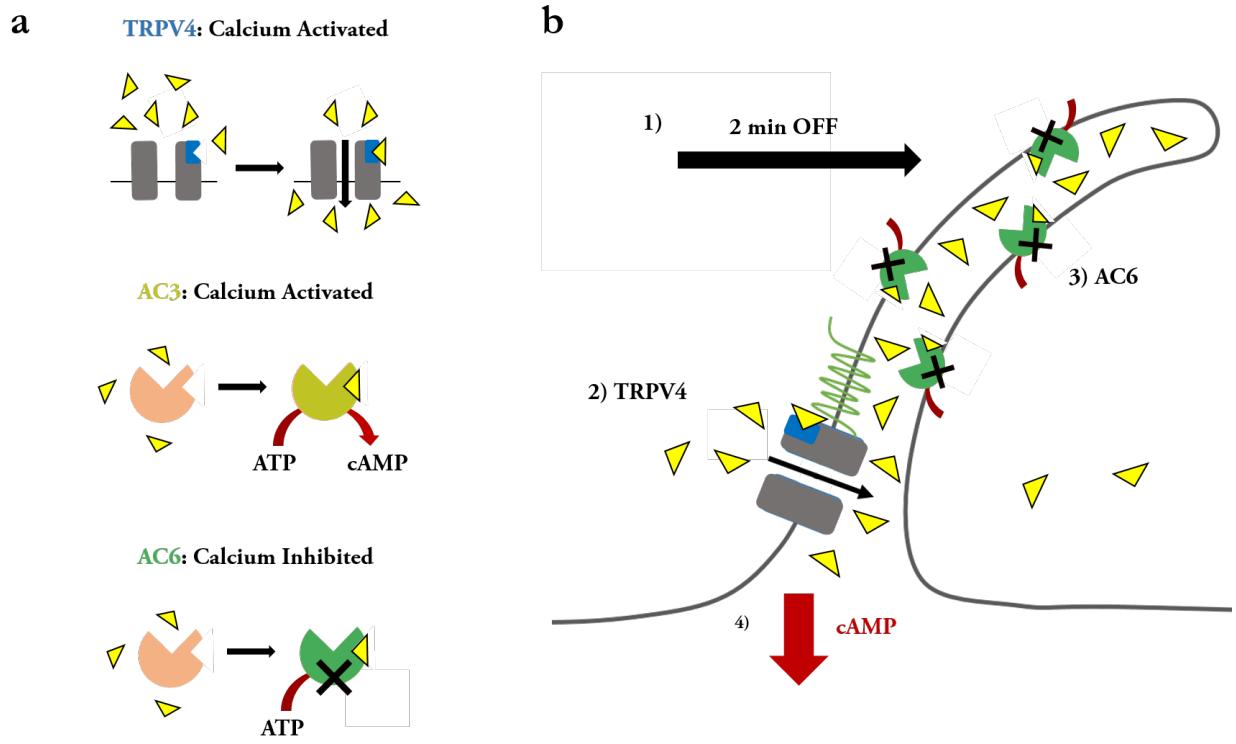

Figure 4.7: Proposed Ca^{2+}/ cAMP dynamics in the osteocyte primary cilium microdomain
(a) Summary of ciliary proteins and the effects of Ca^{2+} binding. (b) Cartoon summarizing our hypothesis of Ca^{2+}/ cAMP dynamics in the osteocyte primary cilium, based on our work to date. We propose that, in the initial onset of fluid shear (1), extracellular Ca^{2+}enters the bent osteocyte cilium by binding TRPV4 to facilitate opening of this channel, resulting in a ciliary influx of Ca^{2+} (2). The Ca^{2+} that has entered the cilium then binds to AC6 (3), inhibiting production of cAMP (4).

Chapter 5: Conclusion

Summary

The overall goal of our work is to study the primary cilium and mechanosensitive cells to identify mechanisms that can be therapeutically manipulated to encourage pro-osteogenic bone maintenance. Collectively, the work in this thesis has revealed an exciting source of osteogenic precursors whose cilia can be targeted to encourage bone generation, potentially *in vivo*. Additionally, these studies identify molecular targets than can be manipulated to tune osteocyte-mediated osteogenesis.

In Chapter 2, we established that the Prx1-expressing population is further restricted to the periosteum in adult mice. We found that mice lacking this cell population were essentially unable to produce bone normally in response to mechanical stimulation. Additionally, we demonstrated that these cells are mechanosensitive and respond to physical stimuli in a pro-osteogenic manner that requires the primary cilium. We propose that this cell source be the preferred source for bone generation strategies, particularly in favor of bone marrow stem cells, since periosteal OCPs are more easily extracted and pre-programmed towards an osteogenic fate.

In Chapter 3, we further characterized the Prx1-expressing population and found these cells are predominantly restricted to the cambium layers of the periosteum/ perichondrium after birth. During juvenile development, these cambium layer osteochondroprogenitors (CLOPs) differentiate into chondrocytes that populate the epiphyseal growth plate to form trabecular bone, as well as osteoblasts that lay down mineralized matrix and eventually become osteocytes embedded in cortical bone. However, mice lacking CLOP primary cilia have significantly shorter and thinner limbs due to disruptions in intramembranous and endochondral ossification.

Finally, we identified key components that mediate Ca^{2+}/cAMP dynamics in the osteocyte primary cilium microdomain. We demonstrated that AC3, AC6, and TRPV4 must bind Ca^{2+} in order to operate normally. Specifically, TRPV4 is unable to facilitate Ca^{2+} influx if its CaM binding domain is removed. Similarly, AC3 and AC6 cannot be activated or inhibited from, respectively, producing cAMP if their Ca^{2+} binding pocket is disrupted. These results provide further evidence that TRPV4 is perhaps the predominant calcium channel in osteocyte mechanotransduction. Additionally, we have established that ACs function to mediate Ca^{2+} and cAMP dynamics during osteocyte mechanotransduction. Interestingly, supranormal levels of AC6 protein were found to lengthen primary cilia, which is known to enhance osteocyte mechanosensitivity and subsequent osteogenesis. These ciliary molecules, particularly AC6, are therefore exciting therapeutic targets to promote bone generation via enhancing osteogenesis.

Future Work

We propose two main experiments that will effectively build upon the work conducted in this thesis. First, we intend to conduct fracture repair studies with our transgenic Prx1 models. The creators of the Prx1CreER-GFP model performed an initial fracture study using a lacZ reporter to track Prx1-expressing OCPs as they populated the fracture callus[53]. This experiment importantly established that Prx1-expressing cells contribute to fracture repair, but there is no insight into a) the mechanism by which these cells participate or b) the extent to which this cell population is required for repair. We propose that the primary cilium will be critical for Prx1-expressing OCPs to populate the fracture callus; therefore, we intend to repeat the initial fracture study with our Prx1CreER-GFP; $Ift88^{fl/fl}$ cilium knockout model to ascertain the necessity of the primary cilium. Another study suggests that periosteal progenitors are the predominant contributor of osteogenic cells in the fracture callus[95]. We will explore this possibility using our

Prx1CreER-GFP; Rosa26^{DTA} ablation model to quantify the contribution of Prx1-expressing periosteal OCPs in fracture repair. We anticipate that both disruptions will negatively impact fracture repair, but the ablation model will be the most severe. At the completion of these studies, we will have a comprehensive picture of the function of Prx1-expressing OCPs and their primary cilia in skeletal development, adult bone maintenance, and, finally, fracture repair.

Second, we wish to build upon the Ca^{2+}/ cAMP studies conducted in Chapter 4. We have generated cilium-targeted biosensors that can quantify Ca^{2+} and cAMP levels distinctly in the cilium. We also possess the tools to simultaneously measure cytosolic changes in these two second messengers. Our plan is to dually transfect MLOY4s with our TRPV4 OE or TRPV4 Mut OE plasmids and our Ca^{2+} biosensor. We will use the biosensor to visualize Ca^{2+} influx into the osteocyte primary cilium when TRPV4 is overexpressed or lacking the CaM domain. We expect that the flow-induced ciliary Ca^{2+} influx will be lost without the TRPV4 CaM domain. Furthermore, we wish to evaluate ciliary cAMP production. We will dually transfect our AC/ Mut OE plasmids with our biosensors and measure cytosolic and ciliary changes in cAMP to gain insight on ciliary/cytosolic relationships during the onset of mechanotransduction. Eventually, we intend to design and test methods that target the osteocyte primary cilium in order to develop pro-osteogenic therapeutics without side effects.

Significance

We believe the work performed in this thesis achieves two significant impacts. First, we have characterized a promising source of osteogenic precursors to generate new bone in areas where it is needed. Furthermore, we have elucidated the importance of the primary cilium in this cell source's ability to respond to mechanical stimuli and differentiate to produce skeletal tissue. This work provides critical insights that can alleviate patients suffering from bone fractures and

critical size defects. Over 1 million surgeries performed each year in the US involve fracture repair, partial excision of bone, and grafting[7,8]. Bone marrow was first identified as a source, but extraction is painful and progenitors require further encouragement towards an osteogenic lineage. The periosteum is a rich source of OCPs and is easily accessible for extraction[84,85]. Furthermore, it may be better suited for bone regeneration since periosteal progenitors largely contribute to deposition of bone and cartilage during bone repair *in vivo*[53,54,95,166]. One strategy to encourage osteogenic differentiation is to target OCP primary cilia[37,48,82,98]. Our lab is among the first to identify the primary cilium as a mechanosensitive signaling nexus that contributes to progenitor activation and osteogenic commitment[39,40,94]. This thesis provides compelling preliminary data indicating Prx1-expressing OCPs and their cilia contribute significantly to juvenile development and adult bone formation. In the long term, the knowledge generated in this research may even make it possible to populate remote sites of bone formation by manipulating cilia, obviating the need for extraction. This contribution is significant because it motivates 1) utilizing the periosteum in the short-term as a primary source of progenitors for regenerative strategies and 2) pursuing ciliary therapies in the long-term to non-invasively generate bone where it is needed. Independently, both of these contributions will ultimately reduce graft donor site morbidity, patient discomfort, and financial burden.

Second, our *in vitro* studies that identify a mechanism for osteocyte mechanotransduction provides unique opportunities to combat osteoporosis in a pro-osteogenic manner. Current pharmaceutical osteoporosis therapies protect or restore bone mass to varying degrees, yet still have adverse side effects. Antiresorptive drugs are associated with increased rate of atypical fractures [2], mandibular necrosis [3], esophageal cancer, and atrial fibrillation [4]. Several anabolic therapies can only be used for a limited time or have a potential risk of osteosarcoma

[5]. Since skeletal loading is a natural anabolic stimulus, targeting the osteocyte mechanosensing system has great potential to uncover new therapeutic strategies. In this thesis, we identified AC6 as a potential target for manipulating osteogenesis that is potentially unique to the osteocyte primary cilium. Furthermore, we identified that AC3 and TRPV4, if properly targeted to the osteocyte primary cilium, can also be potentially manipulated to enhance osteogenesis. These contributions are significant because they are an important advancement in the research continuum leading to novel therapeutics that shift the bone remodeling balance to promote bone formation. It is our hope that pro-osteogenic strategies will minimize adverse side effects and produce longer lasting results that alleviate the taxing dosing regimens associated with current treatments.

References

1. [date unknown]. Products - Health E Stats - Percentage of Adults Aged 65 and Over With Osteoporosis or Low Bone Mass at the Femur Neck or Lumbar Spine: United States, 2005–2010 [Internet].[cited 2017 Jul 26] Available from: https://www.cdc.gov/nchs/data/hestat/osteoporsis/osteoporosis2005_2010.htm.

2. [date unknown]. Facts and Statistics | International Osteoporosis Foundation [Internet].[cited 2017 Jul 27] Available from: https://www.iofbonehealth.org/facts-statistics#category-23.

3. [date unknown]. Hip Fractures Among Older Adults | Home and Recreational Safety | CDC Injury Center [Internet].[cited 2017 Jul 27] Available from: https://www.cdc.gov/homeandrecreationalsafety/falls/adulthipfx.html.

4. Brauer CA, Coca-Perraillon M, Cutler DM, Rosen AB. 2009. Incidence and mortality of hip fractures in the United States.JAMA 302(14):1573–9.

5. Cooper C. 1997. The crippling consequences of fractures and their impact on quality of life.Am. J. Med. 103(2A):12S–17S; discussion 17S–19S.

6. Center JR, Nguyen T V, Schneider D, et al. 1999. Mortality after all major types of osteoporotic fracture in men and women: an observational study.Lancet 353(9156):878–882.

7. Yousefi A-M, James PF, Akbarzadeh R, et al. 2016. Prospect of Stem Cells in Bone Tissue Engineering: A Review.Stem Cells Int. 2016:1–13.

8. Kretlow JD, Mikos AG. 2007. Review: Mineralization of Synthetic Polymer Scaffolds for

Bone Tissue Engineering.Tissue Eng. 13(5):927–938.

9. Weycker D, Li X, Barron R, et al. 2016. Hospitalizations for osteoporosis-related fractures: Economic costs and clinical outcomes.Bone Reports 5:186–191.

10. Kinaci A, Neuhaus V, Ring DC. 2014. Trends in Bone Graft Use in the United States.Orthopedics 37(9):e783–e788.

11. Wagoner Johnson AJ, Herschler BA. 2011. A review of the mechanical behavior of CaP and CaP/polymer composites for applications in bone replacement and repair.Acta Biomater. 7(1):16–30.

12. Lewiecki EM. 2010. Bisphosphonates for the treatment of osteoporosis: insights for clinicians.Ther. Adv. Chronic Dis. 1(3):115–28.

13. Cramer JA, Gold DT, Silverman SL, Lewiecki EM. 2007. A systematic review of persistence and compliance with bisphosphonates for osteoporosis.Osteoporos. Int. 18(8):1023–1031.

14. Black DM, Delmas PD, Eastell R, et al. 2007. Once-Yearly Zoledronic Acid for Treatment of Postmenopausal Osteoporosis.N. Engl. J. Med. 356(18):1809–1822.

15. Odvina C V., Zerwekh JE, Rao DS, et al. 2005. Severely Suppressed Bone Turnover: A Potential Complication of Alendronate Therapy.J. Clin. Endocrinol. Metab. 90(3):1294–1301.

16. Armamento-Villareal R, Napoli N, Panwar V, Novack D. 2006. Suppressed Bone Turnover during Alendronate Therapy for High-Turnover Osteoporosis.N. Engl. J. Med. 355(19):2048–2050.

17. Schneider JP. 2006. Should bisphosphonates be continued indefinitely? An unusual fracture in a healthy woman on long-term alendronate.Geriatrics 61(1):31–3.

18. Lee P, van der Wall H, Seibel MJ. 2007. Looking beyond low bone mineral density: Multiple insufficiency fractures in a woman with post-menopausal osteoporosis on alendronate therapy.J. Endocrinol. Invest. 30(7):590–597.

19. Goh S-K, Yang KY, Koh JSB, et al. 2007. Subtrochanteric insufficiency fractures in patients on alendronate therapy: A CAUTION.J. Bone Jt. Surg. - Br. Vol. 89–B(3):349–353.

20. Neviaser AS, Lane JM, Lenart BA, et al. 2008. Low-Energy Femoral Shaft Fractures Associated With Alendronate Use.J. Orthop. Trauma 22(5):346–350.

21. Lenart BA, Neviaser AS, Lyman S, et al. 2009. Association of low-energy femoral fractures with prolonged bisphosphonate use: a case control study.Osteoporos. Int. 20(8):1353–1362.

22. Fleisch H. 2001. Can Bisphosphonates Be Given to Patients with Fractures?J. Bone Miner. Res. 16(3):437–440.

23. Balemans W, Ebeling M, Patel N, et al. 2001. Increased bone density in sclerosteosis is due to the deficiency of a novel secreted protein (SOST).Hum. Mol. Genet. 10(5):537–43.

24. Li X, Ominsky MS, Warmington KS, et al. 2009. Sclerostin Antibody Treatment Increases Bone Formation, Bone Mass, and Bone Strength in a Rat Model of Postmenopausal Osteoporosis*.J. Bone Miner. Res. 24(4):578–588.

25. MacNabb C, Patton D, Hayes JS. 2016. Sclerostin Antibody Therapy for the Treatment of

Osteoporosis: Clinical Prospects and Challenges.J. Osteoporos. 2016:6217286.

26. Suen PK, Qin L. 2016. Sclerostin, an emerging therapeutic target for treating osteoporosis and osteoporotic fracture: A general review.J. Orthop. Transl. 4:1–13.

27. Ross RD, Edwards LH, Acerbo AS, et al. 2014. Bone Matrix Quality After Sclerostin Antibody Treatment.J. Bone Miner. Res. 29(7):1597–1607.

28. Cosman F, Crittenden DB, Adachi JD, et al. 2016. Romosozumab Treatment in Postmenopausal Women with Osteoporosis.N. Engl. J. Med. 375(16):1532–1543.

29. Ota S, Inoue R, Shiozaki T, et al. 2017. Atypical femoral fracture after receiving antiresorptive drugs in breast cancer patients with bone metastasis.Breast Cancer 24(4):601–607.

30. Ozdemir MT, Kir MÇ. 2011. Repair of long bone defects with demineralized bone matrix and autogenous bone composite.Indian J. Orthop. 45(3):226–30.

31. Farokhi M, Mottaghitalab F, Shokrgozar MA, et al. 2016. Importance of dual delivery systems for bone tissue engineering.J. Control. Release 225:152–169.

32. Islam A, Chapin K, Moore E, et al. 2016. Gamma Radiation Sterilization Reduces the High-cycle Fatigue Life of Allograft Bone.Clin. Orthop. Relat. Res. 474(3):827–835.

33. Ferretti C, Mattioli-Belmonte M. 2014. Periosteum derived stem cells for regenerative medicine proposals: Boosting current knowledge.World J. Stem Cells 6(3):266–77.

34. Yates EW, Boden RA, Suvarna K, Stockley I. 2016. Fresh osteochondral allograft with soft tissue reconstruction for open knee trauma: A 20-year follow-up.Ann. R. Coll. Surg. Engl. 98(2):e34-6.

35. Kwon RY, Temiyasathit S, Tummala P, et al. 2010. Primary cilium-dependent mechanosensing is mediated by adenylyl cyclase 6 and cyclic AMP in bone cells.FASEB J. 24(8):2859–68.

36. Lee KL, Guevarra MD, Nguyen AM, et al. 2015. The primary cilium functions as a mechanical and calcium signaling nexus.Cilia 4:7.

37. Temiyasathit S, Tang WJ, Leucht P, et al. 2012. Mechanosensing by the Primary Cilium: Deletion of Kif3A Reduces Bone Formation Due to Loading.PLoS One 7(3):e33368.

38. Malone AMD, Anderson CT, Tummala P, et al. 2007. Primary cilia mediate mechanosensing in bone cells by a calcium-independent mechanism.Proc. Natl. Acad. Sci. U. S. A. 104(33):13325–30.

39. Hoey DA, Tormey S, Ramcharan S, et al. 2012. Primary Cilia-Mediated Mechanotransduction in Human Mesenchymal Stem Cells.Stem Cells 30(11):2561–2570.

40. Chen JC, Jacobs CR. 2013. Mechanically induced osteogenic lineage commitment of stem cells.Stem Cell Res. Ther. 4(5):107.

41. Chen JC, Hoey DA, Chua M, et al. 2016. Mechanical signals promote osteogenic fate through a primary cilia-mediated mechanism.FASEB J. 30(4):1504–11.

42. Spasic M, Jacobs C. 2017. Lengthening primary cilia enhances cellular mechanosensitivity.Eur. Cells Mater. 33:158–168.

43. Gonciulea A, de Beur SJ. 2015. The dynamic skeleton.Rev. Endocr. Metab. Disord. 16(2):79–91.

44. Clarke B. 2008. Normal bone anatomy and physiology.Clin. J. Am. Soc. Nephrol. 3 Suppl

3(Suppl 3):S131-9.

45. Zhou X, von der Mark K, Henry S, et al. 2014. Chondrocytes transdifferentiate into osteoblasts in endochondral bone during development, postnatal growth and fracture healing in mice.PLoS Genet. 10(12):e1004820.

46. Yang L, Tsang KY, Tang HC, et al. 2014. Hypertrophic chondrocytes can become osteoblasts and osteocytes in endochondral bone formation.Proc. Natl. Acad. Sci. 111(33):12097–12102.

47. Haycraft CJ, Zhang Q, Song B, et al. 2007. Intraflagellar transport is essential for endochondral bone formation.Development 134(2):307–316.

48. Lee KL, Hoey DA, Spasic M, et al. 2014. Adenylyl cyclase 6 mediates loading-induced bone adaptation in vivo.FASEB J. 28(3):1157–65.

49. Leucht P, Kim J-B, Amasha R, et al. 2008. Embryonic origin and Hox status determine progenitor cell fate during adult bone regeneration.Development 135(17):2845–2854.

50. Miller SC, de Saint-Georges L, Bowman BM, Jee WS. 1989. Bone lining cells: structure and function.Scanning Microsc. 3(3):953-60–1.

51. Matic I, Matthews BG, Wang X, et al. 2016. Quiescent Bone Lining Cells Are a Major Source of Osteoblasts During Adulthood.Stem Cells 34(12):2930–2942.

52. Vellasamy S, Sandrasaigaran P, Vidyadaran S, et al. 2012. Isolation and characterisation of mesenchymal stem cells derived from human placenta tissue.World J. Stem Cells 4(6):53–61.

53. Kawanami A, Matsushita T, Chan YY, Murakami S. 2009. Mice expressing GFP and

CreER in osteochondro progenitor cells in the periosteum.Biochem. Biophys. Res. Commun. 386(3):477–82.

54. Ouyang Z, Chen Z, Ishikawa M, et al. 2013. Prx1 and 3.2kb Col1a1 promoters target distinct bone cell populations in transgenic mice.Bone .

55. Tatsumi S, Ishii K, Amizuka N, et al. 2007. Targeted Ablation of Osteocytes Induces Osteoporosis with Defective Mechanotransduction.Cell Metab. 5(6):464–475.

56. Nelson CM, Bissell MJ. 2006. Of Extracellular Matrix, Scaffolds, and Signaling: Tissue Architecture Regulates Development, Homeostasis, and Cancer.Annu. Rev. Cell Dev. Biol. 22(1):287–309.

57. Nguyen AM, Jacobs CR. 2013. Emerging role of primary cilia as mechanosensors in osteocytes.Bone 54(2):196–204.

58. Berridge MJ, Bootman MD, Roderick HL. 2003. Calcium: Calcium signalling: dynamics, homeostasis and remodelling.Nat. Rev. Mol. Cell Biol. 4(7):517–529.

59. Praetorius HA, Spring KR. 2001. Bending the MDCK cell primary cilium increases intracellular calcium.J. Membr. Biol. 184(1):71–9.

60. Nauli SM, Kawanabe Y, Kaminski JJ, et al. 2008. Endothelial Cilia Are Fluid Shear Sensors That Regulate Calcium Signaling and Nitric Oxide Production Through Polycystin-1.Circulation 117(9).

61. Praetorius HA, Spring KR. 2003. The renal cell primary cilium functions as a flow sensor.Curr. Opin. Nephrol. Hypertens. 12(5):517–20.

62. Praetorius HA, Spring KR. 2003. Removal of the MDCK Cell Primary Cilium Abolishes

Flow Sensing.J. Membr. Biol. 191(1):69–76.

63. Nauli SM, Alenghat FJ, Luo Y, et al. 2003. Polycystins 1 and 2 mediate mechanosensation in the primary cilium of kidney cells.Nat. Genet. 33(2):129–137.

64. Bratic I, Trifunovic A. 2010. Mitochondrial energy metabolism and ageing.Biochim. Biophys. Acta - Bioenerg. 1797(6–7):961–967.

65. Wadhwa S, Choudhary S, Voznesensky M, et al. 2002. Fluid flow induces COX-2 expression in MC3T3-E1 osteoblasts via a PKA signaling pathway.Biochem. Biophys. Res. Commun. 297(1):46–51.

66. Seino S, Shibasaki T. 2005. PKA-Dependent and PKA-Independent Pathways for cAMP-Regulated Exocytosis.Physiol. Rev. 85(4):1303–1342.

67. Kiprilov EN, Awan A, Desprat R, et al. 2008. Human embryonic stem cells in culture possess primary cilia with hedgehog signaling machinery.J. Cell Biol. 180(5):897–904.

68. Corbit KC, Shyer AE, Dowdle WE, et al. 2008. Kif3a constrains β-catenin-dependent Wnt signalling through dual ciliary and non-ciliary mechanisms.Nat. Cell Biol. 10(1):70–76.

69. Marszalek JR, Ruiz-Lozano P, Roberts E, et al. 1999. Situs inversus and embryonic ciliary morphogenesis defects in mouse mutants lacking the KIF3A subunit of kinesin-II.Proc. Natl. Acad. Sci. U. S. A. 96(9):5043–8.

70. Gillespie PG, Walker RG. 2001. Molecular basis of mechanosensory transduction.Nature 413(6852):194–202.

71. Su S, Phua SC, DeRose R, et al. 2013. Genetically encoded calcium indicator illuminates calcium dynamics in primary cilia.Nat. Methods 10(11):1105–7.

72. Moore ER, Jacobs CR. 2016. Molecular and Cellular Mechanobiology - Google Books [Internet].Springer :3–26[cited 2017 Jul 31] Available from: https://books.google.com/books?id=21nSDAAAQBAJ&pg=PA25&lpg=PA25&dq=moore+jacobs+primary+cilium&source=bl&ots=K-io-vlGvI&sig=EndtNreOUkyGWhKjmRhbRaEIWv4&hl=en&sa=X&ved=0ahUKEwiQ8_aJtrTVAhWGOj4KHUw9AsIQ6AEIKzAA#v=onepage&q=primary cilium&f=false.

73. Lehman JM, Michaud EJ, Schoeb TR, et al. 2008. The Oak Ridge Polycystic Kidney mouse: modeling ciliopathies of mice and men.Dev. Dyn. 237(8):1960–71.

74. Ishikawa H, Thompson J, Yates JR, Marshall WF. 2012. Proteomic Analysis of Mammalian Primary Cilia. 414-419 p.

75. Mochizuki T, Sokabe T, Araki I, et al. 2009. The TRPV4 cation channel mediates stretch-evoked Ca2+ influx and ATP release in primary urothelial cell cultures.J. Biol. Chem. 284(32):21257–64.

76. Strotmann R, Schultz G, Plant TD. 2003. Ca2+-dependent potentiation of the nonselective cation channel TRPV4 is mediated by a C-terminal calmodulin binding site.J. Biol. Chem. 278(29):26541–9.

77. Masuyama R, Vriens J, Voets T, et al. 2008. TRPV4-Mediated Calcium Influx Regulates Terminal Differentiation of Osteoclasts.Cell Metab. 8(3):257–265.

78. Masuyama R, Mizuno A, Komori H, et al. 2012. Calcium/calmodulin-signaling supports TRPV4 activation in osteoclasts and regulates bone mass.J. Bone Miner. Res. 27(8):1708–1721.

79. Steegborn C. 2014. Structure, mechanism, and regulation of soluble adenylyl cyclases — similarities and differences to transmembrane adenylyl cyclases.Biochim. Biophys. Acta - Mol. Basis Dis. 1842(12):2535–2547.

80. Halls ML, Cooper DMF. 2011. Regulation by Ca2+-signaling pathways of adenylyl cyclases.Cold Spring Harb. Perspect. Biol. 3(1):a004143.

81. Wilsman NJ, Farnum CE, Green EM, et al. 1996. Cell cycle analysis of proliferative zone chondrocytes in growth plates elongating at different rates.J. Orthop. Res. 14(4):562–572.

82. Song B, Haycraft CJ, Seo H, et al. 2007. Development of the post-natal growth plate requires intraflagellar transport proteins.Dev. Biol. 305(1):202–16.

83. Brady RT, O'Brien FJ, Hoey DA. 2015. Mechanically stimulated bone cells secrete paracrine factors that regulate osteoprogenitor recruitment, proliferation, and differentiation.Biochem. Biophys. Res. Commun. 459(1):118–123.

84. Arnsdorf EJ, Jones LM, Carter DR, Jacobs CR. 2009. The periosteum as a cellular source for functional tissue engineering.Tissue Eng. Part A 15(9):2637–42.

85. Castro-Silva II, Zambuzzi WF, de Oliveira Castro L, Granjeiro JM. 2012. Periosteal-derived cells for bone bioengineering: a promising candidate.Clin. Oral Implants Res. 23(10):1238–1242.

86. Arnsdorf EJ, Tummala P, Kwon RY, Jacobs CR. 2009. Mechanically induced osteogenic differentiation - the role of RhoA, ROCKII and cytoskeletal dynamics.J. Cell Sci. 122(4):546–553.

87. Henderson JH, Fuente L de la, Romero D, et al. 2007. Rapid Growth of Cartilage

Rudiments may Generate Perichondrial Structures by Mechanical Induction.Biomech. Model. Mechanobiol. 6(1–2):127–137.

88. Kanno T, Takahashi T, Ariyoshi W, et al. 2005. Tensile mechanical strain up-regulates Runx2 and osteogenic factor expression in human periosteal cells: Implications for distraction osteogenesis.J. Oral Maxillofac. Surg. 63(4):499–504.

89. Robling AG, Turner CH. 2002. Mechanotransduction in bone: genetic effects on mechanosensitivity in mice.Bone 31(5):562–9.

90. Turner CH, Owan I, Alvey T, et al. 1998. Recruitment and proliferative responses of osteoblasts after mechanical loading in vivo determined using sustained-release bromodeoxyuridine.Bone 22(5):463–9.

91. Birkhold AI, Razi H, Duda GN, et al. 2016. The Periosteal Bone Surface is Less Mechano-Responsive than the Endocortical.Sci. Rep. 6:23480.

92. Haycraft CJ, Serra R. 2008. Cilia involvement in patterning and maintenance of the skeleton.Curr. Top. Dev. Biol. 85:303–32.

93. Serra R. 2008. Role of Intraflagellar Transport and Primary Cilia in Skeletal Development.Anat. Rec. Adv. Integr. Anat. Evol. Biol. 291(9):1049–1061.

94. Hoey DA, Kelly DJ, Jacobs CR. 2011. A role for the primary cilium in paracrine signaling between mechanically stimulated osteocytes and mesenchymal stem cells.Biochem. Biophys. Res. Commun. 412(1):182–187.

95. Colnot C. 2009. Skeletal Cell Fate Decisions Within Periosteum and Bone Marrow During Bone Regeneration.J. Bone Miner. Res. 24(2):274–282.

96. Evans SF, Chang H, Knothe Tate ML. 2013. Elucidating multiscale periosteal mechanobiology: a key to unlocking the smart properties and regenerative capacity of the periosteum?Tissue Eng. Part B. Rev. 19(2):147–59.

97. Shimizu T, Sasano Y, Nakajo S, et al. 2001. Osteoblastic differentiation of periosteum-derived cells is promoted by the physical contact with the bone matrix in vivo.Anat. Rec. 264(1):72–81.

98. Haycraft CJ, Zhang Q, Song B, et al. 2006. Intraflagellar transport is essential for endochondral bone formation.Development 134(2).

99. Dempster DW, Compston JE, Drezner MK, et al. 2013. Standardized nomenclature, symbols, and units for bone histomorphometry: a 2012 update of the report of the ASBMR Histomorphometry Nomenclature Committee.J. Bone Miner. Res. 28(1):2–17.

100. Saris DBF, Sanyal A, An K-N, et al. 1999. Periosteum responds to dynamic fluid pressure by proliferatingin vitro.J. Orthop. Res. 17(5):668–677.

101. Klein-Nulend J, Roelofsen J, Sterck JGH, et al. 1995. Mechanical loading stimulates the release of transforming growth factor-? activity by cultured mouse calvariae and periosteal cells.J. Cell. Physiol. 163(1):115–119.

102. Bowers M, Zhang B, Ho Y, et al. 2015. Osteoblast ablation reduces normal long-term hematopoietic stem cell self-renewal but accelerates leukemia development.Blood 125(17):2678–88.

103. Stanger BZ, Tanaka AJ, Melton DA. 2007. Organ size is limited by the number of embryonic progenitor cells in the pancreas but not the liver.Nature 445(7130):886–891.

104. Soleimani M, Nadri S. 2009. A protocol for isolation and culture of mesenchymal stem cells from mouse bone marrow.Nat. Protoc. 4(1):102–106.

105. Koshihara Y, Honda Y. 1994. Age-related increase in collagen production in cultured human osteoblast-like periosteal cells.Mech. Ageing Dev. 74(1–2):89–101.

106. Lim SM, Choi YS, Shin HC, et al. 2005. Isolation of human periosteum-derived progenitor cells using immunophenotypes for chondrogenesis.Biotechnol. Lett. 27(9):607–611.

107. De Bari C, Dell'Accio F, Vanlauwe J, et al. 2006. Mesenchymal multipotency of adult human periosteal cells demonstrated by single-cell lineage analysis.Arthritis Rheum. 54(4):1209–1221.

108. Bei K, Du Z, Xiong Y, et al. 2012. BMP7 can promote osteogenic differentiation of human periosteal cells in vitro.Mol. Biol. Rep. 39(9):8845–8851.

109. Nakahara H, Bruder SP, Haynesworth SE, et al. 1990. Bone and cartilage formation in diffusion chambers by subcultured cells derived from the periosteum.Bone 11(3):181–8.

110. Nakahara H, Dennis JE, Bruder SP, et al. 1991. In vitro differentiation of bone and hypertrophic cartilage from periosteal-derived cells.Exp. Cell Res. 195(2):492–503.

111. Bilkay U, Tokat C, Helvaci E, et al. 2008. Osteogenic Capacities of Tibial and Cranial Periosteum.J. Craniofac. Surg. 19(2):453–458.

112. Nakahara H, Bruder SP, Goldberg VM, Caplan AI. 1990. In vivo osteochondrogenic potential of cultured cells derived from the periosteum.Clin. Orthop. Relat. Res. (259):223–32.

113. O'Driscoll SW, Fitzsimmons JS. 2001. The role of periosteum in cartilage repair.Clin. Orthop. Relat. Res. (391 Suppl):S190-207.

114. Murao H, Yamamoto K, Matsuda S, Akiyama H. 2013. Periosteal cells are a major source of soft callus in bone fracture.J. Bone Miner. Metab. 31(4):390–398.

115. Logan M, Martin JF, Nagy A, et al. 2002. Expression of Cre recombinase in the developing mouse limb bud driven by aPrxl enhancer.genesis 33(2):77–80.

116. Hall BK, Hall BK. 2015. Chapter 10 – Embryonic Stem and Progenitor Cells. In: Bones and Cartilage. p 153–165.

117. Martin JF, Olson EN. 2000. Identification of a prx1 limb enhancer.Genesis 26(4):225–9.

118. White RB, Biérinx A-S, Gnocchi VF, Zammit PS. 2010. Dynamics of muscle fibre growth during postnatal mouse development.BMC Dev. Biol. 10(1):21.

119. Lamon S, Zacharewicz E, Butchart LC, et al. 2017. MicroRNA expression patterns in post-natal mouse skeletal muscle development.BMC Genomics 18(1):52.

120. Richman C, Kutilek S, Miyakoshi N, et al. 2001. Postnatal and Pubertal Skeletal Changes Contribute Predominantly to the Differences in Peak Bone Density Between C3H/HeJ and C57BL/6J Mice.J. Bone Miner. Res. 16(2):386–397.

121. Deren ME, Yang X, Guan Y, Chen Q. 2016. Biological and Chemical Removal of Primary Cilia Affects Mechanical Activation of Chondrogenesis Markers in Chondroprogenitors and Hypertrophic Chondrocytes.Int. J. Mol. Sci. 17(2):188.

122. Anderson CT, Castillo AB, Brugmann SA, et al. 2008. Primary Cilia: Cellular Sensors for the Skeleton.Anat. Rec. Adv. Integr. Anat. Evol. Biol. 291(9):1074–1078.

123. Goetz SC, Anderson K V. 2010. The primary cilium: a signalling centre during vertebrate development.Nat. Rev. Genet. 11(5):331–344.

124. Yang L, Tsang KY, Tang HC, et al. 2014. Hypertrophic chondrocytes can become osteoblasts and osteocytes in endochondral bone formation.Proc. Natl. Acad. Sci. U. S. A. 111(33):12097–102.

125. Chang C-F, Serra R. 2013. Ift88 regulates Hedgehog signaling, Sfrp5 expression, and β-catenin activity in post-natal growth plate.J. Orthop. Res. 31(3):350–6.

126. Ascenzi M-G, Lenox M, Farnum C. 2007. Analysis of the orientation of primary cilia in growth plate cartilage: A mathematical method based on multiphoton microscopical images.J. Struct. Biol. 158(3):293–306.

127. Ascenzi M-G, Blanco C, Drayer I, et al. 2011. Effect of localization, length and orientation of chondrocytic primary cilium on murine growth plate organization.J. Theor. Biol. 285(1):147–155.

128. de Andrea CE, Wiweger M, Prins F, et al. 2010. Primary cilia organization reflects polarity in the growth plate and implies loss of polarity and mosaicism in osteochondroma.Lab. Investig. 90(7):1091–1101.

129. McGlashan SR, Haycraft CJ, Jensen CG, et al. 2007. Articular cartilage and growth plate defects are associated with chondrocyte cytoskeletal abnormalities in Tg737orpk mice lacking the primary cilia protein polaris.Matrix Biol. 26(4):234–246.

130. Rais Y, Reich A, Simsa-Maziel S, et al. 2015. The growth plate's response to load is partially mediated by mechano-sensing via the chondrocytic primary cilium.Cell. Mol.

Life Sci. 72(3):597–615.

131. Tummala P, Arnsdorf EJ, Jacobs CR. 2010. The Role of Primary Cilia in Mesenchymal Stem Cell Differentiation: A Pivotal Switch in Guiding Lineage Commitment.Cell. Mol. Bioeng. 3(3):207–212.

132. Cooper KL, Oh S, Sung Y, et al. 2013. Multiple phases of chondrocyte enlargement underlie differences in skeletal proportions.Nature 495(7441):375–378.

133. Gómez-Casati ME, Murtie J, Taylor B, Corfas G. 2010. Cell-specific inducible gene recombination in postnatal inner ear supporting cells and glia.J. Assoc. Res. Otolaryngol. 11(1):19–26.

134. Huh WJ, Khurana SS, Geahlen JH, et al. 2012. Tamoxifen Induces Rapid, Reversible Atrophy, and Metaplasia in Mouse Stomach.Gastroenterology 142(1):21–24.e7.

135. Langenskiöld A. 1998. Role of the ossification groove of Ranvier in normal and pathologic bone growth: a review.J. Pediatr. Orthop. 18(2):173–7.

136. Bashur LA, Chen D, Chen Z, et al. 2014. Loss of Jab1 in Osteochondral Progenitor Cells Severely Impairs Embryonic Limb Development in Mice.J. Cell. Physiol. 229(11):1607–1617.

137. Corish P, Tyler-Smith C. 1999. Attenuation of green fluorescent protein half-life in mammalian cells.Protein Eng. 12(12):1035–40.

138. Fujii T, Ueno T, Kagawa T, et al. 2006. Comparison of bone formation ingrafted periosteum harvested from tibia and calvaria.Microsc. Res. Tech. 69(7):580–584.

139. Hutmacher DW, Sittinger M. 2003. Periosteal Cells in Bone Tissue Engineering.Tissue

Eng. 9(supplement 1):45–64.

140. Ono N, Ono W, Nagasawa T, Kronenberg HM. 2014. A subset of chondrogenic cells provides early mesenchymal progenitors in growing bones.Nat. Cell Biol. 16(12):1157–1167.

141. Shapiro IM, Adams CS, Freeman T, Srinivas V. 2005. Fate of the hypertrophic chondrocyte: Microenvironmental perspectives on apoptosis and survival in the epiphyseal growth plate.Birth Defects Res. Part C Embryo Today Rev. 75(4):330–339.

142. Takarada T, Nakazato R, Tsuchikane A, et al. 2016. Genetic analysis of Runx2 function during intramembranous ossification.Development 143(2).

143. Lui JC, Nilsson O, Baron J. 2011. Growth Plate Senescence and Catch-Up Growth. In: Endocrine development. p 23–29.

144. Gafni RI, Weise M, Robrecht DT, et al. 2001. Catch-Up Growth Is Associated with Delayed Senescence of the Growth Plate in Rabbits.Pediatr. Res. 50(5):618–623.

145. Marino R, Hegde A, Barnes KM, et al. 2008. Catch-Up Growth after Hypothyroidism Is Caused by Delayed Growth Plate Senescence.Endocrinology 149(4):1820–1828.

146. Huangfu D, Liu A, Rakeman AS, et al. 2003. Hedgehog signalling in the mouse requires intraflagellar transport proteins.Nature 426(6962):83–87.

147. Clement CA, Ajbro KD, Koefoed K, et al. 2013. TGF-β Signaling Is Associated with Endocytosis at the Pocket Region of the Primary Cilium.Cell Rep. 3(6):1806–1814.

148. Lindbæk L, Warzecha C, Koefoed K, et al. 2015. Coordination of TGFβ/BMP signaling is associated with the primary cilium.Cilia 4(Suppl 1):P17.

149. Seo H-S, Serra R. 2007. Deletion of Tgfbr2 in Prx1-cre expressing mesenchyme results in defects in development of the long bones and joints.Dev. Biol. 310(2):304–316.

150. Alvarez J, Sohn P, Zeng X, et al. 2002. TGFbeta2 mediates the effects of hedgehog on hypertrophic differentiation and PTHrP expression.Development 129(8):1913–24.

151. Minina E, Wenzel HM, Kreschel C, et al. 2001. BMP and Ihh/PTHrP signaling interact to coordinate chondrocyte proliferation and differentiation.Development 128(22):4523–34.

152. Li Y, Dudley AT. 2009. Noncanonical frizzled signaling regulates cell polarity of growth plate chondrocytes.Development 136(7):1083–1092.

153. Long F, Zhang XM, Karp S, et al. 2001. Genetic manipulation of hedgehog signaling in the endochondral skeleton reveals a direct role in the regulation of chondrocyte proliferation.Development 128(24):5099–108.

154. Wu LNY, Lu M, Genge BR, et al. 2002. Discovery of Sonic hedgehog expression in postnatal growth plate chondrocytes: Differential regulation of Sonic and Indian hedgehog by retinoic acid.J. Cell. Biochem. 87(2):173–187.

155. Yoon BS, Pogue R, Ovchinnikov DA, et al. 2006. BMPs regulate multiple aspects of growth-plate chondrogenesis through opposing actions on FGF pathways.Development 133(23).

156. Chang H, Knothe Tate ML. 2012. Concise Review: The Periosteum: Tapping into a Reservoir of Clinically Useful Progenitor Cells.Stem Cells Transl. Med. 1(6):480–491.

157. Hu B, Nakata H, Gu C, et al. 2002. A Critical Interplay between Ca2+ Inhibition and Activation by Mg2+ of AC5 Revealed by Mutants and Chimeric Constructs.J. Biol.

Chem. 277(36):33139–33147.

158. Mou T-C, Masada N, Cooper DMF, Sprang SR. 2009. Structural Basis for Inhibition of Mammalian Adenylyl Cyclase by Calcium †.Biochemistry 48(15):3387–3397.

159. Gao MH, Lai NC, Giamouridis D, et al. 2017. Cardiac-directed expression of a catalytically inactive adenylyl cyclase 6 protects the heart from sustained β-adrenergic stimulation.PLoS One 12(8):e0181282.

160. Hu C-L, Chandra R, Ge H, et al. 2009. Adenylyl cyclase type 5 protein expression during cardiac development and stress.Am. J. Physiol. Heart Circ. Physiol. 297(5):H1776-82.

161. Okumura S, Kawabe J, Yatani A, et al. 2003. Type 5 Adenylyl Cyclase Disruption Alters Not Only Sympathetic But Also Parasympathetic and Calcium-Mediated Cardiac Regulation.Circ. Res. 93(4):364–371.

162. Xia Z, Choi E-J, Wang F, Storm DR. 1992. The type III calcium/calmodulin-sensitive adenylyl cyclase is not specific to olfactory sensory neurons.Neurosci. Lett. 144(169):173–169.

163. Upadhyay VS, Muntean BS, Kathem SH, et al. 2014. Roles of dopamine receptor on chemosensory and mechanosensory primary cilia in renal epithelial cells.Front. Physiol. 5:72.

164. Besschetnova TY, Kolpakova-Hart E, Guan Y, et al. 2010. Identification of Signaling Pathways Regulating Primary Cilium Length and Flow-Mediated Adaptation.Curr. Biol. 20(2):182–187.

165. Nguyen AM, Young Y-N, Jacobs CR. 2015. The primary cilium is a self-adaptable,

integrating nexus for mechanical stimuli and cellular signaling.Biol. Open 4(12):1733–8.

166. Colnot C, Zhang X, Tate MLK. 2012. Current insights on the regenerative potential of the periosteum: Molecular, cellular, and endogenous engineering approaches.J. Orthop. Res. 30(12):1869–1878.

167. Chen JC, Moore ER, Jacobs CR. 2018. Prx1-expressing progenitor primary cilia mediate bone formation in response to mechanical loading in mice. In submission. J. Biomech.